SURFACTANT DESIGN FOR EOR PROJECT AND DYNAMIC SURFACE

TENSION FOR FLUID ANALYSIS

A Thesis

by

AASHRIT REDDY BAGAREDDY

Submitted to the Graduate and Professional School of
Texas A&M University
in partial fulfillment of the requirements for the degree of

MASTER OF SCIENCE

Chair of Committee,	David Schechter
Committee Members,	Jenn-Tai Liang
	Juan Carlos Laya Pereira
Head of Department,	Jeff Spath

December 2021

Major Subject: Petroleum Engineering

ABSTRACT

Surfactant flooding has been shown to increase EOR potential in hydrocarbon reservoirs. Chemical surfactants have been demonstrated to potentially improve EOR in unconventional reservoirs such as shale. Surfactants of different types such as cationic, anionic and nonionic surfactants have been studied extensively for their potential to alter wettability of reservoir rock and improving Estimated Ultimate Recovery (EUR). Nonionic surfactants have been shown to be especially effective in altering Eagle Ford shale wettability.

A methodology for effectively screening surfactants for EOR projects is introduced for a well in the Eagle Ford basin. Practical and chemical effects are considered while formulating an optimal injection fluid for good field scale performance. In the pre-injection phase, laboratory measurements like contact angle and spontaneous imbibition experiments are performed to evaluate wettability alteration performance. The effects of chemical additives are also investigated to ensure no interference from other surface-active chemicals. In the post-injection phase, the oil and water production rates are monitored daily. Produced water samples are analyzed to measure residual surfactant concentration in the produced water through a unique dynamic surface tension methodology. Performance evaluation of the EOR project indicates increased oil and water production rates with low residual surfactant concentrations returning to the surface.

Dynamic surface tension methodology was utilized to develop a method to measure adsorption density on rock samples and characterize the performance based on the surfactant type. Results show that nonionic surfactants have a higher adsorption density on limestone and shale rock compared to sandstone rock.

A systematic methodology for performing dynamic surface tension measurements and estimating the surfactant concentrations by quantitative analysis is proposed.

DEDICATION

This study is dedicated to my parents, Mr. Suresh Reddy and Mrs. Shalini Reddy, for motivating me throughout my journey as a graduate petroleum engineering student. The support I have received from them; I will forever be grateful for that. I extend my gratitude to them for believing in my academic pursuits.

ACKNOWLEDGEMENTS

CONTRIBUTORS AND FUNDING SOURCES

Contributors

This work was supervised by a thesis committee consisting of Professor David Schechter and Professor Jenn-Tai Liang from the Department of Petroleum Engineering and Professor Juan Carlos Laya Pereira from the Department of Geology and Geophysics.

All work conducted for the thesis was completed by the student independently.

Funding Sources

NOMENCLATURE

EOR	Enhanced Oil Recovery
EUR	Estimated ultimate recovery
OOIP	Original oil-in-place
E	Displacement efficiency
K	permeability
μ	viscosity
M	Mobility ratio
K_{rw}	Relative permeability to water
K_{ro}	Relative permeability to oil
N_c	capillary number
σ	Interfacial tension
TAN	Total acid number
TBN	Total base number
EO	Ethylene Oxide
CMC	Critical micelle concentration
σ_{sw}	Solid-water interfacial tension
σ_{ow}	Oil-water interfacial tension
S_{wf}	Residual forced water saturation
S_{of}	residual forced oil saturation
I_{A-H}	Amott-Harvey index
ULR	Unconventional liquid reservoirs

TDS	Total dissolved solids
DST	Dynamic surface tension
MBPM	Maximum Bubble Pressure method
P_{max}	Maximum pressure
γ	Surface Tension
bbl.	barrel
Γ	Surface excess concentration
C	Concentration
R	Universal Gas constant
T	Temperature
D	Diffusion coefficient
γ_{eq}	Equilibrium surface tension
SARA	Saturates, aromatics, resins and asphaltenes
g/cm^3	grams per centimeter cube
mN/m	(Millinewton per meter) or (dyne)
EF	Eagle Ford
XRD	X-Ray diffraction
CA	Contact Angle
MD	Measured depth
TVD	True vertical depth
FW	Freshwater

PW   Produced water

MS   Master solution

MIC   Microbially influenced corrosion

LC   Laughlin Cook

ppm   Parts per million

CT   Computerized tomography

wt. %   Percentage by gram weight

lbs.   Pound weight

cc.   Centimeter-cube of volume

ms   Millisecond

TABLE OF CONTENTS

LIST OF FIGURES

xv

1. INTRODUCTION

Enhanced Oil recovery (EOR) is very often incorrectly used interchangeably with Improved Oil recovery (IOR). IOR is a broad concept that encompasses all techniques and methods for ultimate recovery of oil, while EOR is primarily driven by the potential to recover more oil at an economically viable rate [5]

Almost 2.0×10^{12} barrels (0.3×10^{12} m ^{3}) of conventional oil and 5.0×10^{12} barrels (0.8×10^{12} m ^{3}) of heavy oil will be remaining in reservoirs once traditional methods of oil recovery have been exhausted. A major part of these remaining oil reserves is estimated to be recovered using EOR processes [2]. Enhanced oil recovery is an industry-wide technique to unlock greater production from relatively unrecoverable oil reserves. With advancing technologies and rapid progression in injection technologies, numerous EOR methods have been developed that aid in improving tertiary oil recovery. Oil reservoirs generally go through a a cycle of primary, secondary and tertiary production cycles. The primary recovery from an oil reservoir uses the natural pressure difference of the reservoir to drive the crude oil to the surface. Primary recovery generally recovery 5 – 10% of OOIP, hence primary recovery methods are generally considered ineffective due to the lower recovery from OOIP. Secondary recovery is utilized during when the natural energy present in the reservoir has been depleted insufficiently such that it is unable to drive oil production from the reservoir to the wellhead. Secondary recovery involves injection of fluids such as gas or a liquid to regulate reservoir pressure and stimulate oil wells. The injection fluids behave in the manner of an artificial drive. The process is called waterflooding if the injected fluid is a liquid. Secondary stage efficiency for recovery is reported to be around 10 – 40 % of OOIP [6,7,8]. Tertiary recovery processes are used after primary and secondary recovery processes have been exhausted and

1

are unable to generate sufficient pressure difference to produce oil. Tertiary mechanisms include those techniques that improve oil recovery by oil swelling, reducing the viscosity of the fluids or by generated a favorable relative permeability for oil production.
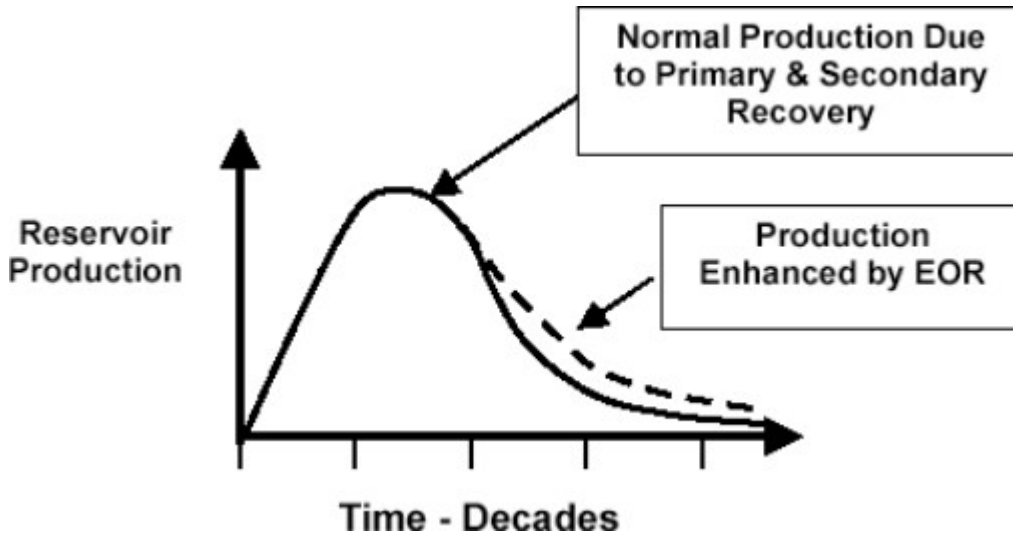
Figure 1: Stages of reservoir production [3]

Tertiary mechanisms are also known as Enhanced Oil recovery (EOR) methods. EOR methods include the injection of fluids that interact with the rock/oil/brine system in the reservoir. These fluids interact with the reservoir to create favorable conditions for oil recovery such as IFT reduction, wettability alteration, oil swelling, favorable phase behavior, oil viscosity reduction [2]. These interactions are brought about by the physical and chemical effects by the injection fluids with the reservoir system.

The potential for oil recovery from EOR processes is massive to recover oil trapped at the pore-scale level after primary and secondary production techniques have been used to recover oil through snap-off caused by changes in capillary pressure.[9] Although the potential is great, choosing the right type of EOR techniques is critical to recovering oil from mature

oil fields in a cost-effective manner. EOR processes can extract more than half of the OOIP and generates significantly more oil production that primary or secondary methods [10].

The displacement efficiency(E) of any oil recovery displacement process can be thought of as the product of microscopic (E_D) and macroscopic (E_V) displacement efficiencies.[11]

$$E = E_D * E_V$$

Eq 1

$$E = E_i * E_a$$

Eq 2

where E_i is the vertical sweep efficiency and E_a is the areal sweep efficiency.

The macroscopic displacement efficiency of a well is an indicator of the effectiveness of the fluid to come in contact with the oil-saturated parts of the reservoir, whereas microscopic displacement efficiency is the indicator of effectiveness of the injection fluid to mobilize the residual oil when it comes in contact with the oil [11]. There are 4 main types of EOR methods:

1) Thermal EOR (TEOR)

2) Chemical EOR techniques (CEOR)

3) Gas Injection EOR technique (GEOR)

4) Microbial EOR (MEOR)

Figure 2 shows the different types of EOR techniques involves in thermal and non-thermal processes.
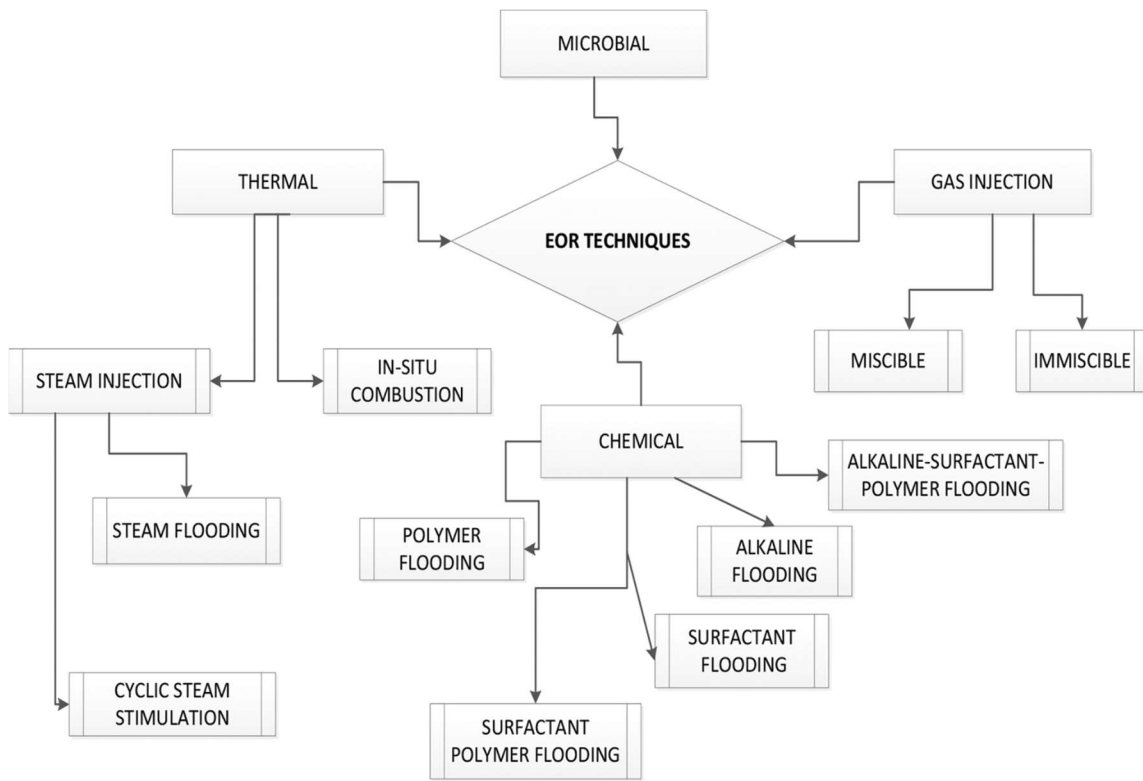
Figure 2: Classification of EOR methods in conventional reservoirs[4]

1.1. Objectives

The objectives of this study were to facilitate the surfactant selection process for a well in the Eagle form formation for the purpose of a surfactant EOR project. Surfactant solutions, especially nonionic surfactants have been shown to be able to successfully alter the wettability of Eagle ford shale rock to water-wet. The application of an aqueous surfactant solution to a well by performing an injection process will be monitored in this study. Studies have shown that dynamic surface tension measurements have the potential

to determine the concentration of surfactant in an aqueous fluid, by comparing the dynamic surface tension between a known solvent and an unknown produced water fluid. The method for analyzing produced water fluids from a production well by using dynamic surface tension analysis and calculating the total surface mass returned to the surface is documented in this study.

The process of measuring surfactant adsorption kinetics onto rock surfaces has historically been performed using UV Visible Spectrophotometry, which is a tedious and expensive process to perform. The lack of an effective and cost-friendly method for measuring surfactant adsorption kinetics at regular intervals is addressed in this study. Dynamic surface tension analysis is also utilized to observe the change in surfactant concentration during surfactant imbibition onto rock samples. The dynamic surface tension methodology is applied to calculate the amount of surfactant adsorbed onto a rock sample, as well as the surfactant adsorption densities. The effect of different rock compositions is also investigated to characterize the adsorption tendencies of surfactants onto rock samples.

1.2. Chemical EOR (CEOR)

Chemical EOR techniques involve injection of chemicals to improve oil recovery. Chemical EOR methods have seen great potential for EOR projects in terms for feasibility, cost effectiveness and performance. Based on the chemical EOR process, the slugs of water with chemicals are used to alter the rock/fluid or fluid/fluid interactions in the

reservoir. The most known chemical EOR processes are polymer, alkaline and surfactant flooding [24].

1.2.1. Polymer flooding

Early water breakthrough can occur during a waterflooding process in a reservoir as result of viscous fingering and gravity effects. High-molecular weight water-soluble polymers are used with the water slug to increase the viscosity of the injection fluid. The increased viscosity helps with mobility control and mitigates viscous fingering. Early water breakthroughs that are generally observed in waterflooding are avoided along with increase in oil recovery. [25]

Polymer flooding increases oil recovery through 3 main mechanisms:

1) <u>Mobility control</u>: Mobility ratio is the ratio of the mobility of the injected fluid to the mobility of the displaced fluid. Equation (3) denotes the mobility ratio of a waterflood where M is the mobility ratio and K and μ denoted the permeabilities and viscosities to water and oil respectively.

$$M = \frac{K_w \mu_o}{K_o \mu_w} \qquad\qquad \textit{Eq 3}$$
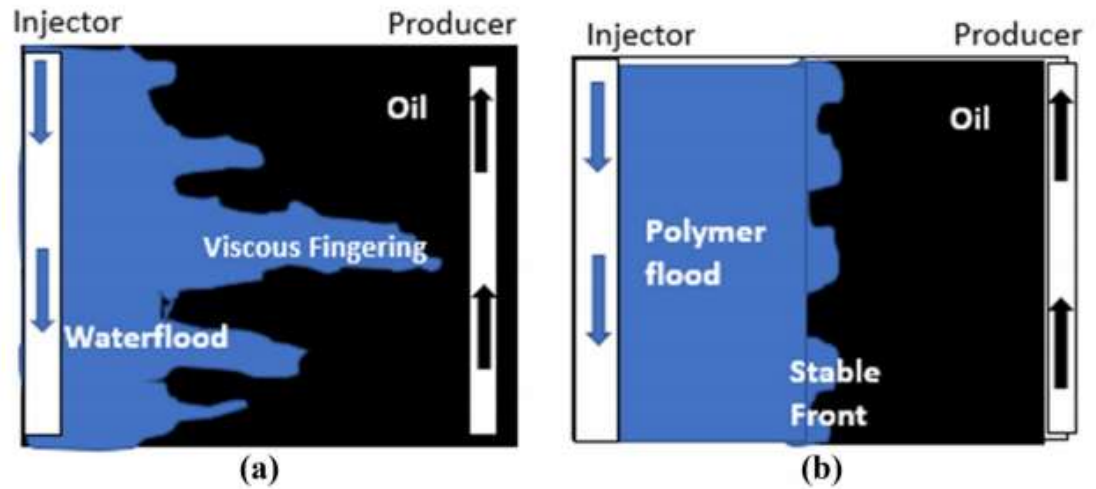
Figure 3: Mobility ratios for a) Waterflooding Process (M > 1) b) Polymer flooding (M <= 1)[26]

Unfavorable mobility ratios caused during waterflooding processes (M >1) leads to viscous fingering of water through oil which causes early water breakthroughs and lower sweep efficiencies. Inclusion of polymer in the injected fluid helps raise the viscosity of the fluid which displaces the oil in the reservoir while maintaining a stable displacement front without any viscous fingering or channeling [26]. A representation of a high mobility waterflood process vs a low mobility polymer flooding process is shown in Figure 3.

2) <u>Disproportionate permeability reduction</u>: Another mechanism by which polymer flooding improves displacement efficiencies is through disproportionate permeability reduction. Heterogenous reservoirs tend to exhibit uneven permeability distribution between zones which can lead to channeling of water through the higher permeability zones. This leads to recoverable oil and gas in the lower permeability zones to be trapped and hence leads to poor oil recoveries

7

in non-tertiary stages of production [41]. Polymer flooding causes the high flow resistances to high permeability parts of the reservoir, lower relative permeability to water (K_{rw}) while not affecting the relative permeability to oil (K_{ro}). Increasing resistance to water flow forces the waterflood front to flow through the low permeability zones hence improving macroscopic sweep efficiencies through different layers of the reservoir.

3) <u>Polymer viscoelasticity</u>: Polymers are a non – Newtonian fluid, so they have the ability to expand and contract (deform) during flow in porous media which is indicative of the viscoelastic properties of polymers. The polymer molecules exhibit increased viscosity due to the viscoelastic properties of the polymers which improves displacement efficiencies. An investigation into the sweep efficiencies of polymer indicated that high elasticity polymer solutions exhibit a high flow resistance through a porous medium, and a stable displacement front [27].

1.2.2. Surfactant flooding

Surfactant flooding is an improvised waterflooding process where an aqueous solution of a surfactant is injected into a reservoir to mobilize trapped residual oil. Surfactants are amphiphilic in nature and have a non-polar hydrophobic tail and a polar hydrophilic head. Surfactants can be of classified into cationic, anionic, nonionic and zwitterionic surfactants depending upon the charge of the hydrophilic head. Surfactant EOR aims to improve oil recovery by reducing water/oil IFT while simultaneously altering the wettability of the reservoir rock which creates favorable capillary pressure conditions

imbibition of the water phase into the pores which mobilizes the trapped oil in porous media. Surfactants have 2 primary mechanisms of improving oil recovery:

1) Interfacial tension reduction: Surfactant EOR improves upon secondary recovery processes such as waterflooding in which displacing trapped oil is difficult at pore scale due to unfavorable capillary pressure distribution. Surfactants aid in reducing the surface tension between the injected surfactant solution and the in-situ fluids, leading to a change in the pore scale capillary pressures. The dimensionless capillary number (N_c) is defined as:

$$N_C = \frac{\mu * v}{\sigma * cos\theta} \qquad\qquad \textbf{Eq 4}$$

Higher values of N_c are a strong indicator of higher oil recoveries. Typical brine floods have an N_c range between 10^{-7} and 10^{-6}. Increasing the value of N_c will lead to an increase in recovery factor, which can be done by increasing injectant fluid viscosity(μ), injectant fluid velocity(v) and/or reducing the interfacial tension (σ). Increasing fluid velocity and can cause fractures in the reservoir rock whereas increasing displacing fluid viscosity only led to an increase in capillary number of less than 100 times [42]. Increase in capillary number by a magnitude of greater than 1000 times can be done by reducing IFT through surfactant flooding [29]. Surfactant flooding works by injecting an aqueous surfactant solution whereby the hydrophilic head interacts with the water phase while the hydrophobic head interacts with the components in the crude oil phase. The surfactant molecules form a layer on the rock which lowers the IFT at the oil/brine interface. This leads

to a reduction in capillary forces trapping the residual oil, resulting in the formation of an oil bank and more effective displacement efficiencies.

2) Wettability alteration: The affinity of a rock surface in the presence of fluids such as brine or crude oil is known as wettability. This concept will be covered thoroughly in the next chapters. Rock wettability plays a major role in the flow regime of fluids in the reservoir. Reservoirs can generally be termed as oil-wet, water-wet and mixed-wet depending upon the state of wettability. The most commonly used methods to measure wettability are contact angle measurements, zeta potential and spontaneous imbibition experiments. In contact angle experiments, the angle between the oil/water interface is measured where a $\theta > 90$ is oil-wet while $\theta < 90$ is said to be water-wet. Wettability alteration from oil-wet to water-wet alters the capillary forces binding the oil at the pore space and allows increased relative permeability to oil. [29]
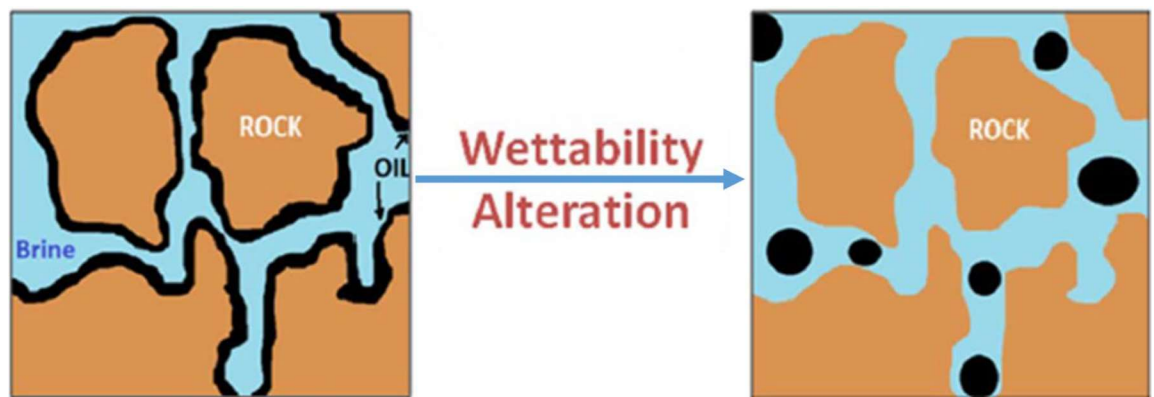
Figure 4: Wettability alteration [30]

Surfactants can be of different types based on the charge of the hydrophilic head group. Surfactants with negative charge on the hydrophilic head are called anionic surfactants and are generally used in sandstone reservoirs. Cationic surfactants are those whose hydrophilic head carries a positive charge. Non-ionic surfactants are those that do not ionize in an aqueous solution [29]. The hydrophilic head consists of non-dissociable groups such as esters, amide, phenols while the hydrophobic group consists of alkyl, alkylbenzene groups. Non-ionic surfactants are water soluble despite being non-dissociable due to their polarity that is brought about by the hydrogen bonds and Vander Waal's forces. Lastly, zwitterionic surfactants are those surfactants that have a both negative and positive charge on the hydrophilic head group, which behave as both a cationic and anionic surfactant upon dissociation.

The use of surfactants for EOR purposes is ultimately dependent on practical issues such as surfactant adsorption. Surfactant adsorption occurs at pore scale in the reservoir due to the interactions between oppositely charges surfactant and surface charge of the reservoir rock. Surfactant effectiveness is also depending on the electrolyte concentrations, the pH and fluid chemistries within the reservoir. Surfactant screening through laboratory experiments to determine the most ideal surfactant for a specific reservoir rock with a specific surface charge to be used in EOR applications.

1.2.3. Alkali flooding

Alkalis are said to be a basic, ionic salt of an alkali metal or an alkaline earth metal. Alkalis can also be defined as a base that dissolves in water. Alkali flooding is unique as it involves

in-situ generation of chemicals for EOR through saponification.[84]. Saponification is the reaction between a caustic alkali and an organic acid to form soap, represented by the chemical reaction in Equation 5.
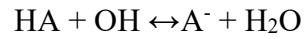
$$HA + OH \leftrightarrow A^- + H_2O$$ *Eq 5*
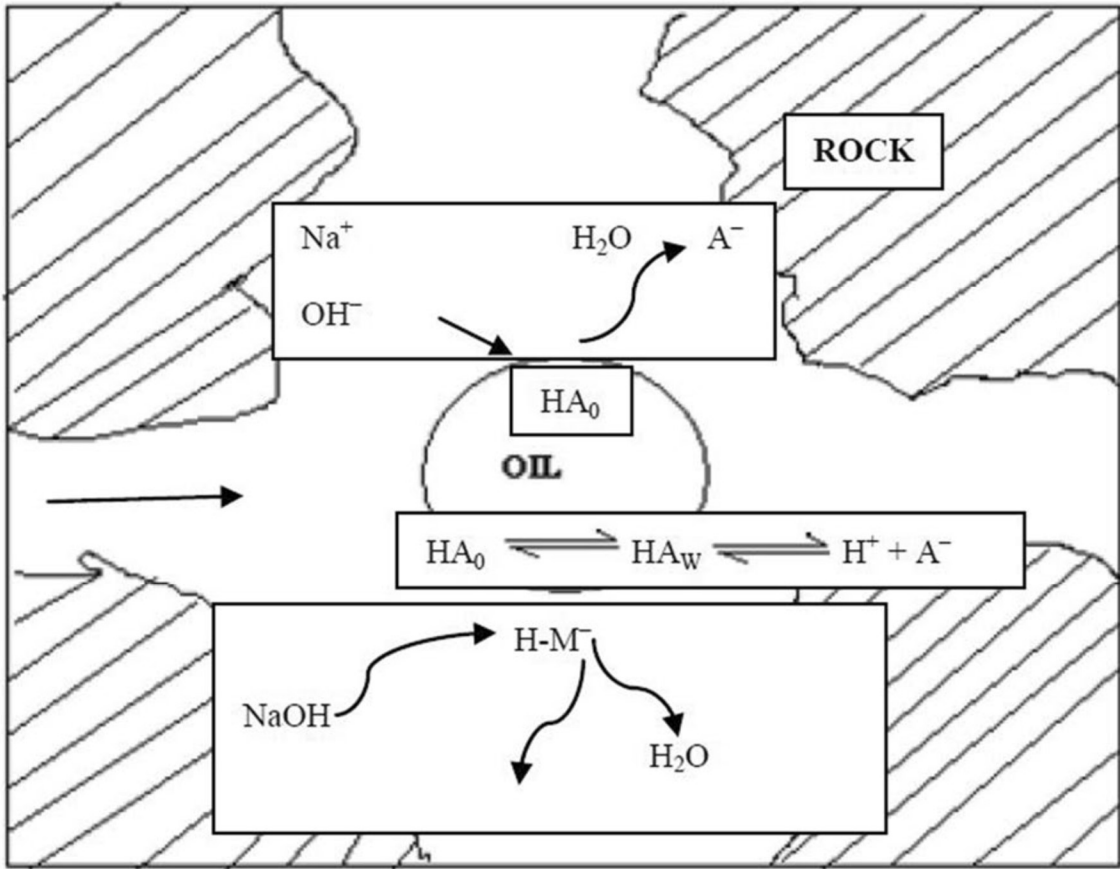
Figure 5: Schematic of alkali flooding [36]

The 'A' in the reaction stands for the alkali. Organic acids in crude oil such as carboxylic acids are the acidic component that react with the alkali to form an in-situ surfactant that

12

lowers IFT and improves oil recovery by emulsifying the oil. [85]. Similar to other chemical EOR processes, alkali flooding increases EOR by oil emulsification, oil swelling, IFT reduction and wettability alteration. The varying chemical characteristics of crude oil and reservoir rock under different conditions like pH, salinity and temperature which then exhibit different mechanisms in alkali flooding.

The most commonly screened alkalis are $NaBO_2$ (Sodium metaborate), Na_2CO_3(Sodium carbonate), NaOH (Sodium Hydroxide), and $NaHCO_3$ (Sodium bicarbonate). Sodium carbonate is optimal due to low-cost and transportability but its limitations are that it reacts with divalent ions (Ca^{2+}, Mg^{2+} etc.) to form precipitates. Similarly, sodium hydroxide reacts with sandstone rock at higher temperature leading to mineral loss. Sodium metaborate is suggested a replacement for sodium carbonate [88] as it has higher tolerance to divalent ions and will produce precipitates.

1.2.4. Foam Flooding

Foams are defined as a dispersion of a gas in a liquid, , with a continuous liquid phase and gas phase that is rendered discontinuous by the lamellae which is a thin film of liquid [29]. One mechanism by which foam flooding improves recovery in EOR is by viscosity increase, which leads to more stable flood front, better mobility ratios and improved oil recoveries. A second mechanism for improved oil recovery is when the bubbles in the foam expand in reservoir rock(porous media) , leading to selective in-situ diversion of injectant fluid from thief zones to lower permeability zones [90]. These characteristics of

foam flooding make it a more effective EOR solution that conventional methods like waterflooding, gas injection or WAG (Water-Alternating Gas) injection.

Foam flooding depends upon the constant regeneration of foam lamellae to propagate through porous media [29,93]. Surfactant and polymer-based foam flooding depend highly on the stability of the lamellae in porous media as they are prone to react to the minerals in the rock, brine and crude oil and adsorb onto the rock surface thereby destroying the lamellae, rendering low effectiveness of the foam flooding EOR process. [96].

2. SURFACTANT EOR IN UNCONVENTIONAL RESERVOIRS

The recovery of hydrocarbons from tight oil reservoirs such as shale is largely reliant on an extensive fracture connectivity of the reservoir from horizontal drilling and hydraulic fracturing. Tight oil reservoirs generally exhibit poor estimated ultimate recovery (EUR) of less than 10% of oil due to the low permeability [31]. A method to improve EUR would be to decrease fracture spacing while simultaneously increasing the injected fluid and proppant volumes in order to improve fluid connectivity to more parts of the reservoir. Reservoir heterogeneity in tight oil reservoirs leads to unsymmetrical fluid completions and fracture propagation from the wellbore.

Instead of relying heavily on the physical fracture distribution of the reservoir, EUR can be enhanced by injection of fluids by different EOR processes. For recovery from unconventional reservoirs, the most widely used injection fluids are gases such as CO_2 and N_2, and chemical EOR based processes such as surfactant injection. Surfactant injection can be performed as an additive to the fracturing fluid or injected as a huff-and-puff procedure as an EOR method. Initially, surfactants were researched as additives to the fracturing fluid to enhance flowback and improve matrix permeability in tight gas reservoirs.[32]. Surfactants were further studied for their role in achieving different ranges of IFT values with the injection fluid and the crude oil in the reservoir. Surfactants can improve matrix permeability by causing low oil-water IFT of around

10^{-2} to 10^{-3} mN/m, which is associated with the removal of water blockages due to 'matrix fracture interaction'[36, 37]. Ultralow IFT values of below 10^{-3} at the oil-water interface

15

can form in-situ emulsions and mobilize the water in the matrix adjacent to hydraulic fractures but is unable to create an environment for 'capillary desaturation' under the production conditions of tight oil reservoirs [34, 38]. This is a fundamental difference between surfactant screening for unconventional versus conventional reservoirs.[48]. Surfactants have also been researched and experimented for altering the wettability of the reservoir rock surface to water-wet, thereby improving the effectiveness of fracturing fluid imbibition. By altering the wettability to water-wet, this allows the injected fluid to displace oil present in really tight pore spaces while simultaneously helping in reducing the produced water disposal costs. Surfactant EOR is the process of injecting surfactants into naturally fractured reservoirs such as carbonate formations where the surfactant changes the wettability from oil-wet to water-wet causing spontaneous imbibition of the injected fluid. (Hirasaki and Zhang 2004). The main driving force behind spontaneous imbibition in surfactant EOR is the change in capillary pressure balance within the pore spaces, hence surfactants that result in ultralow IFT values are not preferred, unless high permeability allows for gravity drainage as the primary recovery mechanism. (Li. et al. 2017). Rocks minerals in tight oil reservoirs like shale are initially water-wet but change to oil-wet upon contact with crude oil components (Hirasaki and Zhang 2004). The negatively charged clay and quartz minerals are generally negatively-charged which adsorbs the organic bases and aromatics in crude oil (Alvarez and Schechter 2017, Liu et al 2019) while the calcite and dolomite which are typically positively charged attract the organic acids in the crude oil. (Hirasaki and Zhang 2004, Gupta and Mohanty 2011), while

the heavier components like asphaltenes are able to adsorb onto both negatively charged and positively charged minerals (Anderson 1986, Das et.al 2013). Most surfactants utilized in surfactant EOR in conventional reservoirs are also effective in altering the wettability in tight rock reservoirs such as shale. Anionics such as sulfates, catatonics such as quaternary ammonium surfactants, and nonionic surfactants such as ethoxylated alcohols. Oil recovery from carbonates is largely dependent on wettability alteration as an adequate capillary pressure gradient may not be achievable. In carbonate rocks, wettability alteration is achieved by two mechanisms depending upon the charge of the surfactant used. Anionic surfactants follow a *coating mechanism* where the surfactant molecules form a layer on the surface of the positively charged carbonate surface through hydrophobic interactions with the negatively charged crude oil components, while cationic surfactant molecules form ion-pairs with the negatively charged acidic oil crude oil components to desorb the oil off the surface, revealing the water-wet rock surface. This is known as the cleaning mechanism.Cationic surfactants have been shown to alter wettability greater than anionic surfactants due to this phenomena of desorption of oil via ion-pair formation. Studies have shown that rock with greater number of positively charged minerals like carbonates and dolomites exhibit greater adsorption rates and oil recoveries with cationic surfactants, which has similar charges (Alvarez and Schechter 2016, Alvarez at.al 2018a,2018b). Similarly, anionic surfactants tend to adsorb at a faster rate onto rock with higher number of negatively charged quartz and clay minerals. (Alvarez and Schechter 2017). The surfactant molecules adsorb onto the rock surface via

polar hydrophobic interactions and electrostatic interactions when the surfactant possesses a similar charge to the minerals on the rock surface.

Surfactants operate differently in conventional versus tight unconventional reservoirs based on the varying heterogeneities and difference of pore space size between them. Conventional reservoirs tend to cause surfactant loss as they have more unproductive pore spaces with no residual oil, which leads to poor relative permeability to oil (K_{or}) and greater relative water permeability (K_{ow}) causing surfactant solution to bypass the oil saturated zones of the reservoir. Unlike conventional, unconventional reservoirs have tight pore spaces into which the surfactant molecules diffuse and adsorb onto the surface altering the wettability to water-wet, resulting in favorable relative permeabilities and spontaneous imbibition of water to displace the oil. A characteristic of unconventional rocks such as carbonates are their large specific surface area values, which causes surfactant "loss" through adsorption, which may lead to hindered flow of injected surfactant molecules Experiments on Marcellus shale using different types of surfactants showed adsorption rates of 1-30mg/g. (Alvarez et al 2017,2018a,2018b). Adsorption rates of around 15mg/g were reported for nonionic surfactants on Marcellus shales. (zelenev at al 2011). (Alvarez at.al 2018a) calculated the surfactant adsorption on Marcellus shale, where cationic surfactants had between 25-30 mg/g adsorption rate while anionic surfactants were lower with 3 – 14 mg/g adsorption rates. (Alvarez et al 2017) experimented with Bakken rock with high quartz and clay content, with a anionic surfactant and reported values of around 6-8mg/g. (Zhang et al. 2016) reported adsorptions

rates of 11 – 33 mg/ g on Bakken sandstones with anionic and nonionic surfactants, with low adsorption rates of 0.5 mg/g with blended ethoxylated nonylphenol surfactants. In order to be an effective EOR process, it is suggested that the adsorption rate must be below 1mg/g (Zhong et al. 2019), but it is yet to be proven that increased surfactant adsorption rates leads to lower oil recovery values. The methodologies for screening surfactants for an EOR project generally begins with macroemulsion and microemulsion tests for the aqueous surfactant solution with crude oil, IFT measurements to ensure low IFT values for favorable capillary pressure generation, contact angle measurements to quantify wettability of the rock surfaces to characterize between water-wet and oil-wet states, and finally spontaneous imbibition experiments to show the potential for increased oil recovery in heterogenous tight rock.

Sandstone reservoirs generally exhibit water-wet to intermediate-wet properties, while carbonates generally exhibit intermediate-wet to oil-wet properties. This is due to the presence of carboxylic acids in the heavier components like resins and asphaltenes. These carboxylic acid molecules act as a bridge for polar interactions between the carbonate surface and the crude oil components, forming a stable layer on the rock surface. (Stadnes and Austad 2003). (Stadnes and Austad 2000) used cationic and anionic surfactants with chalk which showed greater wettability alteration from cationic surfactants, attributed to the ion-pair formation mechanism.

The potential for improved oil recovery in surfactants has been widely studied and documented through spontaneous imbibition experiments. Typical CEOR techniques such as polymer flooding is not effective in tight oil reservoirs as the viscosity increase of the injection fluid is only effective in larger pore spaces to maintain mobility. Alkali flooding is also rendered ineffective in high salinity conditions due to the presence of divalent ions. Surfactant solutions, especially those of non-ionic surfactants diffuse into the reservoir to alter wettability even in small pore spaces, which is also resistant to high degree of salinities. (Nguyen et al. 2014) performed experiments on eagle ford shale outcrop and Bakken core plugs with had high calcite and clay content. The results show improved oil recoveries of about 40 – 50 % of the OOIP using cationic and nonionic surfactants. The presence of high TDS affects the performance of surfactants due to unfavorable interactions with the ions in the brine causing unfavorable IFT generation. (Shuler et al. 2011) compared the performance of different types of nonionic and anionic surfactants with Bakken shale rock, recovering about 15 - 60 % of OOIP, but did not specify the type and molecular structures of the surfactants. The oil recovery was greater compared to traditional brine imbibition experiments. (Wang et al. 2015) performed imbibition experiments with Middle Bakken siltstone, reported increased oil recovery of about 45 – 60% compared to oil lower oil recoveries in the brine imbibition case which recovered 20-25% less OOIP compared to the surfactant solutions. Surfactant adsorption has been shown to been highly dependent on rock lithology, crude oil content, the pH of reservoir fluids, the chemical additives to the injected fluid and in-situ conditions of the reservoir.

2.1. Surfactant EOR and literature review

2.1.1. Wettability of ULR

Anderson 1986a defined wettability as the proclivity of a fluid to adhere or spread on solid surfaces in the presence of other immiscible fluids (Anderson 1986a). For a rock oil brine system, it may be considered as the measure of affinity of the rock surface for crude oil or brine. When the rock is water wet, the rock has a tendency for water to occupy smaller pore spaces and contacts a majority surface area of the rock, whereas when the rock is oil-wet, the rock has a higher affinity for oil instead of water and hence the crude oil occupies the small capillary spaces in the rock and is in contact with the majority of the rock. The interactions between rock, oil and brine affects the wettability of a rock/oil/brine system inside an unconventional reservoir. Neutral wettability is said to exist when the rock is neither oil-wet nor water-wet. According to research, it is proposed that all petroleum reservoirs were strongly water-wet at the time of initial formation, and develop oil-wettability after migration of oil. This is supported by the findings that clean sedimentary rocks are usually strongly water-wet, while sandstone reservoirs are deposited in aqueous environments facilitating an affinity for water before oil migration. (Anderson 1986a). Reservoir wettability can be classified into 3 types:

a) Fractional Wettability: Fractional wettability occurs when the crude oil components are strongly adsorbed onto only specific areas of the rock surface, rendering those areas oil-wet while the rest of the rock is water-wet. This may be due to the heterogeneity of the reservoirs leads to variations in properties in the

21

rock/oil/brine system such as surface chemistry as well as adsorption characteristics. This is also referred to as heterogenous wettability.

b) Mixed wettability: The type of fractional wettability where the oil-wet surfaces of the rock forms continuous paths to oil through the larger pore spaces. This occurs when there is a layer of oil-wet organic molecules from oil deposited on the surface of the rock but unable to spread over the water covered surfaces. Due to this phenomena, the crude oil components are unable to mobilize the water from the smaller pore spaces and they remain water-wet. Mixed wet reservoirs tend to allow a small but finite oil permeability to exist till low oil saturation levels.

c) Homogenous wettability: Homogenous wettability refers to the presence of a relatively uniform rock wettability to oil or aqueous phase.

Heterogenous wettability refers to reservoirs with different affinities for oil and aqueous phases in the same rock (Wang et al. 2011). Conventional reservoirs tend to exhibit homogenous wettability due to uniform mineral compositions and lack presence of organic matter in the rock matrix. Conversely, unconventional reservoir rocks such as shale exhibit heterogenous wettability due to the variations in rock mineralogy and the presence of organic matter along with the impact of the depositional environment.

2.1.2. Factors Affecting Rock Wettability

2.1.2.1. Polar Compounds in Oil

Buckley et.al [47] discussed the various mechanisms by which polar components present in the crude oil can modify the wettability of a mineral surface. The acidic and basic

components comprising of nitrogen, sulfur and oxygen present in the heavier oil fractions like asphaltenes and resins are polar in nature and have significant surface activity. The paper introduced multiple mechanisms by which crude oil crude oil alters the wettability of a rock surface to oil-wet.

1. Oil/Rock polar interactions (Absence of water): The surface-active polar components present in the crude oil which carry negative or positive charges interact with the oppositely charged polar components on the rock mineral surface. This leads to adsorption of the crude oil components onto the rock surface thereby altering the wettability of the rock.

2. Surface precipitation: Heavier components present in the crude oil tend to precipitate in the presence of a weak solvent. If the crude oil is a poor solvent, then the formation of asphaltene precipitate onto the rock surface may occur. This precipitation of heavier asphaltenes onto the rock leads to adsorption of oil molecules onto the surface.

3. Acid/Base interactions (Presence of water): Oil and water both become charged in the presence of water. This leads to the polar components in the crude oil to behave as an acid (giving up a proton to become negatively charged) or as a base (gaining proton and becoming positively charged). These acid/base interactions can alter the stability of the water film present between the crude oil and the rock mineral surface. The repulsion caused by like charges can lead to increased stability of the water film whereas opposite charged cause instability of the water film and

simultaneous breakdown. The adsorption of acidic and basic components of the crude oil onto the rock surface ultimately depend upon the rock mineral surface after the breakdown of the water film. Rock surface has varying surface charges due to the heterogeneity in the mineral composition of the rock. For example, silica surfaces tend to possess a negatively chare which provides a polar site for negatively charged nitrogen compounds to adsorb onto the rock surface.

4. Ion Binding: Divalent cations such as Ca^{2+} and Mg^{2+} can form two covalent bonds, and behave as a medium between the crude oil and rock surface minerals due to their ability to bond with the negatively charged components in both the crude oil and mineral surface.
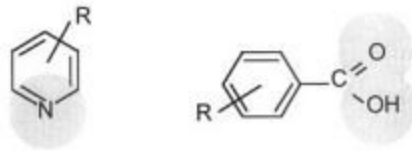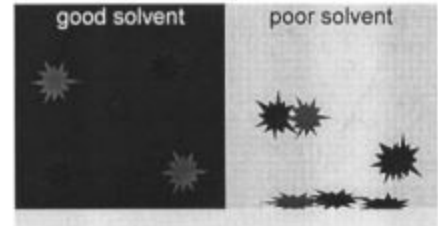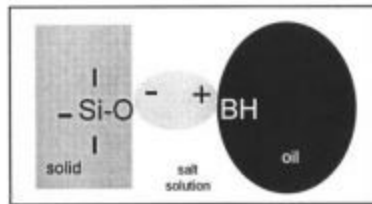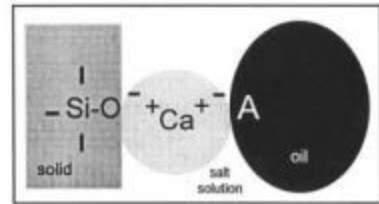
Figure 6: Mechanisms of wettability alteration by crude oil [47]

Acid/base interactions lead to either increased stability or decreased stability of the water film between the oil and the mineral surfaces, where if there exists like charges, the resulting repulsion will lead to stability of the water fil, whereas unlike charges will lead to breakdown of the water film. (Buckley, Liu and Monsterleet 1998)

Stadnes 2000 [60] mentions that it is very important to characterize the TAN (Total Acid Number) and TBN (Total Base number) of the oils, as the author mentions that the partitioning of cationic surfactants into the oil is related to the acid number of the crude oil. High values of TAN will cause high surfactant partitioning. The surfactants dissolve as 1:1 ion pair with the organic carboxylates, while similarly the desorbed carboxylates will form 1:1 ion pair complex with the surfactants that will dissolve in the oil phase or micelles. Thus, the surfactants dissolved in the oil phase as ion-pairs will probably not be active in the wettability alteration process. The oil wetting nature of carbonates increases as the acidic number of the crude oil increased (Stadnes et al. 2002[58])

2.1.2.2. Brine Salinity

The salinity and pH of the brine have been observed to affect the surface charge of a rock surface. Anderson 1986a [49] investigated the effect of pH on surface charge on silica and discovered that silica is positively charged at low pH and becomes negatively charged as the pH goes above 4, while carbonate rock was positively charged till 8 pH above which it developed a negative charge. Sandstone surfaces and carbonate surfaces interact differently with different types of ionic surfactants depending upon the charge of the brine

phase and its pH levels. At neutral pH levels, silica is negatively charged and attracts organic bases while carbonate rock has an affinity for organic acids as they are typically positive at neutral pH conditions.

Seethipalli et.al 2004 [51] investigated the effect of wettability alteration by anionic surfactants in the presence of sodium carbonate (Na_2CO_3). The results indicated that the addition of sodium bicarbonate salt suppressed the adsorption of surfactants as increase in carbonate can alter the zeta potential of the carbonate surface unfavorably. Aqueous phase studies were conducted which showed that Na_2CO_3 reacted with the naphthene molecule to form in-situ surfactants, similar to alkaline flooding EOR processes. The increase in concentration of these "in-situ" surfactants caused formation of micelles beyond the critical micelle concentration of the surfactant and caused the oil molecules to solubilize into the micelles present in the aqueous phase which caused the aqueous phase to turn darker with the formation of a microemulsion. The further increase in Na_2CO_3 decreased the solubility of the surfactant molecules and the oil molecules gradually partitioned back into the oil-phase. An optimal salinity level is said to exist for wettability alteration by surfactants where the presence of salts can be conducive to solubilization of oil into the aqueous phase by surfactant micelles while not lowering the solubility of the surfactant in the aqueous phase itself. IFT reduction is maximum at the optimal salinity after which the interfacial tension increases with the increase in salt content.

The brine found in carbonate reservoirs are typically basic with pH of about 7 to 8. Higher concentrations of Ca^{2+} exist relative to CO^{3-}, causing the rock-water interface to attain a

positive charge. The carboxylic acid components in the crude oil partly dissociate causing the oil/water interface to be negatively charged. The presence of opposite charges on either side of the oil/water/rock surface leads to instability and breakdown of the water film. Through this mechanism, crude oil leads to wettability alteration in the presence of a water film depending on the surface charges of the phases.

Karimi et al. 2015 [52] investigated the effects of multivalent ions Mg^{2+} and divalent ions in the presence of cationic surfactants DTAB and reported that the multivalent ions aided in the wettability alteration performance through the interaction with the carboxylic acid molecules on the oil-wet rock surface.

2.1.2.3. Effect of Temperature

Stadnes et al (2000) reported that the properties of oil and solubility of crude oil is different depending on the change in temperature. Stadnes et al (2002) reported that carbonate reservoirs become more water-wet as the temperature increases, while sandstone reservoirs tend to become less water-wet with increase in temperature. Zhang and Austad 2006 reported that in the presence of a fixed concentration of positive multivalent ions, the wettability alteration performance of SO^{2-} ions increased with increase in temperature. Das et al 2018 investigated the effects of temperature on the wettability alteration performance of nonionic surfactants with varying sizes of hydrophobic Ethylene Oxide (EO) tail group sizes and reported that the increase in temperature resulted in greater water wetness (lower contact angles). This may be explained by the decrease in solubility with increase in temperature as the strength of the hydrogen bonds weakens. At higher

temperatures, hydrophilic interactions decrease while the intensity of hydrophilic interactions increases. Gupta and Mohanty 2011 [53] investigated the effect positive effect of temperature on the wettability influencing potential of sulfate (SO_4^{2-}), calcium (Ca^{2+}) and Magnesium (Mg^{2+}) on oil-wet calcite. Oil viscosity decreases with the increase in temperature as their ability to desorb acidic molecules present in the crude oil increases. The increase in temperature may lead to increased surfactant adsorption like in nonionic surfactants while it may lead to lower surfactant adsorption due in ionic surfactants depending upon the surfactant concentration and surface activity. Zhang & Austad 2006 [54] reported similar results where the increase in temperature resulted in increase of SO_4^{2-} adsorption onto the oil-wet surface in the presence of calcium ions.

2.1.2.4. Potential Determining Ions (Multivalent Ions)

Multivalent ions such as Ca^{2+}, Mg^{2+}, SO_4^{2-} etc have the ability to lower the solubility of surfactants in aqueous phase, increasing the amount of surface activity of the surfactant at the interface, hence potentially increasing adsorption of surfactant onto the oil-wet rock surface for wettability alteration. Cations such as calcium and magnesium are able to facilitates the polar interactions between crude oil and rock and behave as a bridge between similarly charged crude oil and rock minerals [49].

Zhang and Austad [54] investigated the effect of investigated the effect of divalent ions such as SO_4^{2-} , Ca^{2+} and CO_3^{2-} on the wettability of oil-wet carbonate surfaces. It reported that the increase in the concentration of sulfate ions led to increase wettability alteration performance. Calcium ions were also a potential determining ion, but the sulfate ions

showed greater wettability alteration in the presence of other divalent ions such as calcium and magnesium. It is theorized that the increase in sulfate ion concentration leads to adsorption of SO_4^{2-} onto water-wet sites of the rock, while leads to less positive / more negatively charged rock surface which can result in desorption of negatively charged carboxylic acid molecules in the oil. Increased adsorption of sulfate ions with increase in temperature is said to occur due to lowered solubility of sulfate in water due to the weakening of hydrogen bonds between sulfate ions and water molecules. Similar studies [55] have also found that wettability alteration can be brought about by potential determining ions such as sulfate and calcium ions from oil-wet to water-wet at higher temperatures. Studies have shown that optimizing the salinity and the ion composition of injected brine fluid into a reservoir can significantly improve oil recovery. Yousef et al 2014 [56] provided studies with previous work showcasing the ability of potential determining ions like sulfate, calcium and magnesium and reported similar findings.

2.1.2.5. Surfactant concentration

The concentration of surfactant in an aqueous solution can affect the amount of surfactant that is surface active at an interface and hence affects the amount of adsorption onto a rock surface to alter wettability. The critical micelle concentration (CMC) of a surfactant is the concentration of a surfactant in an aqueous solution above which the surfactant monomers forming aggregates called "micelles". A typical micelle is an aggregate with the hydrophilic head of the surfactant molecules in contact with the surrounding. The CMC is considered an important factor for reduction of IFT and wettability alteration through

surfactant adsorption [59]. Austad et al. (1997) reported increasing surfactant adsorption on the chalk surface with increasing surfactant concentrations. Zhang et al (2010) [57] investigated the effects of cationic surfactants on a quartz surface and reported the effects of increasing surfactant concentration on adsorption characteristics. As surfactant concentrations increased, the monolayer adsorption layer developed into a bilayer adsorption layer. Below the CMC, the quartz surface became hydrophobic with increasing surfactant concentration with the hydrophilic head attached to the quartz surface. As the surfactant concentration approached CMC, surfactant adsorption bilayer was formed with the hydrophilic head oriented towards the aqueous phase rendering the surface more hydrophilic and decreasing contact angle.

2.1.2.6. Interfacial Tension

The interfacial tension of an oil/rock/brine system is a key parameter in the selection of surfactant systems for enhanced oil recovery. The role of surfactants is to alter the capillary pressure at the entries of the smaller pore spaces in the rock in order to promote spontaneous imbibition of the water phase into the pores to displace the residual oil. Surfactant molecules have the ability to attach to the rock surface in order to increase hydrophilicity of the rock surface and decrease the surface tension between oil and water. The adsorption of surfactant molecules onto the surface lowers the surface tension of the oil/water system thereby lowering entry capillary pressure, while spontaneous imbibition of water phase occurs due to the alteration of surface wettability of the rock surface to

water-wet conditions. Stadnes et al. 2002 investigated the effects of cationic ($C_{12}TAB$) and nonionic (EO tail group) on the interfacial tension of oil/surfactant aqueous phase and reported decreasing IFT values with increasing surfactant concentrations. The CMC of a surfactant impacts the IFT of an oil/water system. The CMC of a surfactant solution can be determined from the IFT characteristics of the surfactant. As surfactant concentration in a solution increased, the reduction of IFT occurs until a certain point at the CMC of the surfactant where the surfactant molecules start forming micellar aggregates. Above the CMC, surfactant molecules tend to move to the micelles in the aqueous phase than the oil/water interface for interfacial reduction. A plateau is observed in IFT after the CMC. [58, 59].

2.1.3. Wettability analysis measurements

Wettability is a surface phenomenon that occurs everywhere in our daily life between surfaces around us, due to their characteristic surface chemistries. Wettability plays a vital role in enhanced recovery processes in crude oil reservoirs. In conventional reservoirs, the process of oil drainage by altering the capillary pressure is also aided by gravity and viscous forces due to the large pore sizes in conventional rocks such as limestone or sandstone which have greater porosity and permeability paths. Unconventional reservoirs, on the other hand, consist of small pore spaces and limited permeability pathways in the reservoir due to the tight packing of the formation. As per the definition, wettability can be interpreted as the preference of a solid for a specific fluid.

2.1.3.1. Contact Angle

Contact angle is defined by the tangent to the water-oil interface at the point of intersection with the rock sample. The rock sample should be flat and smooth to avoid significant errors in the measurements. Other limitations in these measurements are contact angle hysteresis due to surface heterogeneity, and failure to represent the wettability of whole system. The contact angle hysteresis is the difference between the advancing contact angle and the receding contact angle measurements, which might be caused by surface roughness, surface heterogeneity, and surface immobility.
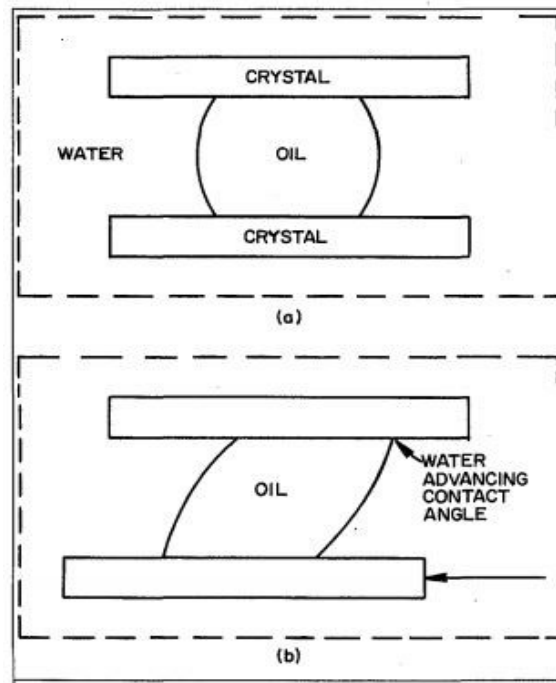
Figure 7: Contact angle hysteresis [50]

Sessile drop, captive bubble, tilting plate, and capillary rise, among others, are some of the methods used to measure contact angles. Contact angle is most commonly measured

by captive bubble method. At equilibrium, the forces are balanced and the liquid will not continue wetting the surface and it will stay as a drop with a specific contact angle over the surface. This is expressed by the Young's Equation:

$$\sigma_{os} = cos\theta\ \sigma_{ow} + \sigma_{sw}$$

<div align="right">*Eq 6*</div>

Tangential forces of oil-solid (σ_{os}) interface are equal and contrary to the sum of the forces of solid-water (σ_{sw}) and oil water (σ_{ow}).
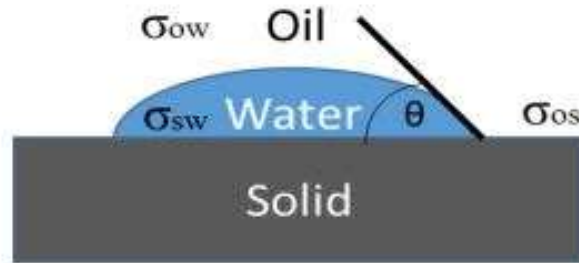
Figure 8: Contact angle

Contact angles can explain different situation like for example, when the angle is $\theta=0°$, water will uniformly wet the surface. Then, when the angle increases, a droplet is formed and water will wet the surface at a specific angle. Finally, when the angle is $\theta=180°$, water will not wet the surface. Although the relationship between the phases can be well explained by the Young equation, surface tension is a property that fails to describe the microscopic forces that involve wettability. Hirasaki (1991) describes these microscopic forces as electrostatic, Van der Waals and structural forces. Electrostatic forces depend on

the type of minerals, and fluid properties such as pH, salinity and composition. Van der Waals and electrostatic forces are related to the disjoining pressure which is the force that acts to separate the two interfaces and it is the result of ionic and molecular interactions in the crude-oil/brine/rock system.
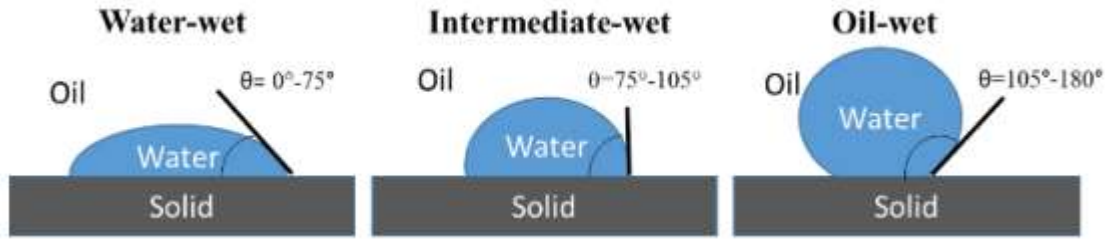
Figure 9: Contact angle measurement

2.1.3.2. Amott-Harvey Method

The Ammott Harvey index is a method to quantify the wettability of a core of rock by measuring the amount of wetting fluid that is imbided into the rock and simultaneously the amount of fluid that is able to displace a non-wetting fluid from the rock matrix. Hey the armored Harvey method is a combination of spontaneous imbibition as well as forced displacement of a non-wetting fluid to measure the wettability of a core. Viscosity and initial saturation can be adjusted using the ratio of spontaneous imbibition to force imbibition. Initial water saturation is calculated by flooding or centrifuging the samples with water and then oil. Then, four steps are archived as follows

S_{wf} is the water saturation after forced imbibition of aqueous phase and S_{of} is oil saturation after oil imbibition of oil phase. Once the saturations are measured, the Amott-Harvey index is calculated by the following equations:

$$I_w = \frac{(S_{ws}-S_{iw})}{(S_{wf}-S_{iw})} \qquad\qquad ....Eq\ 7$$

$$I_o = (S_{os} - S_{or})/(S_{of} - S_{or}) \qquad\qquad ....Eq\ 8$$

$$I_{A-H} = I_w - I_o \qquad\qquad ....Eq\ 9$$

For strongly water-wet systems, I_{A-H} is 1 and for strongly oil-wet systems I_{A-H} is -1. A water-wet system is between 0.3 and 1, and oil-wet between -1 and -0.3

The main disadvantage of this method is the inability of measuring intermediate-wet states. Also, the initial saturation of the rock is a main factor to measure wettability. (Anderson 1986b)

2.1.3.3. USBM Method

The USBM approach is comparable to the Amott-Harvey method, with the added benefit of accounting for intermediate-wet conditions. This method, like the Amott-Harvey index method, calculates the average wettability of a core and compares the work (W) required to centrifugate the non-wetting fluid. For the area under capillary pressure curves, the work is computed using Eq. 6. The amott Harvey approach is analogous to the USB M method.

$$W = log(A1/A2) \qquad\qquad \textbf{\textit{Eq 10}}$$

The area under the capillary pressure curve is denoted by A1 and A2. When W is larger than zero, the core is water-wet, oil-wet when W is less than zero, and intermediate-wet when W is near to zero. The gap in area under capillary curves is related to the ease with which water may absorb into a water-wet surface, and the difficulty with which oil can be displaced on the same surface.

Zeta Potential

The use of zeta potential measurements in ULR can be used to address variations in wettability in the material. A thin water film is formed on the surface of a shale rock, and the stability of the film is measured in order to evaluate the rock's affinity for water. At the interface between rock and fluid, the zeta potential is the electrical potential across a double layer, and its magnitude is related to the surface charges at the contact. In the presence of an increase in electrical potential on the double layer, stable liquid films may be observed, which shows that there is a repulsion that changes rock wettability from water-wet to water-dry by detaching the oil from the surface of the rock. Unstable thin water films can be viewed as exhibiting intermediate and even oil-wet characteristics. The thickness and stability of the water layer between the rock surface and the oil are determined by the charges applied to the oil, water, and rock surface. Hirasaki (1991)

The zeta-potential of the rock-water interface and the charge of the oil-water interface determine the stability of the water film between the rock and the oil, which is commonly

addressed in terms of disjoining pressure. This is determined by the pH and potential-determining ions, CA^{2+} and $(CO_3)^{2-}$, which are both present in the carbonate structure and are responsible for the zeta potential of the carbonate-water interface. Specifically, the zeta potential quantifies the difference in electrical charge between the dense layer of ions around the particle and the charge of the bulk of the suspended fluid surrounding the particles in a colloidal solution. (2006) (Zhang and Austad 2006) (Zhang and Austad 2006)

2.1.4. Wettability alteration mechanisms

The wettability of oil-wet or intermediate-wet reservoirs can be altered by addition of surfactants to shift rock wettability to water-wet. Surfactants are amphiphilic compounds that have both a hydrophobic and a hydrophilic group. Based on their head group, surfactants are most commonly classified in cationic (positive charge), anionic (negative charge), nonionic (no charge) and zwitterionic or amphoteric (positive and negative charge).

2.1.4.1. Cationic Surfactants

(Stadnes 2000b) and (Stadnes 2000a) detailed the mechanism by which cationic surfactants interacted with negatively charged rock surfaces (in this case, chalk). It is called the *"**Ion-Pair Formation mechanism**"*. The surfactants monomers and micelles exist in equilibrium in this scenario, and the cationic monomers interact with the adsorbed negatively charged anionic materials on the rock surface (such as carboxylic acids), to create an "ion-pair" resulting from electrostatic interactions. This causes the desorption of these anionic components, making the surface more water wet. Some of the desorbed

material will also dissolve into the micelles. This combined mechanism of ion-pair formation and micellar dissolution leads to the rock surface becoming more water-wet. As a result, capillary forces now dominate the imbibition process and water will pour into the pour to imbibe onto the water-wet rock.

In addition to electrostatic interactions, the hydrophobic interactions also play a great role in changing the wettability. If the hydrophobic part of the cationic surfactant is more hydrophobic, it will easier for the surfactant to come into contact with the adsorbed carboxylic acids (negatively charged) and hence lead to faster desorption.

Thus, the main factors affecting wettability alteration by surfactants (in this case, cationic surfactants) is:

1) The formation of ion-pairs leading to the desorption of the negatively charged carboxylic acids

2) The hydrophobicity of the surfactant

3) Imbibition of water onto the rock by capillary forces
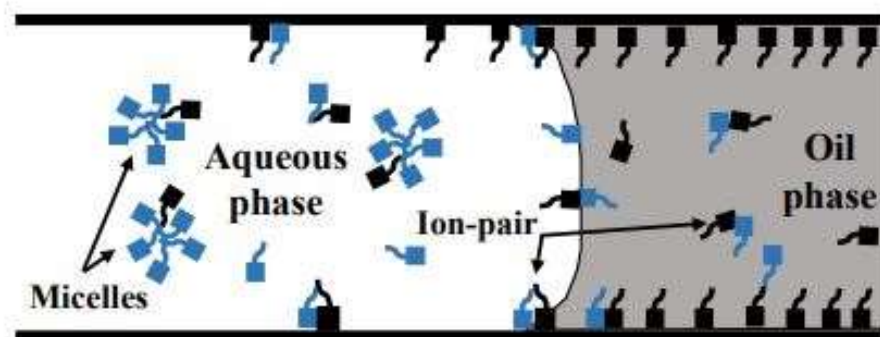
Figure 10: Ion-Pair formation mechanism

2.1.4.2. Anionic Surfactants

Austad (1997) and Stadnes (2000) proposed the mechanism of ***"surfactant adsorption"***, instead of ion-pair formation mechanism. In this paper, anionic surfactants were used to alter the wettability of a chalk surface that was also slightly negatively charged, hence ion-pair formation due to electrostatic interactions was not possible.

The anionic surfactants, containing EO-groups (ethylene oxide groups) in the hydrophilic head, alter the wettability by forming a bi-layer. The hydrophobic tail of the surfactant attaches itself to the hydrophobic surface of the rock, and the hydrophilic part containing the EO-groups will cause the contact angle to decrease below 90°, forming a small water-zone between the organic coated surface and the oil. This creates weak capillary forces during the imbibition process which can alter the wettability to weakly water-wet and promote water imbibition. It is observed that the imbibition of the surfactant increases with increasing number of EO-groups.

This formation of a surfactant double layer cannot be considered as a permanent wettability alteration mechanism as the hydrophobic bonds between the hydrophobic tail and hydrophobic surface are weak, and the wettability alteration is very likely to be completely reversible due to this.
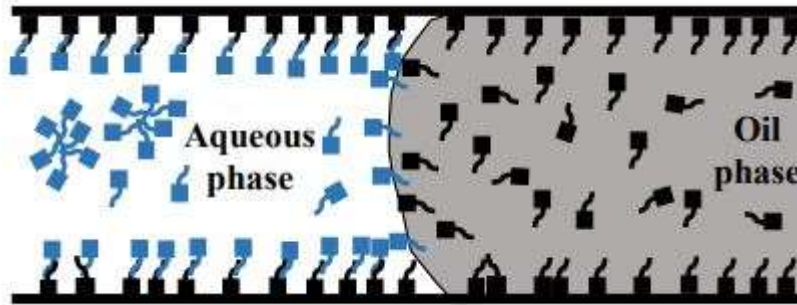
Figure 11: Surfactant adsorption mechanism

Seethipalli (2004) investigated the behavior of anionic surfactant adsorption on carbonate surface in the presence of Na_2CO_3. Surfactant adsorption was seen to increased non-linearly for the anionic surfactants as the concentrations increased. The surfactant adsorption decreased significantly in the presence of Na_2CO_3. The presence of Na_2CO_3 raised the pH of the surfactant brine solution to greater than the zero charge point for calcite (which should be noted is around 8.2), thus this causes the calcite surface to acquire negative charges and repel the like-charged anionic surfactant, and thus suppress it's adsorption.

(Stadnes 2002) conducted experiments on a carbonate surface with a cationic surfactant. The C12TAB (cationic surfactant) alters the wettability from oil-wet to strongly water-wet by actively desorbing the carboxylic compounds from the carbonate surface (carboxylates are the most strongly adsorbed surface-active material).

2.1.4.3. Nonionic Surfactants

(Das 2018) mentioned the mechanism by which non-ionic surfactants interacted with mineral surfaces to cause wettability alteration, called *"coating and sweeping"*

mechanism. Initially, the hydrophobic tails of the surfactants adsorb onto the mineral surface. This causes a temporary hydrophilic surface due to which the surfactants molecules interact with the water molecules near the surface. The hydrophilic components reduce the water-calcite surface energy, which results in water, aided by surfactant molecules, sweep the oil away, exposing the solid mineral surface. Initially, the interactions are more hydrophobic-interaction dominated, due to the interactions between the oil-wet surface and the hydrophobic chains. As the oil is swept away, more of the substrate gets exposed to water and the hydrophilic interactions with calcite and water molecules increase and start dominating. It was concluded that the final contact angle did not depend as much on the hydrophobic group, rather it depended on the hydrophilicity of the surfactant. As the number of EO groups increased, the hydrophilicity of the surfactant increased, thus decreasing the hydrophobic interactions of the surfactant-surface, and hence the surfactant was not as effective at wettability alteration and the final contact angle was higher. This is due to the better hydration by the water molecules, thus rendering lesser surfactant molecules available for adsorption. This applies comfortably to surfactants with small hydrophilic groups, as they are less hydrophilic. But surfactants with larger hydrophilic groups causes hydrophilic repulsions between the polar head groups due to accumulation of hydrophilic heads near the surface. In the case of bulkier hydrophile groups, the final wettability state is then determined by the effective surfactant-water-surface interactions instead of being monotonically dependent on the hydrophilicity.
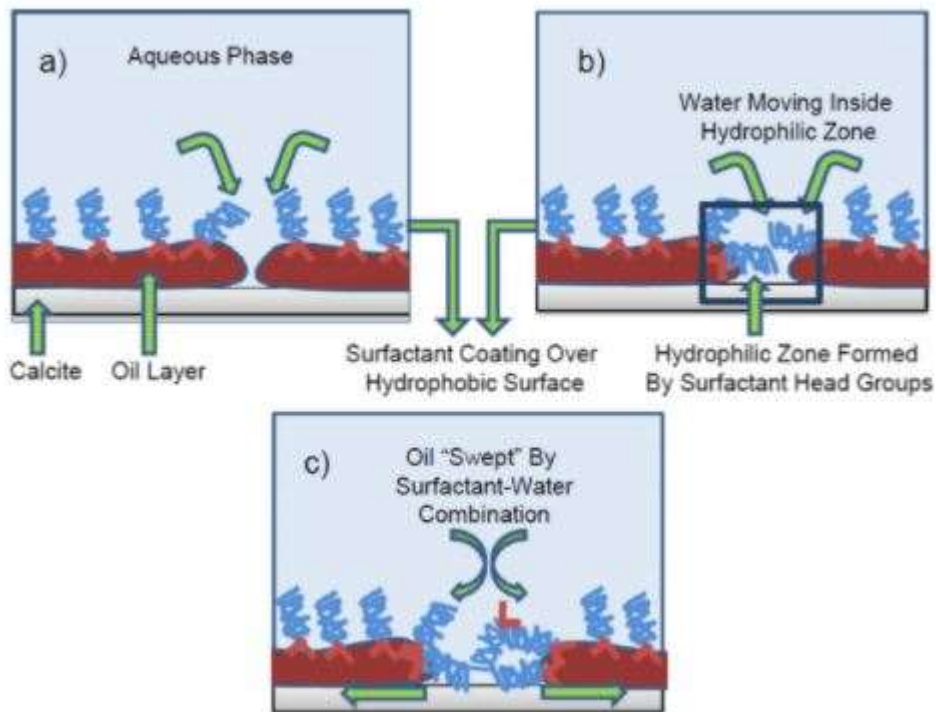
Figure 12: Mechanism of coating and sweeping

(Stadnes 2002) conducted experiments on a carbonate surface with a nonionic surfactant (Ethoxylated Alcohol). The brine used on the experiments had a total TDS of 9%. The nonionic surfactant altered the wettability to slightly water-wet by forming a bilayer

2.2. Dynamic surface tension of surfactants

Surfactant EOR is dependent on the effectiveness of surfactants to alter the oil/brine IFT values inside the reservoir in order to generate capillary desaturation of oil. Interfacial processes such as wettability alteration are highly dynamic and equilibrium conditions are rarely achieved.

The dynamic surface tension of any aqueous solution is representative of the phenomena that govern the interfacial characteristics of surfactant molecules and its interaction at the interfacial surfaces such as brine and rock. In dynamic surface tension analysis, the surface tension of a newly formed surface is equal to that of the pure liquid. The surface tension decreases as the surface age increases due to the increased adsorption of surfactant at the air/liquid interface. The DST of surfactant solutions is dependent on the charge, length and size of the polar hydrophilic head of the surfactant molecule, as well as salts and additives present in the solution.

2.2.1. Maximum Bubble Pressure Method (MBPM)

The maximum bubble pressure method (MBPM) is a useful technique to characterize the dynamic surface tension properties of surfactant solutions and the adsorption kinetics at the surface. Surfactant adsorption is typically a fast process with surface adsorption occurring quickly when it is above the critical micelle concentration (CMC). The maximum bubble pressure apparatus involves a gas-feeding system along with a bubble rate measuring system and a pressure measuring system. The gas-feed mechanism comprises of a pressure regulator, capillary, and a flow control meter for purifying the gas. The pressure variation can be measured using an in-built pressure transducer.

The capillary is immersed into a solution like aqueous surfactant solutions at a depth h below the liquid surface. Then the gas pressure P is related to the radius of the gas/liquid interface at the bubble formed by the Laplace equation (Equation 6)

$$P_{max} = P - P_0 = 2\frac{\gamma}{R} + \rho g h \qquad \textbf{\textit{Eq 11}}$$

When the bubble radius reaches the radius of the capillary then the pressure P reaches a maximum of P_{max}. P_0 is the atmospheric pressure, γ is the surface tension, ρ is the density of the solution, g being the constant from acceleration due to gravity and R is the radius of the capillary tip. Due to the variations in the operational conditions and the capillary radii, the equipment must be calibrated accordingly. Calibration for equipment must be performed against a known surfactant solution, like deionized water whose surface tension is 72 mN/m at room temperature conditions.

The maximum bubble pressure method has been shown to be effective for the accurate measurement of dynamic surface tension of surfactant solutions with good reproducibility. It is effective for measuring surface tension of non-ionic and ionic surfactants at high concentrations as well as low concentrations below the CMC, different organic solutions and liquids.

2.2.1.1. DST Curves
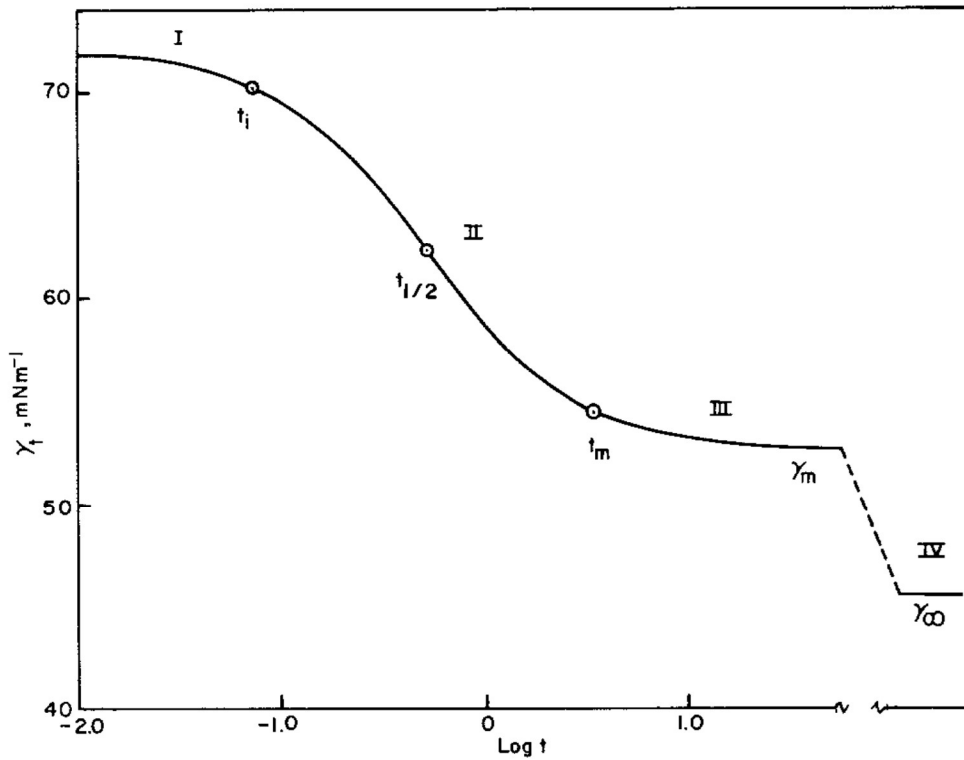
Figure 13: Dynamic Surface tension versus log t(time) Region I: Induction; Region II: rapid fall; Region III: meso-equilibrium; Region IV: equilibrium [40]

The dynamic surface tension of the surfactant solutions changes with time in a pattern that is typically represented by the generalized curves shown in Figure 13 [40]. The regions I, II, III and IV are defined as the

$$\gamma_t - \gamma_m = \frac{\gamma_0 - \gamma_m}{1 + \left(\frac{t}{t^*}\right)^n} \qquad\qquad Eq\ 12$$

45

induction, rapid fall, meso-equilibrium and equilibrium regions respectively. Regions I, II and III are of importance in fast dynamic processes involved in surfactant chemistry. t_i is defined as the final time at end of the induction region and t_m is defined as the time when the curves develop to the meso-equilibrium region. The time for the surface pressure to reach half of its value at meso-equilibrium is termed as $t_{1/2}$. The relationship between these variables is defined by the equation 7, where γ_m is defined as the meso-equilibrium surface tension and t^* is a constant with similar units as t, while n is a dimensionless constant. The surface pressure $\prod$ is the difference between the surface tension of a pure solvent γ_0 and γ_t, which is the surface tension values at time t.

Equation 7 can be represented in the form of equation 8.

$$\frac{\gamma_0 - \gamma_t}{\gamma_t - \gamma_m} = \left(\frac{t}{t^*}\right)^n \qquad\qquad\qquad \textbf{\textit{Eq 13}}$$

The left side of equation 8, $\frac{\gamma_0 - \gamma_t}{\gamma_t - \gamma_m}$ is the ratio of the depression of the surface tension at t, where the depression of surface tension is the surface pressure at meso equilibrium $\prod_m$ and the surface pressure at time t is $\prod_t$. According to the literature, the region I ends when the ratio reaches 1/10 and the Region II ends when the ratio reaches 10. The ratio is 1 when it is at the midpoint between γ_m and γ_0.

2.2.2. Measurement inaccuracies with bubble pressure method

The bubble pressure method can be accurately implemented to measure the dynamic surface tension of surfactant solutions, but there exist several issues with the measurement

techniques. The main issues are related to the measurement of bubble formation frequency, bubble pressure and estimation of surface lifetime and effective surface age [42]. The inaccuracies regarding measurement of bubble pressure can be mitigated through usage of relatively large volume of solutions in comparison with the volume of the bubble formed at the capillary. Small volumes of solution have been reported to increase the error in surface tension measurements.

2.2.3. Dynamic surface tension (DST) kinetics

The equilibrium dynamic and statis behavior of surface tension properties of surfactants are reported to be diffusion-limited and dependent on the surfactant monomer concentrations. The surface adsorption can be characterized by measuring the surface excess concentration of the surfactant below the CMC is given by the Gibbs Adsorption Isotherm (Equation 9)

$$\Gamma = \frac{1}{nRT} \left(\frac{\partial \gamma}{\partial \ln C} \right)_{T,p} \qquad\qquad Eq\ 14$$

Where the Γ is the surface excess concentration, n is the degree of dissociation depending upon this dissociation constant of the surfactant, γ is the equilibrium surface tension of the solution, C is the concentration of the surfactant.

Ward and Todai [44] proposed that for a diffusion-controlled surfactant adsorption, the characteristic time would proportional to the $1/c^2$ in Equation 10.

A characteristic time (τ) is defined for the dynamic surface tension curves obtained in order to quantify the adsorption kinetics during dynamic surface tension analysis. It is defined as the time required to reach half of the drop of the surface tension (Equation 10)

$$\tau = \frac{\pi}{D}\left(\frac{\Gamma}{4c}\right)^2 \qquad\qquad \textit{Eq 15}$$

Which can then be put into the form of Equation 11

$$\log\tau = = \frac{-2\log\pi}{D}\left(\frac{4c}{\Gamma}\right) \qquad\qquad \textit{Eq 16}$$

Where D is the diffusion coefficient of the surfactant which can be derived from the Stokes-Einstein equation [45]. The surface excess concentration is indicative of the number of surfactant monomers adsorbing at the air/water interface during surface tension measurements. τ initially decreases rapidly with the increase in surfactant concentration below CMC, in a manner that is proportional to $1/c^2$, which indicates that the process is diffusion controlled. This has been validated by numerous studies on surfactant CMC measurements using interfacial tension method [43]. The change in τ rapidly decreases and is negligible once CMC is crosses as monomer concentration of the surfactant does not change with increasing bulk surfactant concentrations. Qazi et al. [43] suggested that the formation of micelles above the CMC does not affect the surfactant adsorption significantly as there is no change in surfactant monomer concentration upon micellization.

2.2.4. Surfactant concentration measurements by DST

Dynamic surface tension measurements have the potential to estimate the surfactant concentration in an unknown fluid. Rane et. al 2014(61) introduced a methodology for measuring the concentration of surfactant in produced water samples using dynamic surface tension measurements. The methodology proposed was for low concentrations of 100 ppm (0.01 wt.%) to 1000ppm (0.1 wt. % gr/L) of an unknown surfactant.
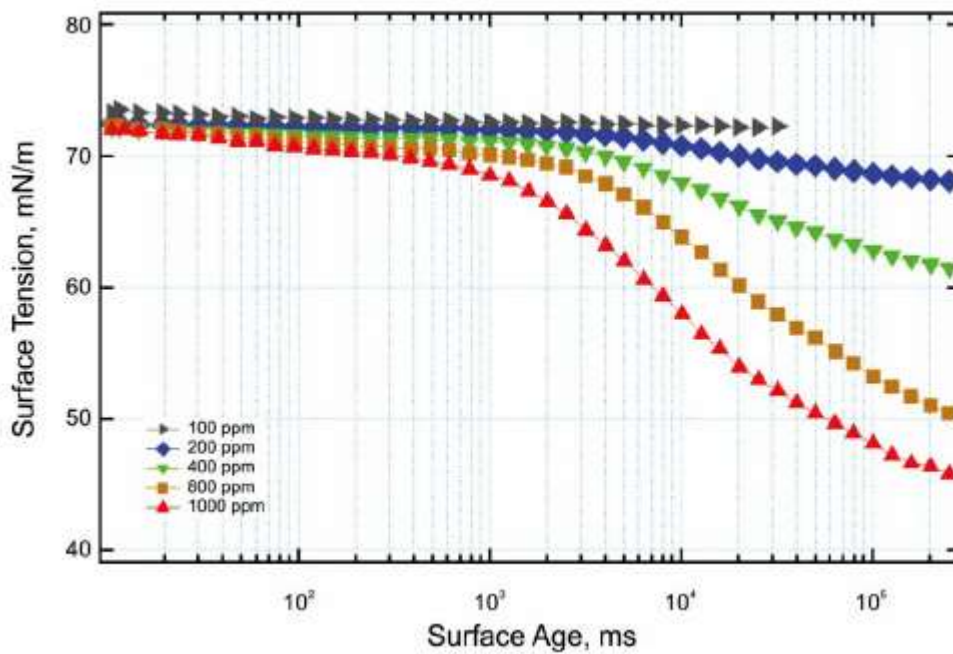

Figure 14: Surfactant calibration curves in DI [61]

Figure 15 shows an example of DST calibration curves for a surfactant in DI water, as presented in the paper by Rane et. al. 2014 [61]. At short bubble times, the adsorption can be defined by the Ward-Todai equation for short times. (Equation 17)

49

$$\gamma_{t \to 0} = \gamma_0 - 4RTC \left\{ \frac{Dt}{\pi} \right\}^{1/2} \qquad \textbf{\textit{Eq 17}}$$

According to the study, the slopes for the DST curves when plotted against the square root of time follow a linear pattern. When the slopes are plotted against the respective concentrations, a linear trend is observed. This generates a trend line as shown in Figure 16.
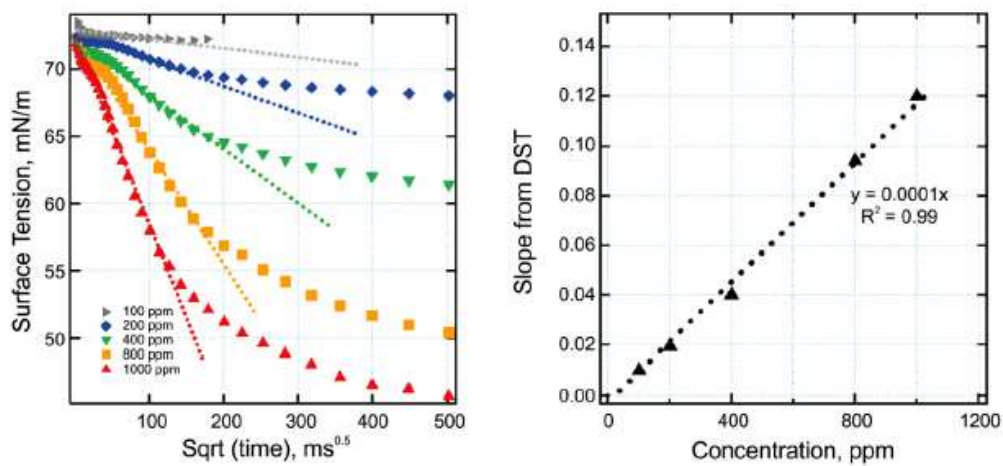

Figure 15: A) Slope trendlines for DST Curves B) Slopes vs Concentrations [61]

Applying this methodology, it is theoretically possible to measure the surfactant concentration of an unknown fluid by finding the X-intercept for the slope of the DST curve of an unknown fluid.

Figure 17 shows the comparison between the prediction of surfactant concentrations between UV-Vis and dynamic surface tension measurement. The results show high accuracy for estimating the surfactant concentrations in aqueous surfactant solutions.
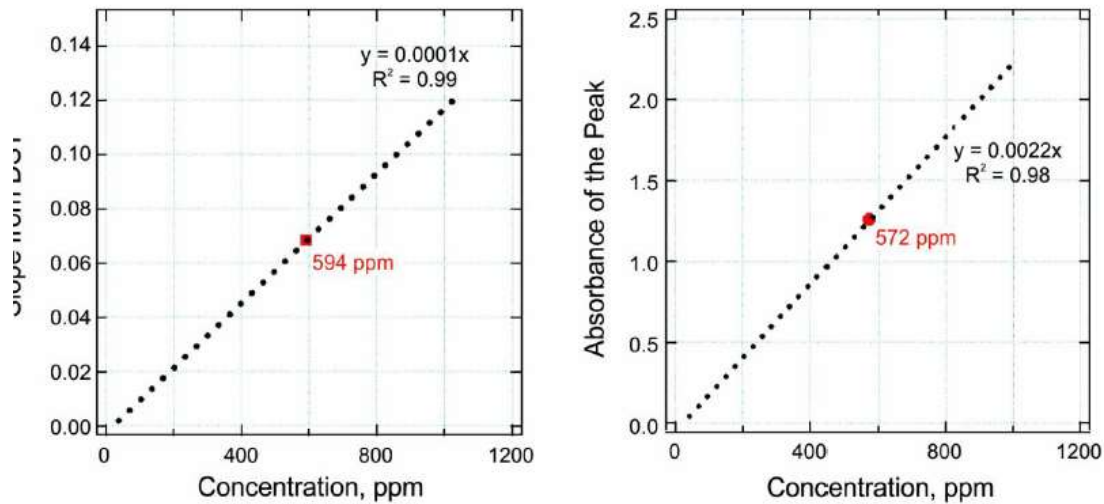
Figure 16: Evaluation of surfactant concentration: UV-Vis versus DST Measurement [61]

The implementation of this methodology is observed in this study. A different quantitative methodology is proposed for higher concentrations, and for surfactants whose trends deviates from the short-time diffusion-controlled Ward-Todai equation. A method of estimating surfactant concentrations for highly deviant DST curves by using an optimal bubble surface age selection is developed in this study and applied to quantify surfactant concentration change for adsorption experiments and measure the residual surfactant returned in produced fluid for a surfactant EOR project.

2.2.5. Effects of temperature on DST

Fainerman et al. 1994 [42] measured the dynamic surface tension of anionic surfactants sodium hexadecyl sulphate and sodium tetradecyl sulphate and nonionic surfactant Triton-100 were evaluated at different temperatures which showed that the temperature affects the dynamic surface tension of surfactants, with equilibrium surface tension decreasing as

51

the temperature was increased. Hue et al 1987 [41] investigated the effect of temperature on a solution of sodium 2-ethylhexyl sulfosuccinate and also reported similar findings, where the temperature was varied from 10 deg. C to 45 deg.C.

2.2.6. Effects of salinity on DST

The presence of salts can significantly affect the equilibrium behavior of surfactant by altering the CMC, the equilibrium surface tension (γ_{eq}), and micellar aggregation number and Kraft temperature [43]. Studies have been performed previously investigating the effect of salts on the dynamic surface tension of surfactants. Qazi et al. 2020 [43] investigated the effect of increasing NaCl concentrations on dynamic surface tension of ionic (CTAB) and nonionic (Tween 80). The increases in salt concentrations resulted in shift of CMC to lower concentrations for ionic surfactants until a certain concentration with decrease in equilibrium surface tension as well. The CMC and surface tension of nonionic Tween-80 was not affected by salt, but this is attributed to its low CMC concentration resulting in low surfactant monomer concentrations. This can be attributed to the electrostatic interactions with the cationic surfactant and salt anions which is conducive to micelle formation. Low surface excess concentration calculations have been reported [43] for ionic surfactants with addition of salt which has been hypothesized to be due to ion-pair formation between salt anions and cationic surfactants, neutralizing the surface charge.

2.2.7. Effects of surfactant concentration on DST

Experiments have shown that the increase in surfactant concentration leads to lower equilibrium surface tension values. The equilibrium surface tension decreases linearly with increasing surfactant concentrations, although this may be affected by dissolved solids [43]. Hua et al [46] conducted experiments with nonionic surfactant and reported decreasing surface tension values for increasing surfactant concentrations. Increase in surface excess concentrations and decrease in equilibrium surface tension (γ_{eq}) were reported based on molecular structure of the surfactants where increase in hydrophobicity through increasing ionic strength of ionic surfactant solutions, decreasing EO groups in nonionic surfactants or increase alkyl chain. [46]

3. EXPERIMENTAL METHODOLOGY AND MATERIALS

3.1. Oil Properties

The crude oil used in this study are 2 crude oils from 2 nearby wells in the Eagle Ford basin, EF1 and EF2. The crude oil EF1 is produced from the well that is being documented in this study. A SARA analysis was performed to measure the composition of saturates, aromatics, resins and asphaltenes in the crude oils. The composition of the crude oil EF1 was 27% saturates, 53% aromatics, 16% resins and 4% asphaltenes. The composition of crude oil EF2 was similar with 34% saturates, 49% aromatics, 15% resins and 2% asphaltenes. The oil has a large number of intermediate weight components such as aromatics. The densities of the crude oil EF1 was 0.9038 g/cm^3, 0.8659 g/cm^3 and 0.8549 gm/cm^3 at 70 °F, 170 °F and 200 °F temperatures respectively. The density of the crude oil EF2 was 0.9064 gm/cm^3, 0.8686 gm/cm^3 and 0.8572 g/cm^3 at 70°F, 170°F and 200 °F respectively. The API gravities of the oil were similar with EF1 and EF1 having densities of 24.25 API and 23.97 API respectively.
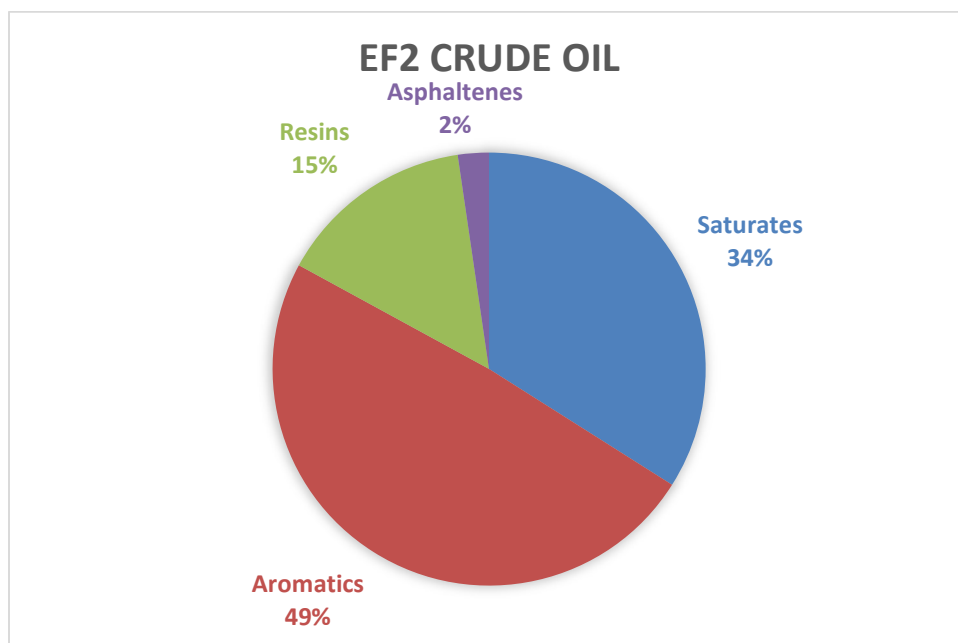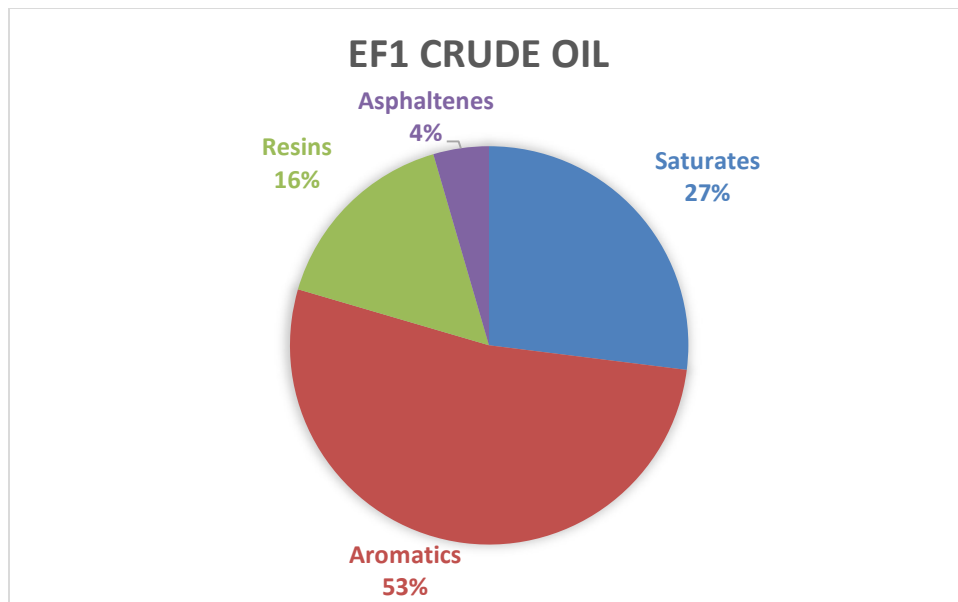
EF1 CRUDE OIL

Asphaltenes
4%

Resins
16%

Saturates
27%

Aromatics
53%

EF2 CRUDE OIL

Asphaltenes
2%

Resins
15%

Saturates
34%

Aromatics
49%

Figure 17: SARA Analysis of crude oil A) EF1 B) EF2

3.2. Rock Properties

The rock composition was measured using X-Ray Diffraction (XRD) analysis. The rock samples were initially crushed with a mortar and pestle and then grounded to particles of 40 microns using a micronizing mill. The powder is then packed into samples containers and processed on a Rigaku MiniFlex 600 X-Ray Diffractometer. The X-Ray tube was operated at 40 kV and 15 mA. The scans were analyzed using "Whole Pattern Profile Fitting" with refinement based on ICDD/NIST/FIZ databases.

The rocks used for this study are chosen to evaluate the performance of wettability alteration by surfactants in the unconventional shale rock in the Eagleford Basin. The rock types used are 2 different samples from shale cores drilled from the same well at different depths. The compositions of Eagle Ford (EF) shale samples 1 and 2 are described in Figure 19 and 20. Eagle ford shale sample 1 has a composition of calcite, quartz, illite, dolomite and other small minerals (Figure 19). The most abundant mineral is calcite at 67% followed quartz and illite at approximately 12% and 9% respectively. The Eagle Ford shale sample 2 has a similar composition with higher calcite content at 76% followed by Quartz and Illite at 6% and 14% respectively. (Figure 20)
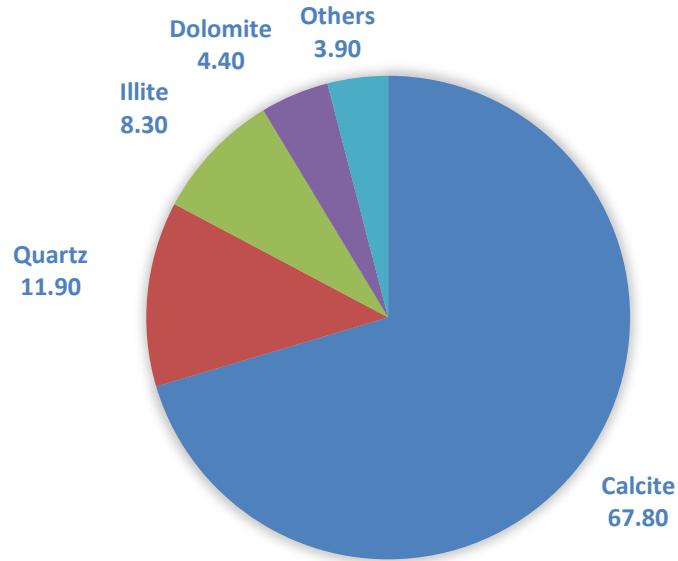
EAGLEFORD SHALE SAMPLE 1

- Others 3.90
- Dolomite 4.40
- Illite 8.30
- Quartz 11.90
- Calcite 67.80

Figure 18: XRD Analysis of Eagleford Shale sample 1(EF Shale 1)

EAGLEFORD SHALE SAMPLE 2

- Others 4.2
- Illite 13.9
- Quartz 6
- Calcite 75.8
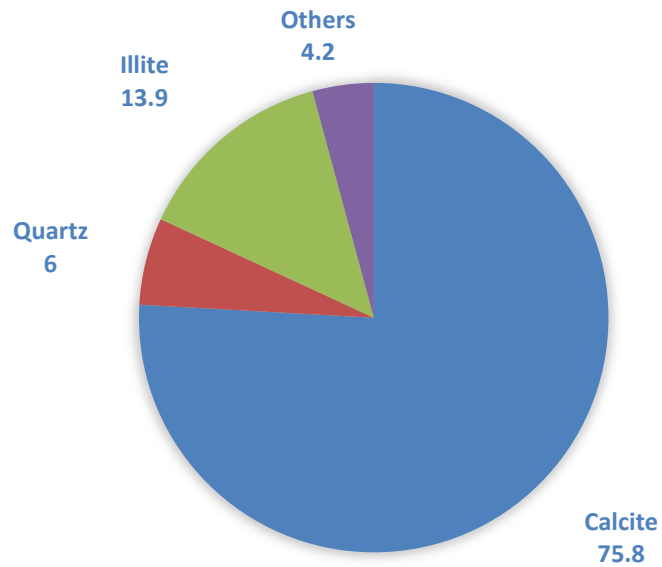
Figure 19: XRD analysis of Eagle ford Shale sample 2(EF Shale 2)

57

LIMESTONE OUTCROP

Quartz
2%

Calcite
98%
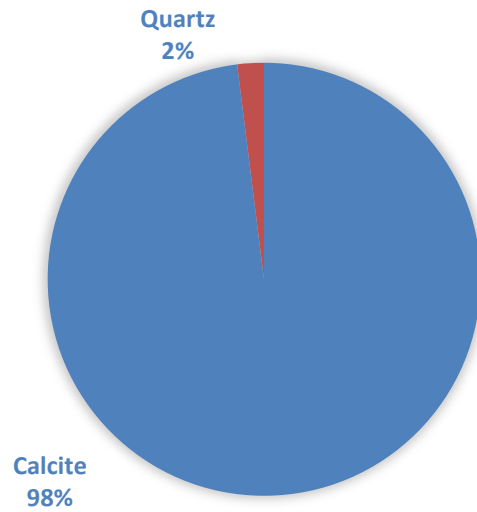
Figure 20: XRD analysis of limestone outcrop (LS)

SANDSTONE OUTCROP

Albite
6.3

Microdine
6.4

Chlorite
4.1

Kaolinite
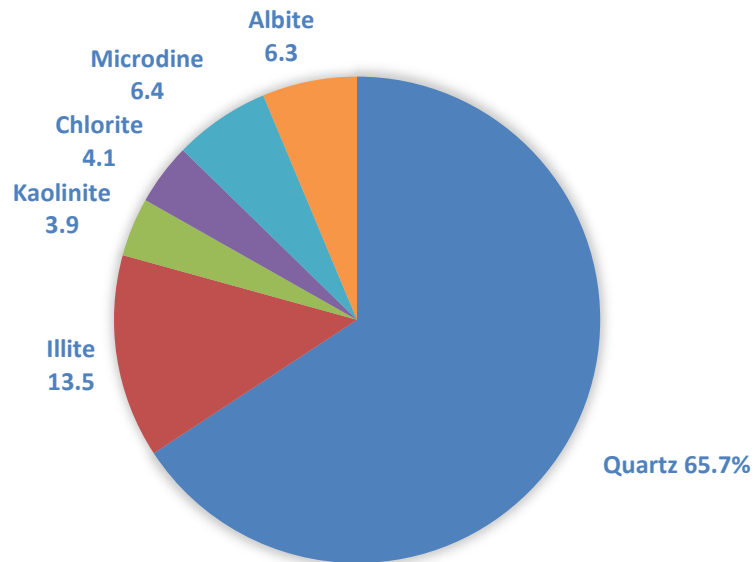3.9

Illite
13.5

Quartz 65.7%

Figure 21: XRD analysis of sandstone outcrop (SS)

Eagle Ford Shale sample 1 is the focus of this study as the contact angle and interfacial tension measurements will be performed using this rock sample to evaluate surfactant performance for wettability alteration. Sandstone outcrop is used for dynamic surface tension (DST) measurements whose composition comprised of quartz, illite, kaolinite and other minerals with quartz being the largest component at 65%, followed by illite at 13.5%. The composition is given in Figure 21. Limestone outcrop samples are also used for DST measurements whose composition is detailed in Figure 22. The composition of the limestone rock was 98% calcite and 2% quartz. This indicates that the limestone sample is mostly made up of carbonates (calcium carbonate) with negligible amount of silica minerals such as quartz.

Rock samples from sandstone and limestone outcrop were used for dynamic surface tension measurement experiments along with Eagle Ford Shale Sample 2. These samples will be used to evaluate the kinetics of surfactant adsorption through dynamic interfacial tension measurement.

3.3. Brine and surfactant solution properties

The TDS of the produced water from the well of interest is about 12% TDS. The TDS is measured in terms of percentage of weight of solute (grams) in weight of the solvent. This applies to weight percentages of surfactant solutions and surfactant brine solutions. The brine samples used for wettability performance evaluation was a 6% TDS brine which is

a diluted version of the 12% TDS produced water. The ratios of ions are preserved to mimic the in-situ brine composition.

The composition of the 6% TDS brine is shown in Figure 23. The brine is largely comprised of NaCl and KCl salts along with salts with divalent ions such as $CaCl_2.2H_2O$ and $MgCl_2.6H_2O$. The concentration of individual ions is shown in Figure 24. The most abundant ions are sodium (Na^+) and chlorine (Cl^-) with concentrations of approximately 20664 ppm and 36324 ppm respectively, followed by divalent ions Ca^{2+} and Mg^{2+} with concentrations of 2057 ppm and 337. The concentration of bicarbonate (HCO_3^-), sulfate ions (SO_4^{2-}) and potassium ions (K^+) are 290 ppm, 331ppm and 283 ppm respectively.

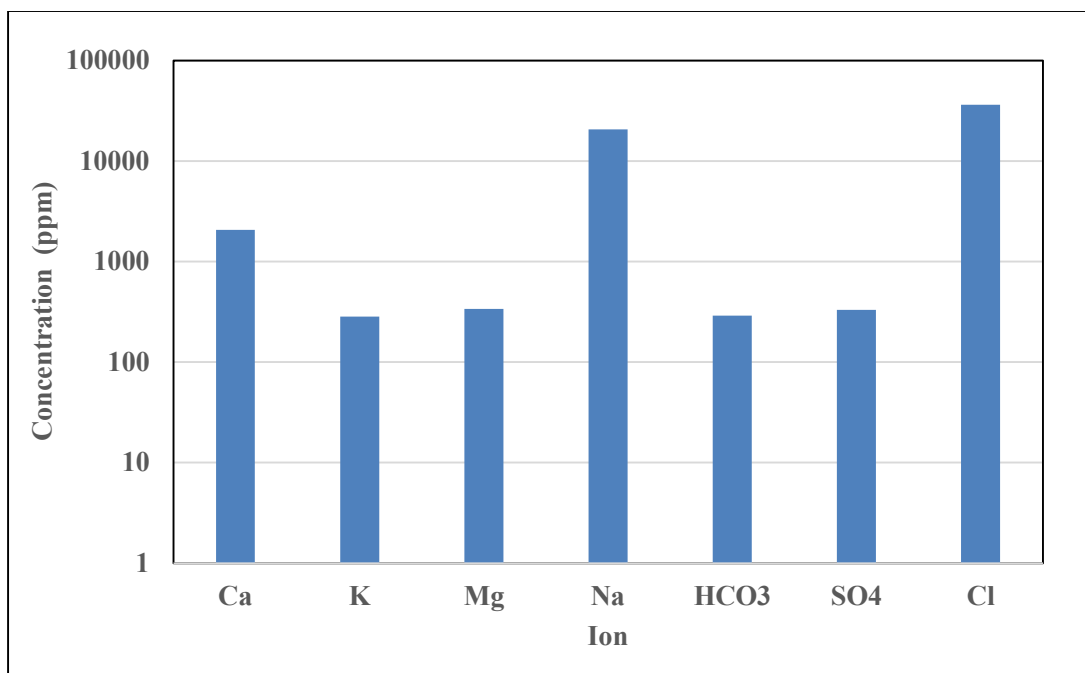| SALT	CONCENTRATION (ppm)
NaCl	51597
$CaCl_2+2H_2O$	7512
$NaHCO_3$	398
$MgCl_2+6H_2O$	2812
Na_2SO_4	487
KCl	538
Total TDS	63,344 mg/L = **6% by wt. TDS**

Figure 22: Salt concentrations in 6% PW

Figure 23: Ion concentrations in 6% Brine

The surfactant solutions used in this study for wettability alteration are 0.2 wt. % surfactant solutions. The surfactant solution is prepared in the respective aqueous phase by weighing the mass of surfactant and mixing in the required weight of brine to achieve the desired concentration. Surfactant concentrations of 0.4, 0.2, 0.1, 0.05, 0.025, 0.0125, 0.0062, 0.0031, 0.0015, 0.0007 and 0.0003 by percentage of weights are used for dynamic surface tension measurements to build surface tension calibration curves in order to estimate the surfactant concentrations in produced water samples that will be presented in further sections. The list of surfactants used for this study are given in Figure 20. Nonionic surfactants N1, N2 , N3 and N4 have similar tail (C12-14) groups with different EO(23, 22 and 12) groups. Cationic surfactants C1 and C2 have different tail groups of C12 and C18 with similar tail group TAC (trimethyl ammonium chloride). Sulfate based anionic

61

surfactants used are S1 and S2 that have similar head groups of IOS (internal olein sulfates) with different tail groups (C_{15-18} and C_{20-24}).
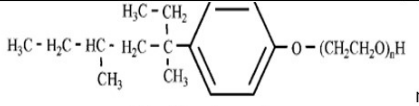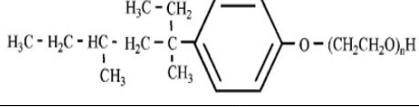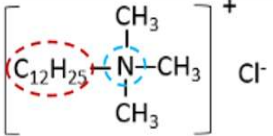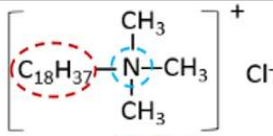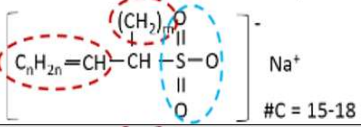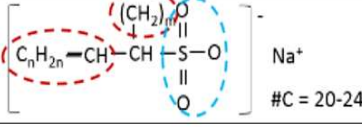
Name	CHARGE	MAIN CONTENT	TAIL	HEAD	STRUCTURE
N1	NONIONIC	ALCOHOL ETHOXYLATE	C12-14	23 EO	$CH_3-(CH_2)_n-O(CH_2CH_2O)_y$ n=11-13, y=23
N2	NONIONIC	ALCOHOL ETHOXYLATE	C12-14	22 EO	$CH_3-(CH_2)_n-O(CH_2CH_2O)_y$ n=11-13, y=22
N3	NONIONIC	ALCOHOL ETHOXYLATE	C12-14	12 EO	$CH_3-(CH_2)_n-O(CH_2CH_2O)_y$ n=11-13, y=12
N4	NONIONIC	ALCOHOL ETHOXYLATE	C12-14	12 EO	$CH_3-(CH_2)_n-O(CH_2CH_2O)_y$ n=11-13, y=12
N5	NONIONIC	NONYLPHENOL ETHOXYLATE	NONYLPHENOL	12 EO	nonylphenol ethoxylate structure, n=12
N6	NONIONIC	NONYLPHENOL ETHOXYLATE	NONYLPHENOL	30 EO	nonylphenol ethoxylate structure, n=30
C1	CATIONIC	C12-TRIMETHYLAMMONIUM CHLORIDE	C12	TAC	$[C_{12}H_{25}-N(CH_3)_3]^+$ Cl^-
C2	CATIONIC	C18-TRIMETHYLAMMONIUM CHLORIDE	C18	TAC	$[C_{18}H_{37}-N(CH_3)_3]^+$ Cl^-
A1	ANIONIC	C15-18 INTERNAL OLEIN SULFATE	C15-18	INTERNAL OLEIN SULFATE	$C_nH_{2n}=CH-CH-(CH_2)_m-SO_3^-$ Na^+, #C = 15-18
A2	ANIONIC	C20-24 INTERNAL OLEIN SULFATE	C20-24	INTERNAL OLEIN SULFATE	$C_nH_{2n}=CH-CH-(CH_2)_m-SO_3^-$ Na^+, #C = 20-24

Figure 24: List of surfactants used

3.4. Contact Angle Experiments

Contact angle measurements are performed to evaluate oil/rock/brine wettability in the presence of surfactants by observing the angle of a drop of crude oil on the surface of a rock chip. Angles between 0 – 75 ° are considered to be water-wet, 75 – 110° are considered to be intermediate-wet and angles between 110 – 180° are oil-wet.

CA measurements were performed on a Data physics OCA 15 Pro device using the captive bubble method with the aid of a video-based optical measurement system. The apparatus consists of the imaging system, dispensing system, and the heating system, all controlled by a drop shape analyzer (DSA) software. ULR rock wettability was determined by oil-rock CA in the presence of an aqueous solution with and without surfactants. The rock chips for contact angle measurements were cut from Eagle Ford shale sample 1. The rock chips were cut and polished to minimize errors in the contact angle measurements due to surface roughness. The chips were cleaned with toluene and methanol (2 days and 1 day respectively) in order to displace the contaminants from the rock surface that might have been present due to improper core handling and core preservation. This cleaning process also displaced hydrocarbon components, thus altering the wettability to water-wet. After cleaning, the water-wet rock chips are aged in crude oil for 6 weeks to restore original reservoir wettability, i.e., alter the wettability of the chips to oil-wet. The measurements are taken at temperatures up to 170 °F to evaluate wettability of rock at high temperatures.
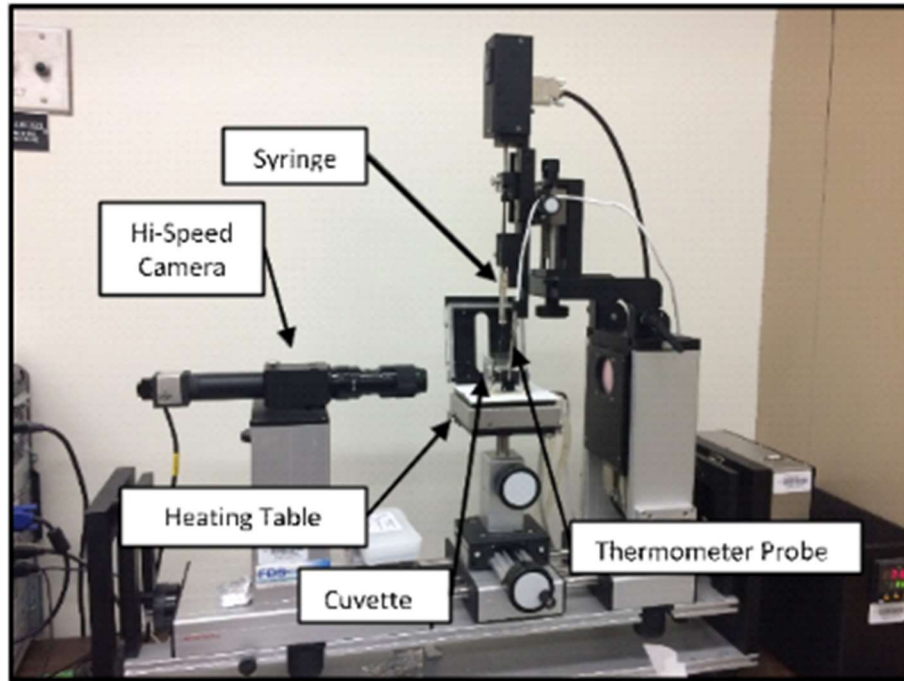
Figure 25: Contact angle measurement on DataPhysics OCA 15 Pro

The procedure to measure the contact angle using the Data physics OCA 15 Pro device is as follows:

1) A syringe attached to a J-shaped needle is filled with the reservoir crude oil.

2) The rock chip under observation is placed in a cuvette filled with the respective brine or surfactant solution and placed onto the Data Physics OCA 15 platform. (Fig 26)

3) A stage is placed inside the cuvette to support the rock chip and allow for bottom to top measurement with the syringe. (Fig 27)

4) The oil drop is dispensed from the syringe and allowed to adhere onto the bottom surface of the rock chip. The contact angle is measured using the captive bubble

method in the DSA software. The OCA 15 Pro apparatus uses a high-speed camera

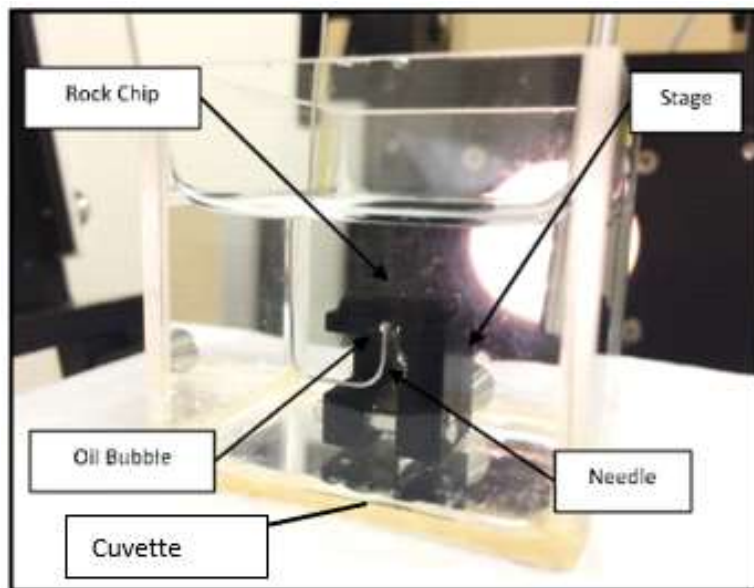to measure the contact angle of the oil on the rock chip

Figure 26: Contact angle measurement set up

3.5. Interfacial/Surface Tension Measurements

Static IFT experiments were performed using a Data physics OCA 15 Pro apparatus by

the pendant drop method and a Grace Instruments M6500 Spinning Drop Tensiometer by

spinning drop method at reservoir temperature using reservoir crude oil, brine and

surfactants. The pendant drop method is very reliable for IFT values higher than 1 mN/m;

for lower values spinning drop method is used. These experiments will also help select

proper surfactant type and concentration. Pendant drop bottoms up method aided by a

video-based optical measurement system, as shown in Figure 28, consisted on dispensing

oil from the capillary needle into a frac fluid solution and measuring IFT when the drop

leaves the needle. In addition, to verify low IFT values (less than 1 mN/m) a spinning drop tensiometer was used. Then, an oil drop was inserted inside the sample tube previously filled with frac fluid and rotated to deform the drop and calculate drop diameters.
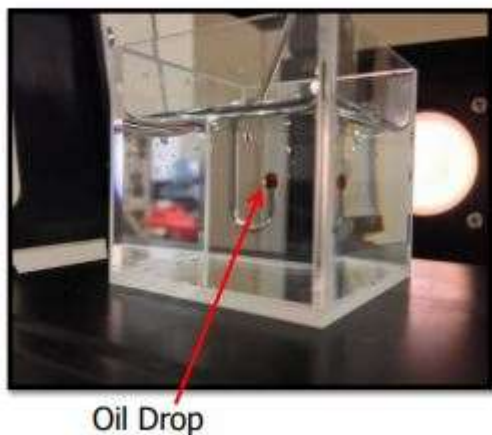

Oil Drop

Figure 27: IFT measurement on Data physics

IFT is determined as follows:

1. Aqueous solutions, with and without surfactants, were placed inside a quartz cuvette and heated until reservoir temperature was reached.

2. Crude oil from Eagle Ford wells were dispensed through a j-shaped capillary needle facing upwards into the aqueous solution. The experiment was recorded using a high-resolution camera and the frame that captured the moment when the drop was about to detach from the needle was used for analysis.

3. Using the DSA software and the density at reservoir temperature of the oil and aqueous solutions, IFT values were calculated by fitting the drop shape profile to the Laplace equation.

3.6. Spontaneous Imbibition Experiments

The spontaneous imbibition experiment is a method of measuring the wettability of a bulk porous medium as compared to contact angle measurements which only indicate the surface wettability characteristics of the rock. Spontaneous imbibition experiments can be performed by soaking an oil-saturated rock core in a wetting aqueous phase such as brine or surfactant solutions. This causes imbibition of aqueous phase into the rock and displacement of oil from the pore spaces due to the reduction in capillary pressures. Spontaneous imbibition experiments are carried out in Modified Ammott cells as shown Figure 29.

Figure 28:Modified Ammott Cell

Cylindrical rock cores of width 1 inch and length 2 inches were cut from Eagle Ford Shale sample 1 were saturated in crude oil at reservoir temperature of 200 °F for 6 weeks to saturate the core with oil and restore reservoir wettability The rock cores are weighed to determine the original oil-in-place (OOIP) of the core by weighing the difference in weight during the aging process. The core plugs are cleaned in toluene and methanol for 2 weeks by utilizing a Dean-Stark apparatus. The amott cell is a glass structure with a dome-shaped base and tall neck with a graduated measuring scale engraved to measure the volume of fluid change in the Amott cell. The imbibition of aqueous phase into the core displaces the oil and it rises to the top of the Amott cell where observations are made noting down the total oil recovered. A time-lapse plot can be graphed of the recovery factor as a function

68

of time for different aqueous surfactant and brine solutions. The spontaneous imbibition experiment is a good indicator of wettability alteration performance by surfactant additives due to the inclusion of complex pore structure and mineral heterogeneity of reservoir rock.

3.7. Dynamic Surface tension measurements

Dynamic surface tension is a method to quantify the dynamics of surfactant adsorption. As the area of the air/water interface increases, the amount of surfactant monomers interacting at the surface increase. This leads to reduction in surface tension as the bubble surface age increases. The dynamic surface tension of a surfactant can be measured using a bubble pressure tensiometer. The KRUSS BPT Mobile apparatus is used to measure the dynamic surface tension at the air/water interface of aqueous surfactant solutions. The surface tension measurements in the tensiometer are related to the hydrostatic pressure of the surrounding fluid by the Young-Laplace equation. A volume of greater than 20 cc was used for measurements to avoid inaccuracies due to low volume of fluid. A capillary tip made of coated with hydrophobic material is immersed in the aqueous fluid. The BPT generates surface tension values for a range of bubble surface ages.

Figure 29: DST measurements with Kruss BPT

The concentration of a surfactant in an aqueous fluid can be estimated through dynamic surface tension measurements. DST calibration curves are generated for a range of surfactant concentrations below CMC and above CMC. The concentrations used are 0.2 wt. %, 0.1 wt.%, 0.05 wt.%, 0.025 wt.%, 0.0125 wt.%, 0.00625 wt.%, 0.0031wt.%, 0.0015 wt.%, 0.0007 wt.% and 0.0003 wt. %. Integration of the dynamic surface tension of an aqueous surfactant solution with the respective calibration curve provides a unique method of estimating the surfactant concentration in a fluid. Figure 26 shows an example of

estimating the surfactant concentration wherein the concentration in produced water sample 1 is 0.00625% and the concentration in produced water sample 3 was nearly 0%.
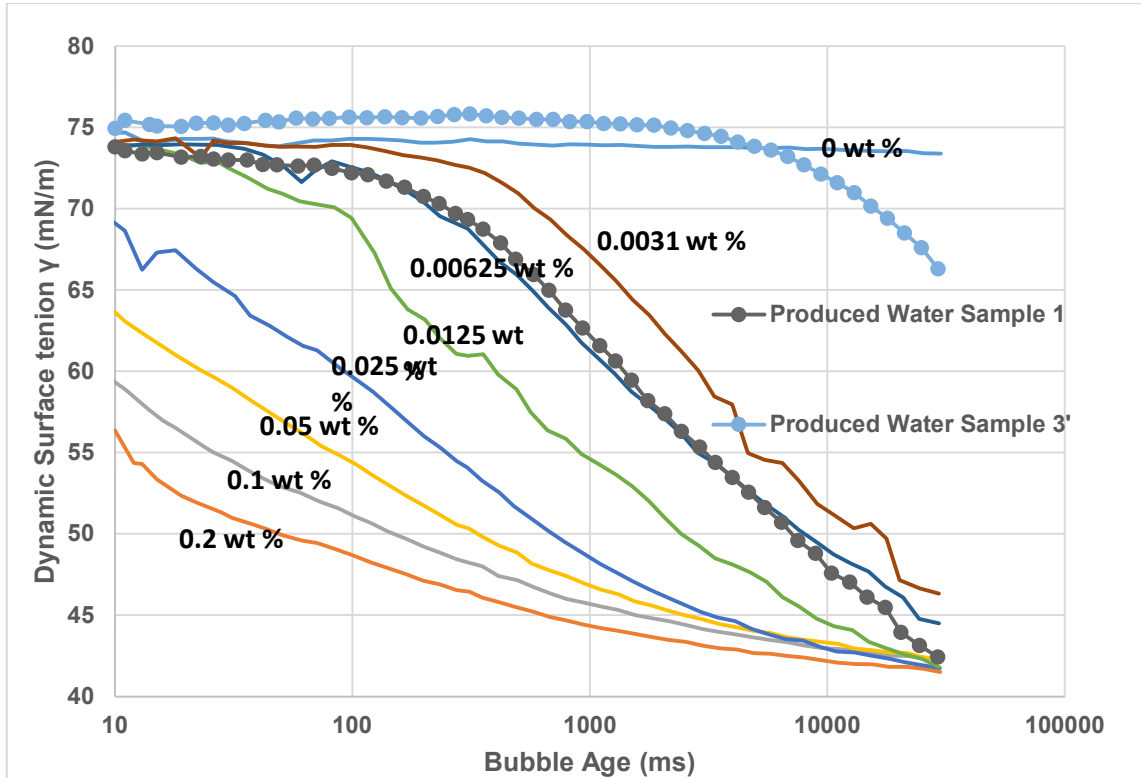

Figure 30: Surfactant concentration measurement

3.8. Produced Water preparation

Produced water samples used in this study were received in plastic containers, as shown in Figure 32. The samples are contaminated with oil forming oil-in-water emulsions and other organic matter such as algae.
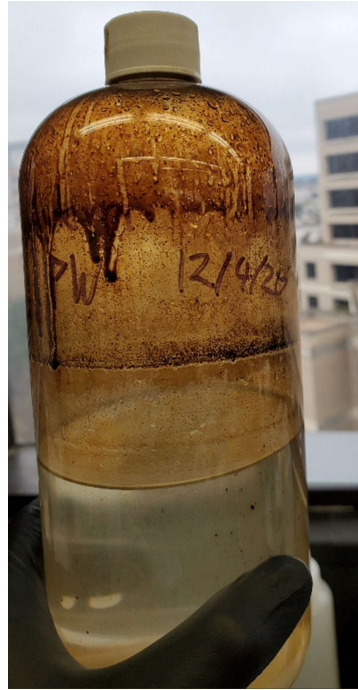
Figure 31 : Produced water container

These samples were prepared for TDS measurements and surfactant concentration measurements were prepared by following a 2 Step process:

1. Produced Water was extracted from the container and centrifuged at 5000 rpm for 1 hr using a centrifuge machine, to separate out the emulsified oil from the produced water.

2. The produced water is then extracted from the centrifuge vials and filtered with 10-micron filter to remove solid particles and contaminants which may cause erroneous measurements. (Figure 33).

3. TDS measurements were taken by drying 20 grams of the produced water sample placed in an aluminum plate in a vacuum oven at 250 deg. C to vaporize all the

water and particles with low vapor points (Figure 34). The TDS is measured by observing the different in weights of the samples in the aluminum plates.
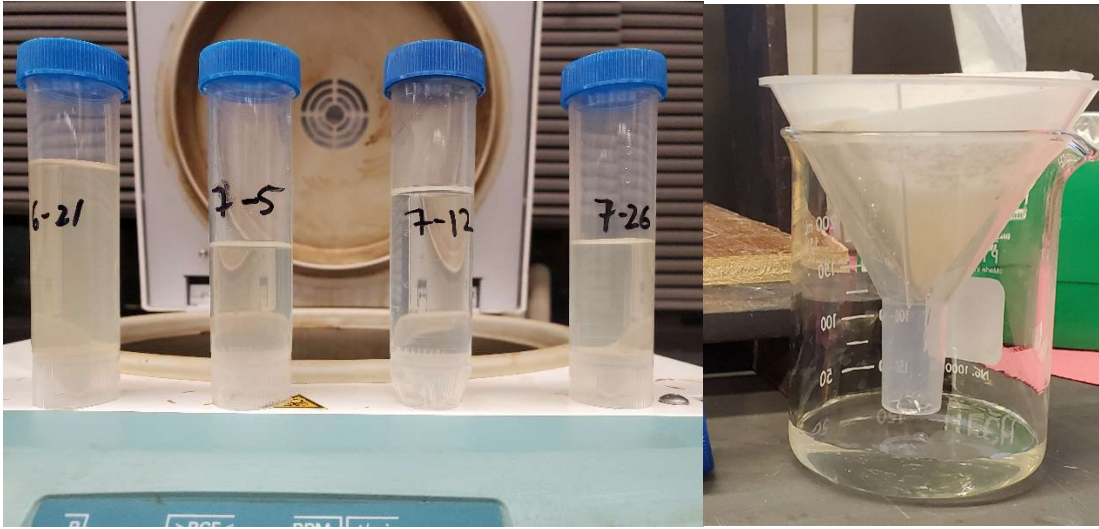

Figure 32: PW centrifuge and filter process

Figure 33: TDS measurements

4. SURFACTANT DESIGN FOR EOR PROJECT IN THE EAGLE FORD BASIN

4.1. Workflow for Surfactant EOR project

A workflow is developed for performing a comprehensive laboratory analysis of processes involved in a surfactant EOR project (Figure 25). The pre-injection phase of a surfactant EOR project involves a surfactant screening phase wherein contact angle, interfacial tension and spontaneous imbibition experiments will be performed to validate the wettability alteration performance of surfactants. Following surfactant screening, gel formation tests and cloud point tests are performed to ensure pumpability of surfactant solution and surfactant stability at high temperatures. The selected surfactant solution will be used to create a concentrated master solution at offsite mixing facilities. The master solution will be transported to the wellsite via mixer trucks, where the MS will be mixed with fresh water (FW) and produced water (PW) from the field to in aboveground Storage Tanks (AST) (Figure 25) at the wellsite to fabricate the injection fluid.

Figure 34: Aboveground storage tank (AST)

The well is to be stimulated with the injection fluid by injecting approximately 15000 bbls of injection fluid into the well and shutting the well in to allow the reservoir rock to soak

in the surfactant solution. The soaking process of 1 month is allowed to ensure maximum surfactant penetration into the rock matrix and effective wettability alteration.

Once production has begun, the produced water and crude oil will be analyzed and the concentration of residual surfactant in the flowback fluids will be determined using dynamic surface tension analysis. The oil recovery will be observed to summarize the impact of surfactant EOR on oil recovery in mature unconventional shale reservoirs.
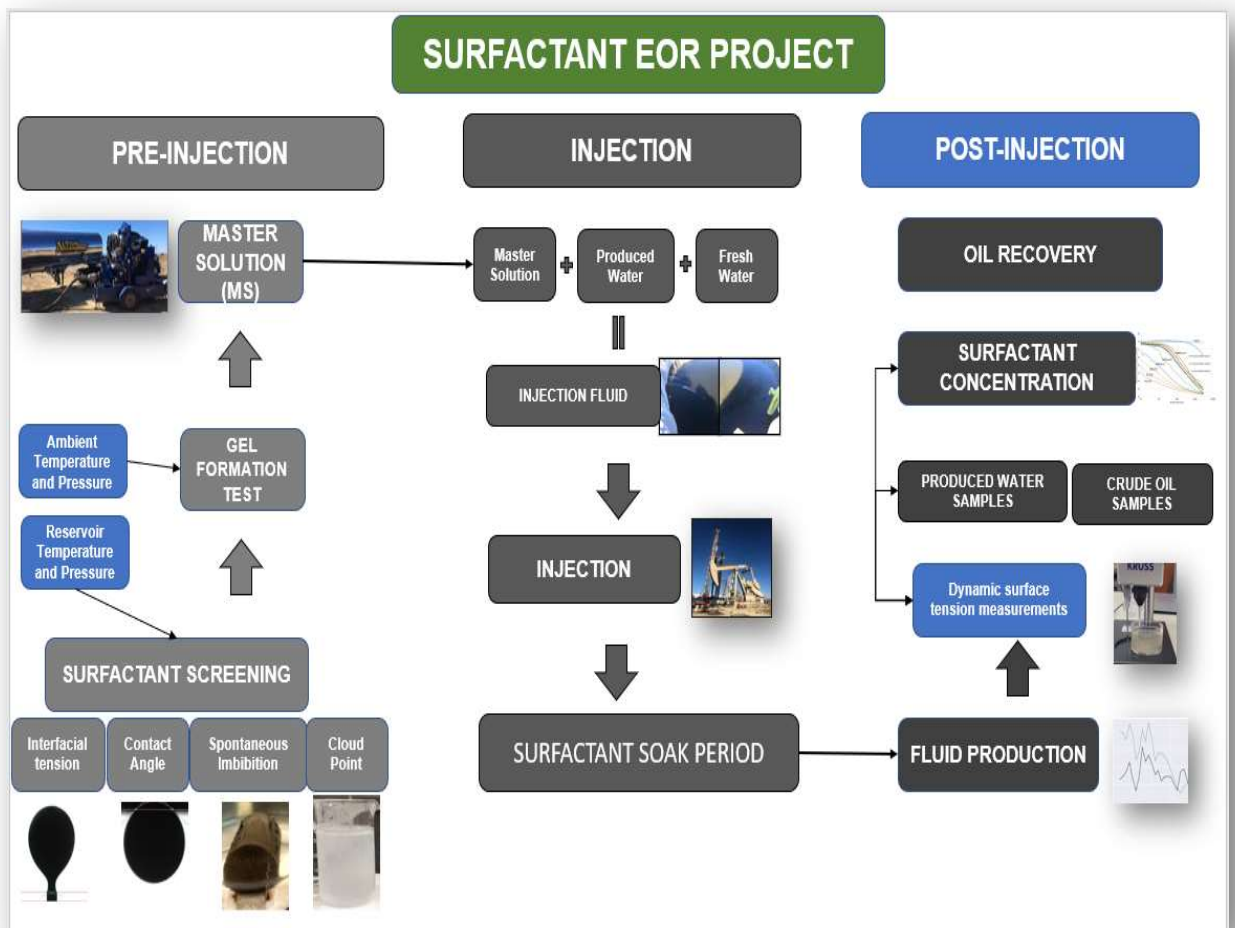

Figure 35: Surfactant EOR project workflow

4.2. Pre-Injection

4.2.1. Well Information and History

The aim of this study is to apply surfactant EOR methodologies to a mature well (Laughlin Cook 1H) located in the Eagleville field of the Gonzales County in Texas. The task at hand is to improve the estimated ultimate recovery (EUR) of the well by injecting stimulation fluid comprising of a surfactant solution. The Laughlin Cook 1H well located in the Eagle Ford Shale formation and is a tight oil reservoir. The Eagle Ford shale is bounded by the Austin Chalk and Buda Limestone. The date of injection for the Laughlin Cook well was decided to be in December of 2020. The injection would follow a 1-month shut-in period to allow the reservoir to soak in the injection fluid to allow maximum surfactant penetration and wettability alteration.
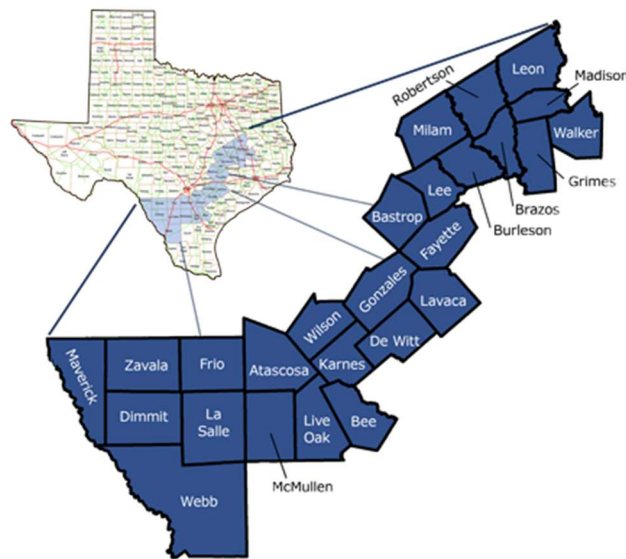

Figure 36: Texas counties in Eagle Ford formation

The well was originally completed by Forest oil on September 20th, 2012.The well was stimulated in 25 different stages with hydraulic fracturing fluids (Slick water, Borate Surface and Down Hole Cross linker system) by utilizing a 'plug-and-perf' methodology. The well was drilled to a measured depth of 13,064 ft (MD), with a 'toe-down' lateral direction running from true vertical depth (TVD) of 7000 to 7340 ft. The depths and elevations for the well are given in Figure 13.

Laughlin-Cook 1H

Depths & Elevations:			
KOP:	6,203' MD		
Depth to 30 Deg Inc:	6,626' MD		
Curve Landed:	7,416' MD		
TD OHL MD:	12,974' MD	KB:	381'
PBTD (CT Tag):	12,927' KB	GL:	359'

Figure 37: Laughlin Cook well information.

The maximum recorded Bottom Hole Temperature (BHT) was 221 deg. F. The temperature of the reservoir, along with the properties of the rock and fluid determine the potential for an enhanced oil recovery through stimulation by a surfactant solution. A figure showing the summary of the plug-and-perf frac stages are showing in Figure 14.

Stage Number	Plug Depth	Top Shot	Top Shot	Top Shot	Top Shot
1	12,927	12,917	12,862	12,807	12,752
2	12,725	12,697	12,642	12,587	12,532
3	12,505	12,477	12,422	12,367	12,312
4	12,285	12,257	12,202	12,147	12,092
5	12,065	12,037	11,982	11,927	11,872
6	11,845	11,817	11,762	11,707	11,652
7	11,625	11,597	11,542	11,487	11,432
8	11,405	11,377	11,322	11,267	11,212
9	11,185	11,157	11,102	11,047	10,992
10	10,965	10,937	10,882	10,827	10,772
11	10,745	10,717	10,662	10,607	10,552
12	10,525	10,497	10,442	10,387	10,332
13	10,305	10,277	10,222	10,167	10,112
14	10,085	10,057	10,002	9,947	9,892
15	9,865	9,837	9,782	9,727	9,672
16	9,645	9,617	9,562	9,507	9,452
17	9,425	9,397	9,342	9,287	9,232
18	9,205	9,177	9,122	9,067	9,012
19	8,985	8,957	8,902	8,847	8,792
20	8,765	8,737	8,682	8,627	8,572
21	8,545	8,517	8,462	8,407	8,352
22	8,325	8,297	8,242	8,187	8,132
23	8,105	8,077	8,022	7,967	7,912
24	7,885	7,857	7,802	7,747	7,692
25	7,665	7,637	7,582	7,527	7,472

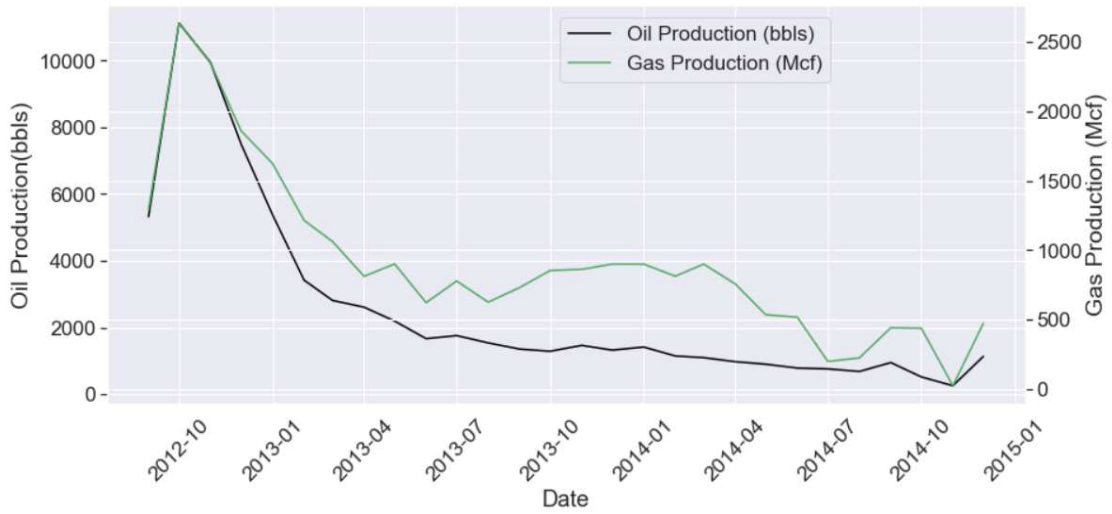**Figure 38: Perforation and plug depths for Laughlin Cook**

Figure 39: Initial production of Laughlin Cook - 2012 to 2015

The **Figure 28** shows the oil and gas production from the well following the completion of the well. It was set on production in 2012 and initially produced close to 11,000 bbls of oil during the Month of October 2012. Since then, the well has been on a slow decline with the monthly production reaching about 500 barrels by the end of 2015.
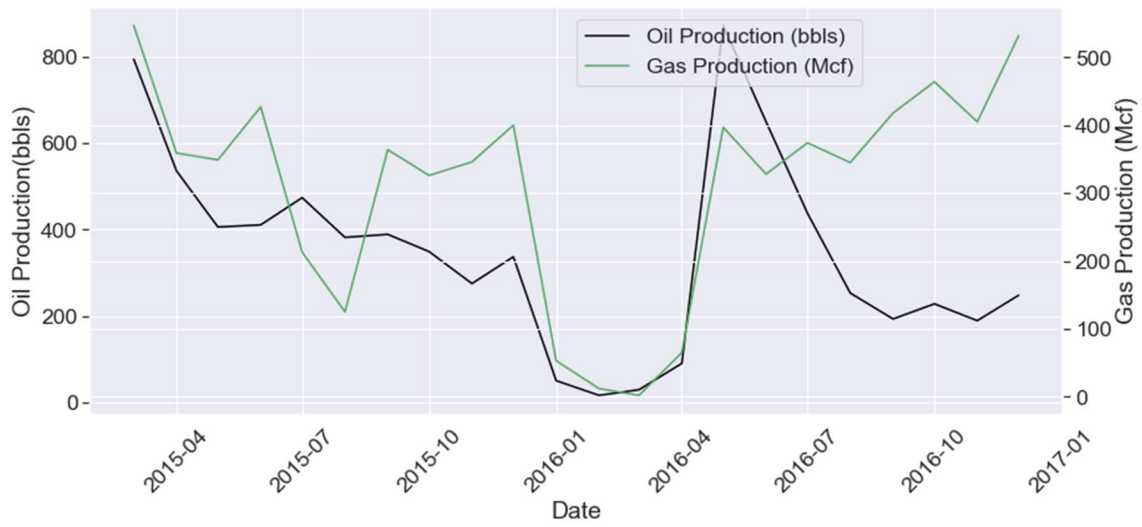
Figure 40: Production decline of Laughlin Cook (2015 to 2017)

The Figure 29 shows the rate of production decline after 2015. The well has begun to decline in production and the operators begin shutting the production of the well to allow the reservoir pressure to replenish in order to promote a favorable pressure gradient for hydrocarbon production. From the 2016, there is a steady decline in production which has decreased to around 150 bbls of oil per month.
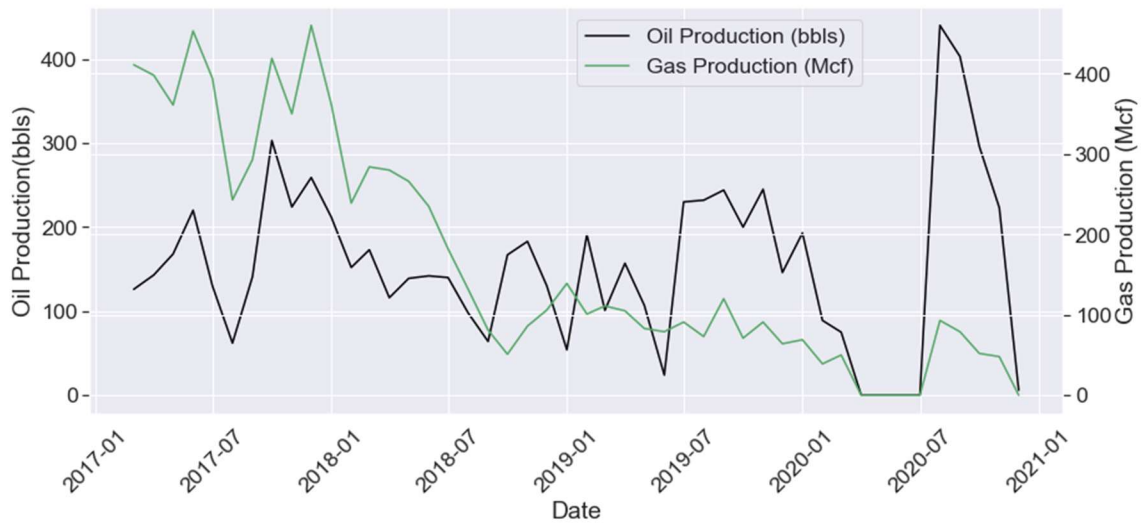
Figure 41: Further decline from 2017

Beginning from 2017, the oil production has dropped down to about 200 bbls per month. This is followed by a further decline in the oil production towards the beginning of 2020. The well has been producing for nearly 9 years and it can be considered to be a mature well. Such wells are generally not able to recover enough crude oil from the reservoir to make it a financially viable option to justify the costs associated with labor and operation costs. The primary and secondary recovery have been exhausted from this well and tertiary methods of recovery such as surfactant flooding can be used to increase oil production and improve the Estimated Ultimate Recovery (EUR) of the well. The purpose of this study is to design a surfactant formulation for an EOR project for the Laughlin Cook well based on experimental laboratory methodology depending upon the operating conditions of the well during injection and the in-situ properties of the rock and fluid.

4.2.2. Injection Plan

The operational philosophy behind surfactant injection for this EOR project was to transport a concentrated 'master solution' of surfactant injection fluid (MS) to the wellsite by means of large concrete mixer trucks which. The concentrated injection fluid (MS) would then be diluted at the wellsite by mixing with freshwater (FW) and produced water (PW) mixed in a suitable ratio. The 'stim fluid' is mixed with the FW and PW according to the most optimal combination of surfactant concentration and salinity for effective wettability alteration and improved oil recovery. A low concentration of a biocide is used at concentrations of 64 ppm or approximately 0.01 wt. % concentrations in the final injection fluid to control microbial growth. A description of the biocide is summarized in the next subsection. The impact of biocide on the wettability alteration performance of surfactant solutions is to be measured through contact angle measurements to ensure the stability of the non-ionic surfactants in the presence of biocides.
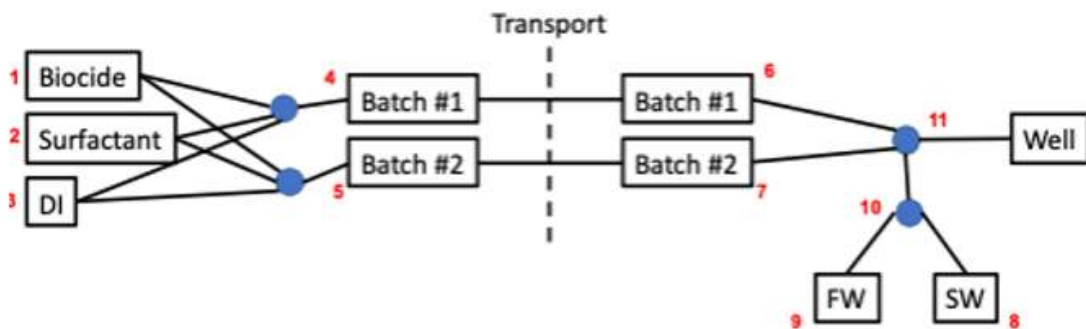
Figure 42: Injection plan

Figure 31 shows the steps involved in mixing, transport and injection of the surfactant solution in the well. The steps for carrying out the injection process are detailed as follows:

A. Blending of surfactant with DI water and biocide at high concentrations to allow easier transport of injection fluid to the wellsite into a concentrated solution MS which will be transported by mixer trucks.

B. The blended solution MS will be transported to the wellsite in 2 mixer trucks

C. The concentrated MS will be diluted with freshwater (FW) and produced water (PW) to achieve suitable concentrations of surfactant and salinity which correspond to laboratory experiments.

D. Injection fluid comprising of FW, PW and MS will be injected into the well

4.2.2.1. Biocide

The inclusion of biocides in the injection fluid is important for aqueous fluids entering the wellbore. Processes such as hydraulic fracturing and waterflooding which involve the use of large amounts of aqueous fluid which are generally sourced from the produced water of the wells or natural sources. The proliferation of bacteria, plankton and other microbes may lead to degradation of chemical additives, plugging of subsurface equipment and generation of H_2S by effect of microbially influenced corrosion (MIC) in flowlines [51]. Thus, the use of biocides is critical to the mitigation of microbial growth which may hinder or disrupt injection fluids in the wellbore. The biocide used for this study is Glutaraldehyde. Glutaraldehyde is an electrophilic biocide which operates by accepting

protons from basic amines or thiols present on the cell membrane of microbes. It contains highly reactive aldehyde carbons that can readily accept electrons from amine groups present on the cell membranes of microbes. The molecular formula of glutaraldehyde is $C_5H_8O_2$. The molecular structure is similar to that of an Ethylene oxide group (C_2H_4O). The surface activity of glutaraldehyde will be evaluated by comparing the performance of surfactant solutions with and without addition of biocide.
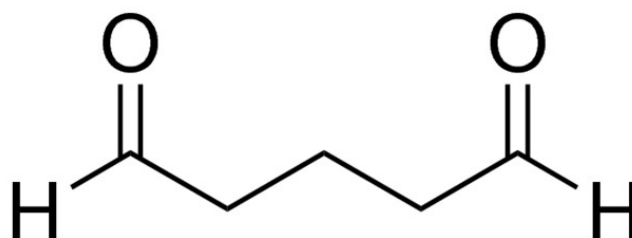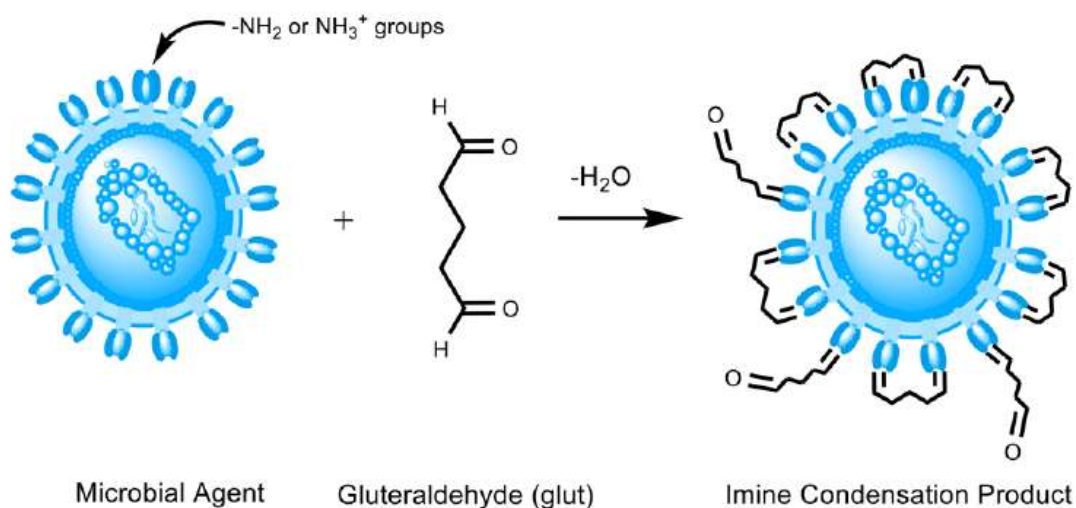
Figure 43: A) Glutaraldehyde with microbe B) Molecular structure [51]

4.2.3. Produced Water and Oil Analysis

The produced water from the Laughlin Cook well is analyzed using ion-chromatography (IC) to compare the concentration of cations in the produced water. The results are compared to the ion analysis of the produced water from Laughlin Cook 1H (LC) from another close by well in Gonzales County within the same Eagle Ford formation, Springs Patteson 2H (P2H), for reference. The results show that the total concentration of cations such as Mg^{2+}, Ca^{2+} and K^+ are nearly similar between both produced water fluids. The concentration of potential determining multivalent ions such as Mg^{2+}, Ca^{2+} and SO_4^{2-} affect the rock wettability and surfactant interaction with the oil/rock/brine chemistry present in the reservoir by allowing covalent bonds to form between similarly charged fluids to bond together forming a bridge between them. The salinity of the Laughlin Cook produced water is around 12.1 wt. %, or roughly 121349 ppm. The salinity percentage (g/L) can be calculated by dividing the total 'ppm concentration' by 10000.
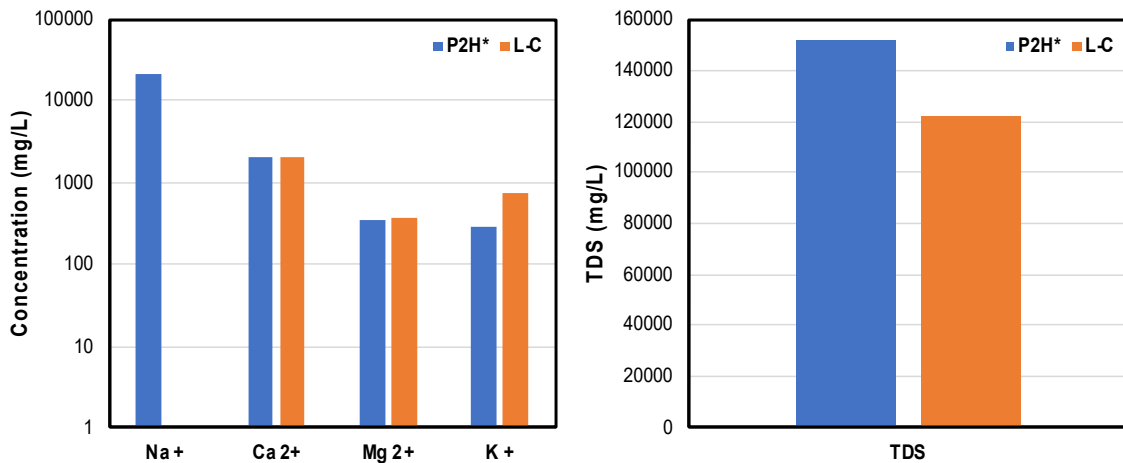
	P2H*	L-C
Na +	20939	
Ca 2+	2085	2086
Mg 2+	342	369
K +	287	737
TDS	151800	121349

Figure 44: A) Produced water ion concentrations B) Total TDS

Figure 19 shows the change in produced water salinity of the well from October 2019 to July 2020, which shows the TDS of the produced water to be around 12 – 14 % salinity. The measurements were performed by an external organization, to which the laboratory TDS measurements presented in Figure 18 match up to. The salinity of the produced water was around the 14% TDS mark. The TDS comparison between the P2H well and LC show that the salinities of the wells in the same field in the Eagle Ford formation are close in values.

87
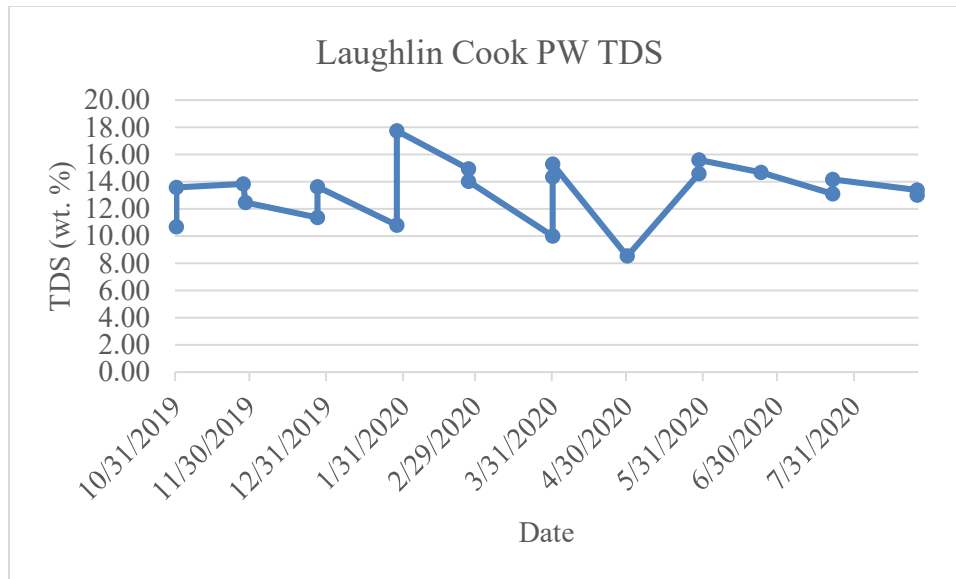
Figure 45: Laughlin Cook produced water TDS (before stimulation)

A SARA analysis is done on the crude oil produced from the Laughlin Cook well to quantify the amount of saturates, aromatics, resins and asphaltenes present in the crude oil. The composition of the crude oil is high in lighter components such as saturates in aromatics with 27% saturates and 53% aromatics along. The heavier components of the consist of 4% asphaltenes and 15% of Resins. The crude oil has a high number of saturates and aromatics, followed by resins and does not contain a lot of asphaltenes.

Comparison between the SARA components of the crude oil from Springs Patteson 2H (P2H) and Laughlin Cook 1H (LC) show that the composition of the oil remained relatively same across wells in the same field in the Eagle Ford shale formations. The density of the LC crude oil is 0.8997 g/cm^3. The density of crude oil produced from P2H

was also similar with API densities of about 24 at room temperature. The density of the crude oil decreases linearly with the increase in temperature.

LAUGHLIN COOK 1H

- Asphaltenes 4%
- Resins 16%
- Saturates 27%
- Aromatics 53%
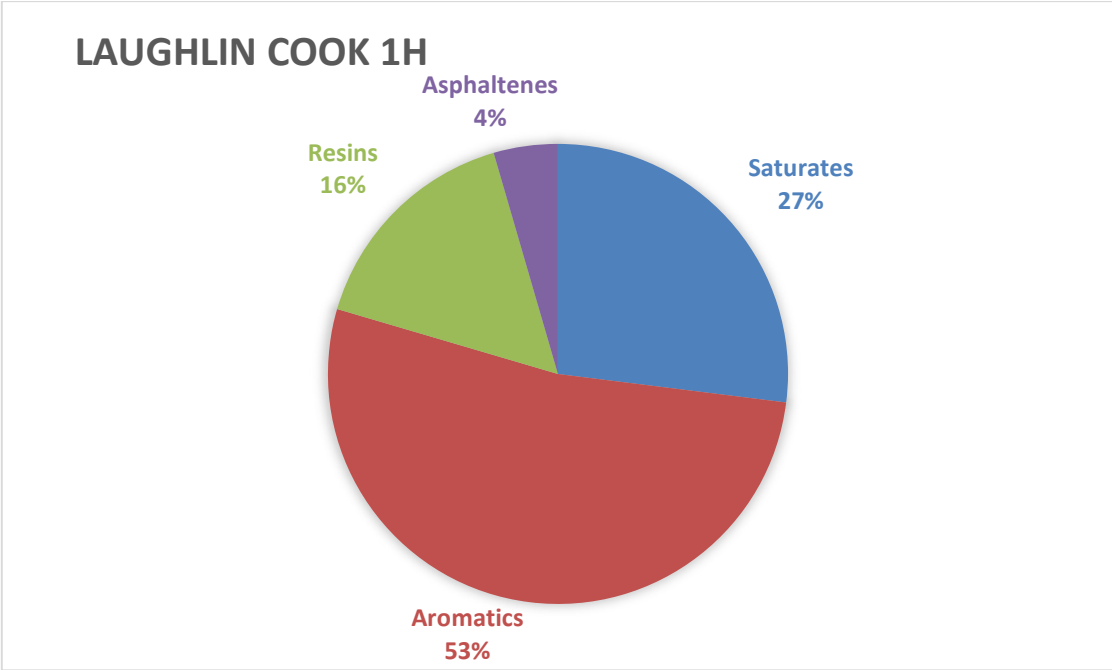
Figure 46: SARA analysis of LC crude oil
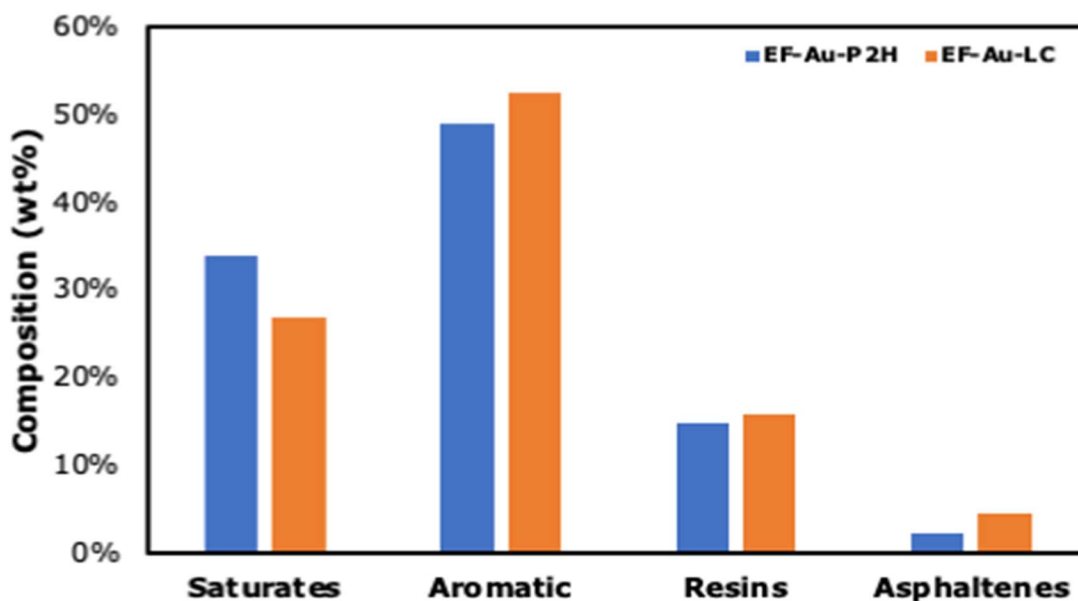
Figure 47: Comparison of SARA analysis between P2H and LC

4.2.4. Surfactant Screening

The surfactants chosen to be screened were 2 types of nonionic alcohol ethoxylate surfactants with C_{12-14} and a range of EO groups in the hydrophilic tail ranging from 12 EO to 22EO. The performance of these nonionic surfactants was evaluated to assess the feasibility for performing an EOR project in the Eagle Ford basin.

4.2.4.1. Cloud Point Measurements

The cloud point of nonionic surfactants is the temperature at which the solubility of surfactant begins decreasing with the increase in temperature. The solubility of nonionic surfactants depends upon the strength of hydrogen bonds between the EO groups in the hydrophilic tail of the surfactant and the aqueous phase. Studies have shown that the solubility of a nonionic surfactants increases with the increase in size of EO groups. As

90

the temperature increases, the hydrogen bonds become weaker causing the surfactant molecules to phase out of the aqueous phase depending upon the size of the EO groups. Surfactants with similar head groups will exhibit increasing cloud point temperatures for increasing number of EO groups. In addition to this, the presence of ion concentrations affects the solubility of surfactants in aqueous phases due to the presence of excess ions in a limited volume of solvent. The cloud point temperatures of nonionic surfactants increase as the salinity increases.

Figure 22 shows the cloud point temperature measurements of 0.2 wt. % surfactant solutions of N1, N2, N3 and N4 as a function of increasing salinities and increasing temperature. The measurements were taken at atmospheric pressure conditions. The cloud points of surfactants N3 and N4 were similar and lower than 212 °F at 208 °F and 199 °F respectively. The cloud points of surfactants N2 and N1 at lower salinities of 2% TDS and 0% TDS were above 212 °F (boiling point of water at atmospheric pressure). The different in cloud point performance between surfactants N1/N2 and N3/N4 are the different in sizes of the EO groups in the hydrophilic heads. There is a trend showcasing the property of nonionic surfactants to decrease in solubility with the increase in salinity as temperature increases as demonstrated by cloud point formation. The cloud points of N3 and N4 are not suitable for the LC well with reported maximum bottom hole temperature (BHT) of 220 °F.
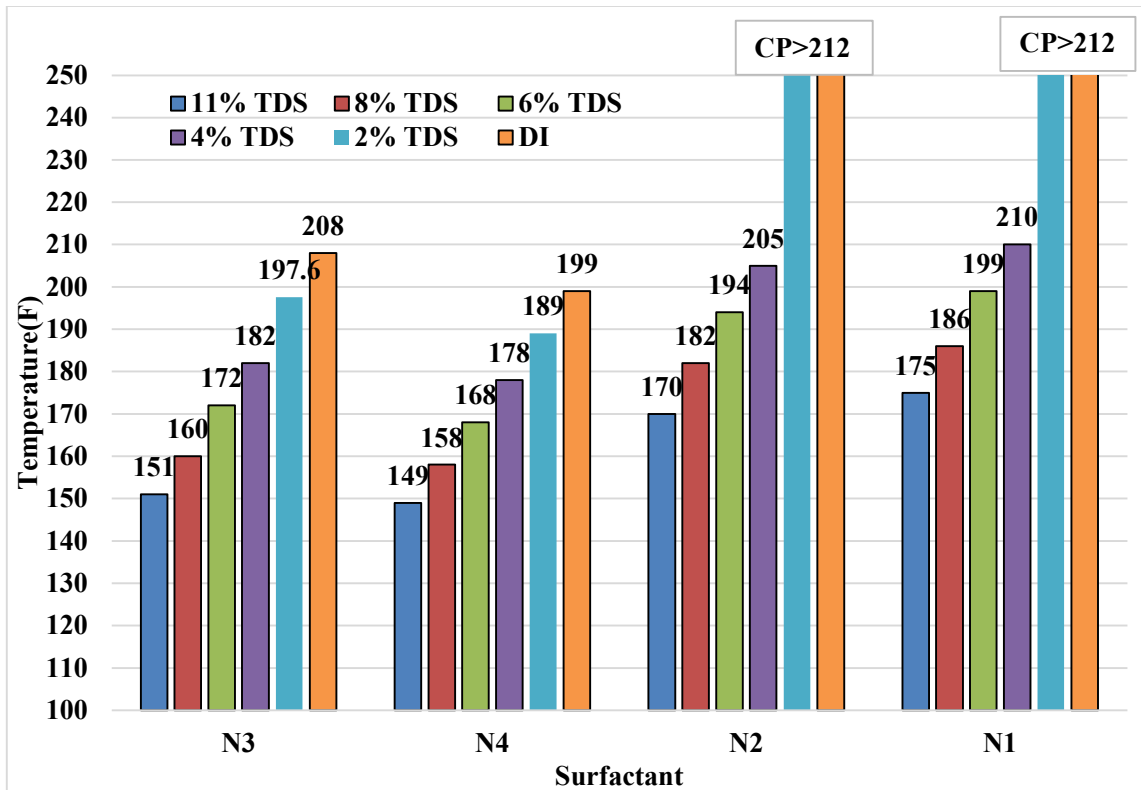
Figure 48: Cloud Points temperatures of N1, N2, N3 and N4

Cloud point measurements are performed again with surfactants N1 and N2 in high pressure conditions. The cloud points of the surfactants N1 and N2 in the same range of temperatures and salinities are observed at a pressure of 250 psia. This experiment serves to mimic the in-situ reservoir temperature and pressure conditions to observe the effect of pressure on cloud points temperatures of the chosen surfactants and to ensure cloud point stability at temperatures above 212 °F. Figure 23 shows the cloud point temperatures of surfactants N1 and N2 with the increase in temperature. At high pressure of 250 psia, the 4% TDS case has the clous points nearly similar to that of the bottom hole temperature of

the well (~220 °F). The cloud point temperatures of the 2% TDS and 0% TDS solutions are above the expected reservoir temperature, which make them suitable for higher temperatures. Cloud point stability is important as the formation of cloud point results in the phasing out of the surfactant from the aqueous phase which may lead to surfactant loss during the injection process before the injection fluid has penetrated effectively into the matrix to alter wettability of the oil-wet rock.
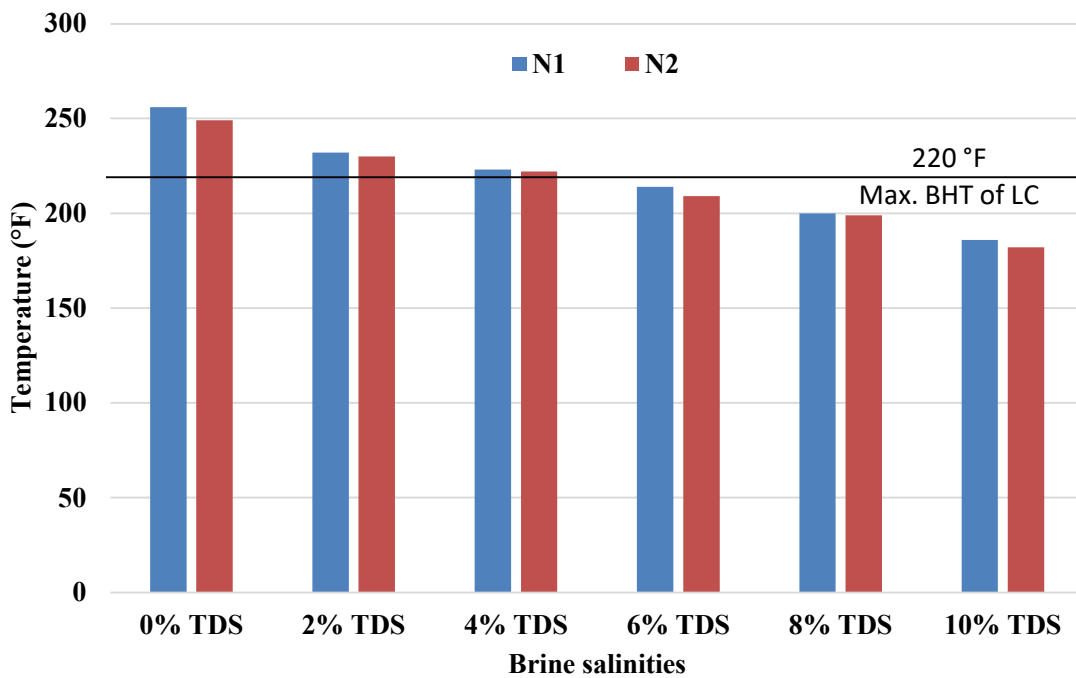
Figure 49: High Pressure High Temperature (HPHT) Cloud point measurements

4.2.4.2. Interfacial Tension Measurements

The performance of surfactants to alter the wettability of a oil-wet porous rock is the ability to alter the interfacial tension between the oil/water interface. The capillary pressure

required at the entry of the throat of the pore spaces in tight unconventional rock is high and therefore IFT reduction mechanisms such as surfactant flooding allowing increases imbibition of the aqueous injection fluid phase into the rock matrix. The decrease in capillary pressure leads to the displacement of the trapped oil in the pore capillaries by the aqueous surfactant solution which results in surfactant molecules coming in contact with rock surface to alter wettability. The alteration of wettability from oil-wet to water-wet results in spontaneous imbibition of the aqueous surfactant solution. IFT is therefore a critical parameter to be considered to assess the wettability alteration performance of surfactants. The IFT of surfactant solutions is affected by temperature and salinity conditions of the system. The IFT of a solution (in presence or absence of surfactant) decreases with the increase in temperature.

Figure 24 shows the results of interfacial tension measurements of brines with different range of salinities as a function of increasing temperature. The IFT of solutions tends to increase with increasing salinity. Some studies have reported similar trends with increasing IFT values as the concentration of salts increase in the solutions in the absence of surfactants, while the general conclusion so far has been than IFT does not show a clear trend with change in salinities as this may also depend on the interactions between the salt ions and the components in the crude oil being used for oil/water IFT measurements.
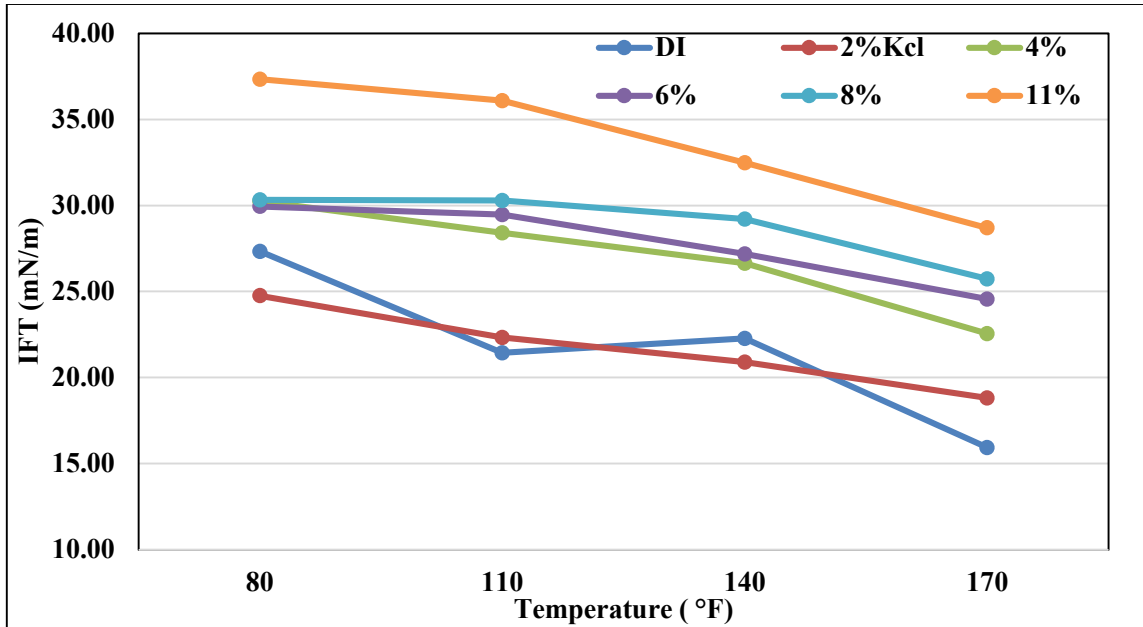
Figure 50: Interfacial tension measurements (brines without surfactant)

Figures 25 and 26 show the interfacial tension measurements on the surfactants N1 and N2. A clear trend is observed with the IFT values of surfactant N1 and N2 where the IFT values decrease with increase in temperature. The IFT values are also impacted by the salinity of the brine where the IFT decreases with increasing salinity across the range of temperatures. This may be explained by the phenomenon of lowered solubility of surfactant solutions in the presence of excess concentration of salt ions. As the concentration of salt ions in the aqueous surfactant solution increases, the solubility of the surfactant decreases due to electrostatic interactions between the surfactant and salt ions which leads to increases surface activity of the surfactant at the oil/water interface, thus leading to lower IFT values. The surfactant N1 and N2 are both able to reduce the IFT values as compared to the IFT without surfactant. (Figure 24)
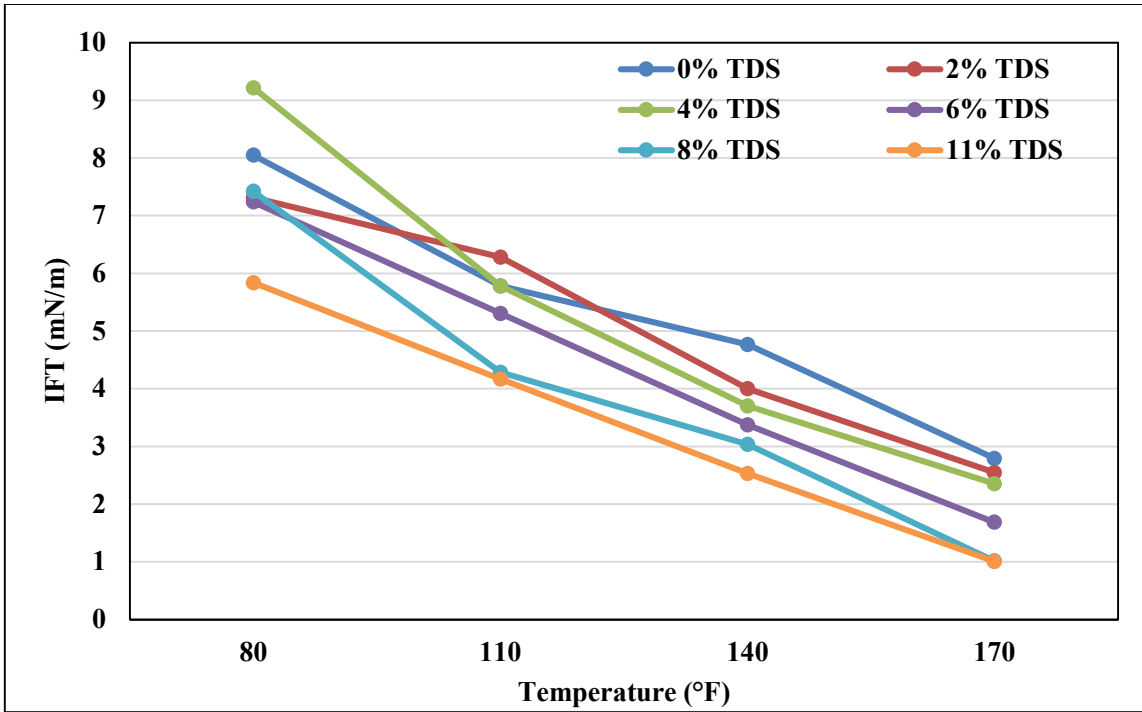
Figure 51: IFT measurements with N2
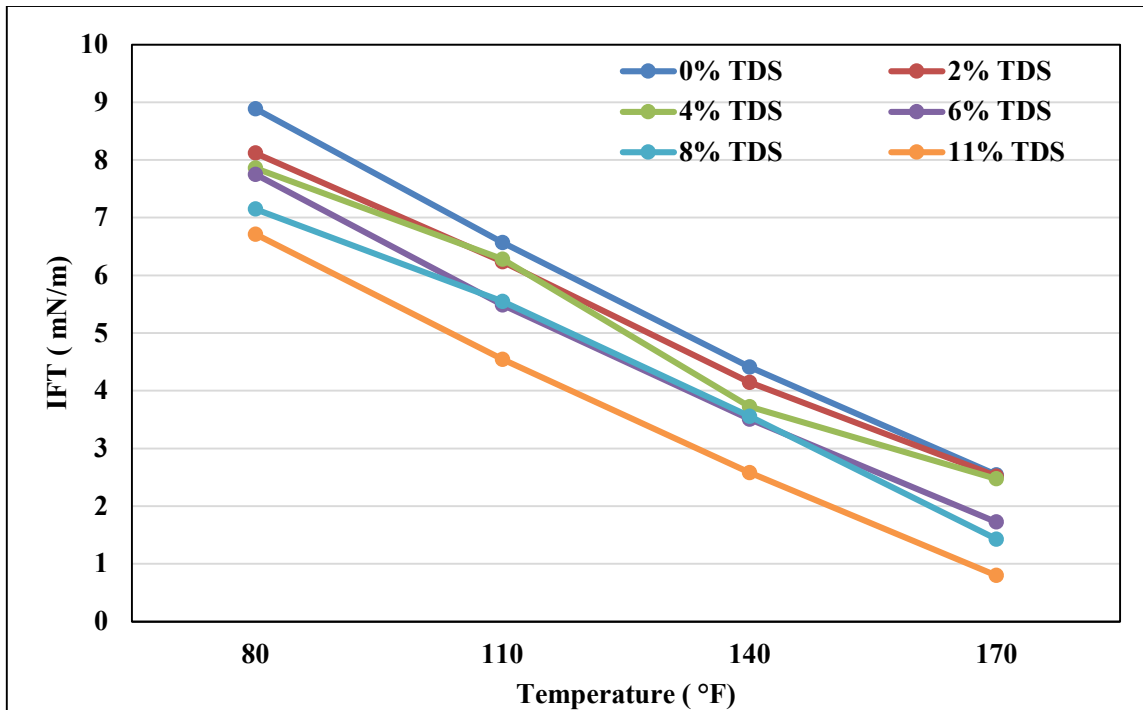
Figure 52: IFT measurements with N1

IFT measurements with surfactants N3 and N4 that have lesser number of EO groups compared to the surfactants N1 and N2 are shown in Figures 27 and 28. The IFT was successfully reduced compared to the case with no surfactant in Figure 24. No noticeable trends were found to be observed in the IFT values as a function of temperature and salinity. This may be due to the impact of cloud point temperatures on the solubility of nonionic surfactants, especially those with smaller EO group sizes. The cloud points of surfactants N3 and N4 are shown in Figure 22 which may explain the hysteresis in interfacial tension measurements as the temperature increases and approaches the cloud point temperature. This is further exaggerated by the presence of high concentrations of salt ions which further lower solubility of the surfactant in the solution. This unstable behavior of interfacial tension for surfactants N3 and N4 due to cloud point issues may

lead to unexplained behavior during wettability alteration processes at reservoir conditions.
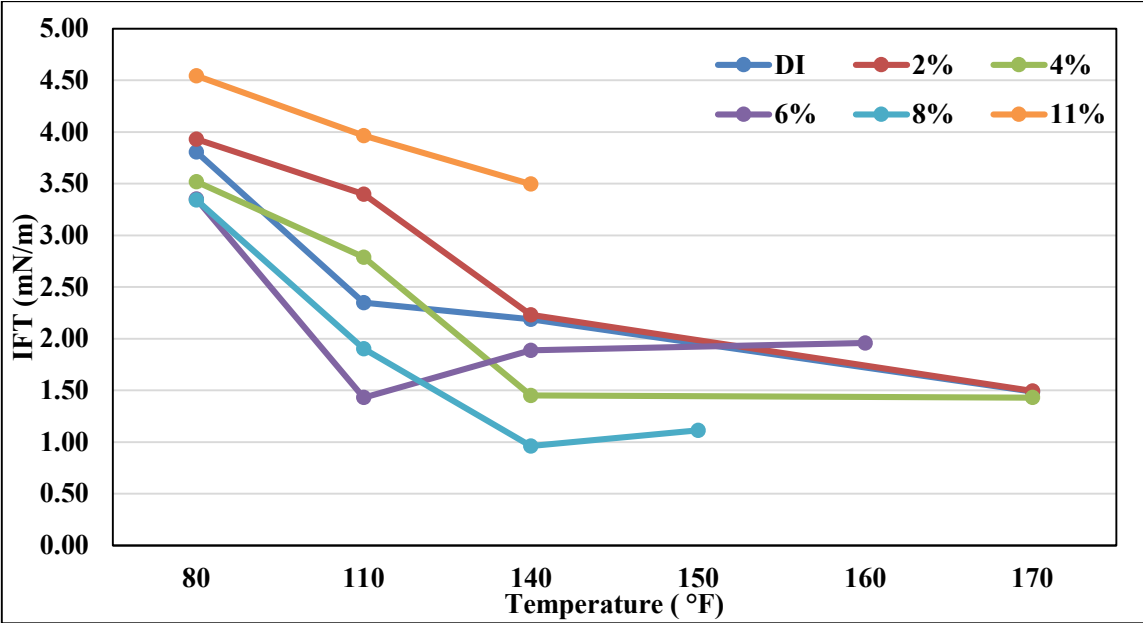
Figure 53: IFT measurements with N3
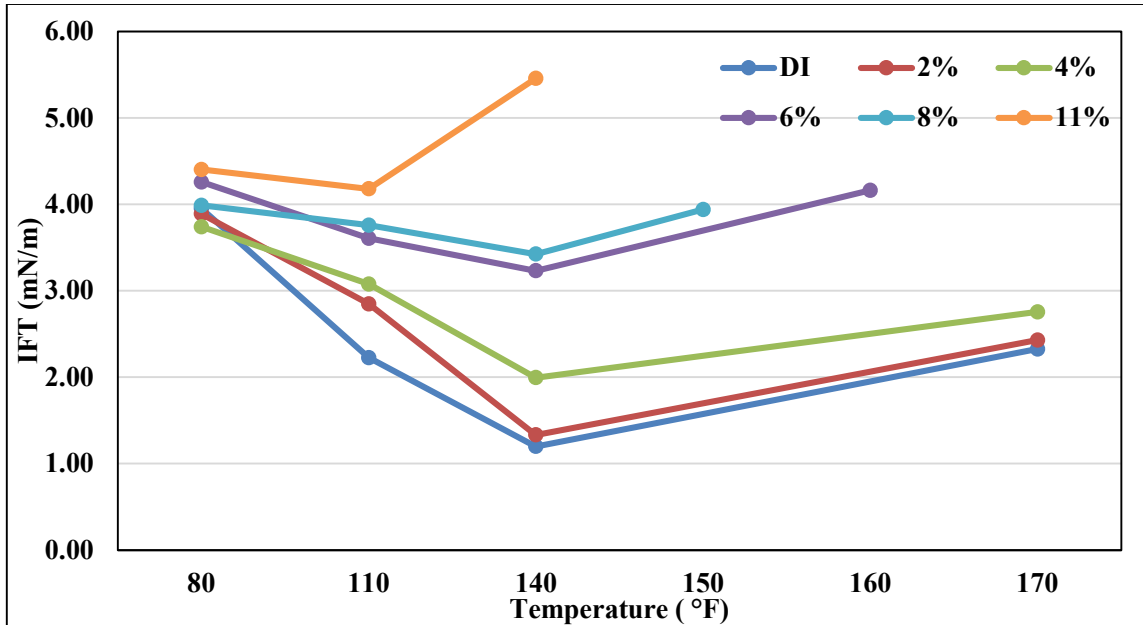
Figure 54: IFT measurements with N4

4.2.4.3. Contact Angle Measurements

Following the initial cloud point tests and interfacial surface tension tests, contact angle measurements are performed on rock chips from the eagle ford shale sample 1 using EF1 and EF2 crude oils. The rock chips are initially aged in the respective crude oils for 6 weeks to achieve original reservoir wettability. The alteration of wettability of the rock by EF1 and EF2 crude oils is shown in Figure. The measurements were performed at 170 °F and the brine used is the 6% diluted PW solutions. The initial wettability of the rock chips before aging are 34 degrees and 28 degrees for the EF1 and EF1 oil/brine/rock system, showing that the chips are initially water-wet prior to aging. As can be observed, the aging process alters the wettability of the rock surface from intermediate-wet at 2 weeks to gradually oil-wet at 6 weeks of aging. The final contact angles of rock chips with the

99

respective oil aged chips are 123 ° for EF1 and 127 ° for EF2 showing that the chips were oil-wet.
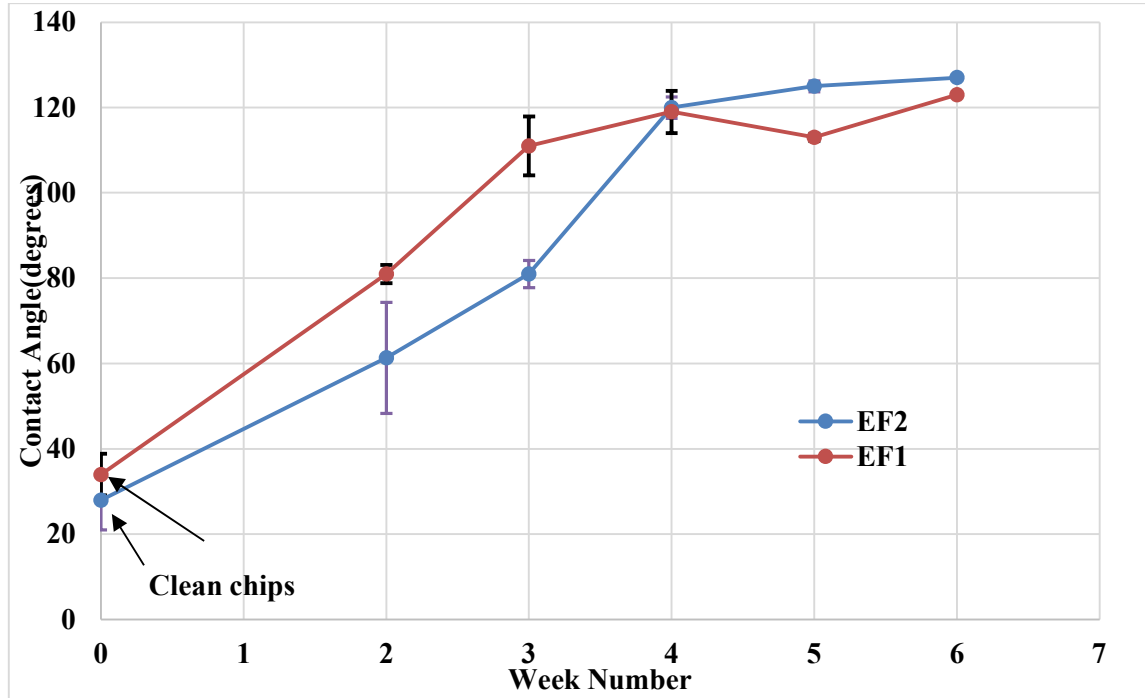
Figure 55: Contact angle values for crude oil/brine/rock system after aging

The wettability alteration performance of nonionic surfactants N1, N2, N3 and N4 are evaluated through contact angle measurements on oil-wet rock chips aged in EF1 crude oil with eagle ford sample 1 rock chips, as shown in Figure 44. Concentration of 0.2 wt. % of surfactant is used for the measurements. The results show that all the nonionic surfactants are able to successfully alter the wettability of the rock at high temperature of 170 °F from oil-wet to water-wet angles below 75 °. The inclusion of biocide does not seem to affect the wettability alteration performance of surfactants.

100

The contact angle of the water-wet chips was nearly 40 ° showing good wettability alteration performance.
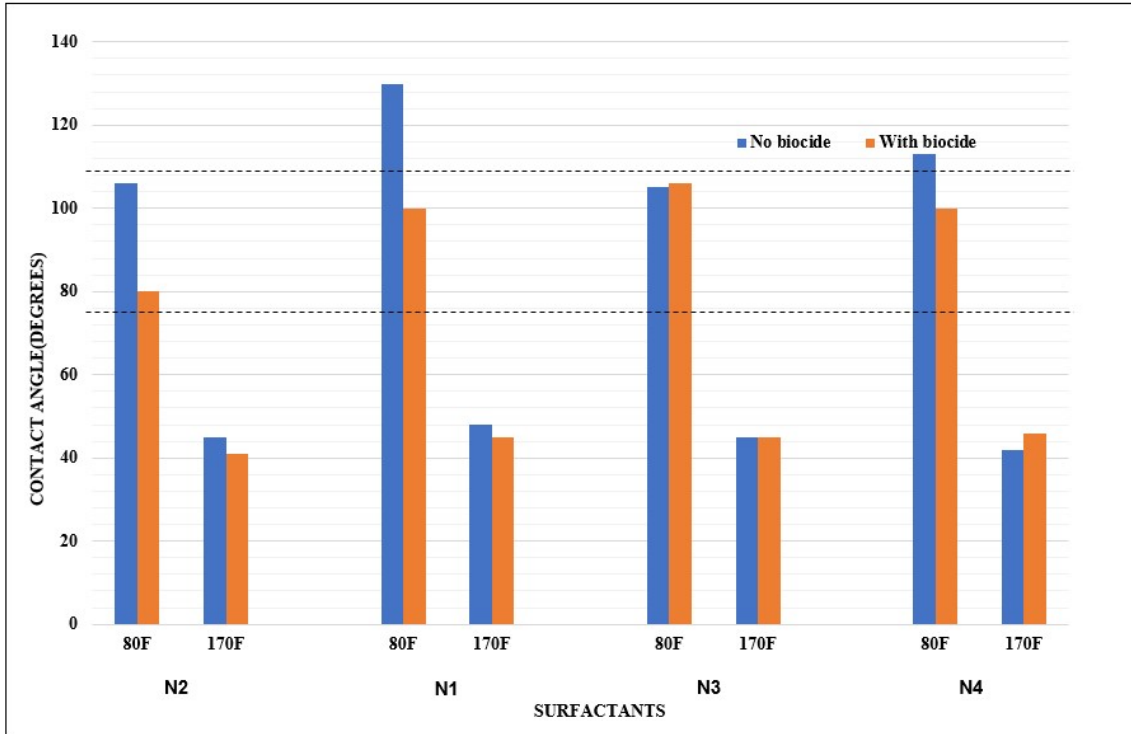
Figure 56: Contact angle measurements on oil-wet rock chips

The 0.2 wt.% surfactant solutions of N1 and N2 with 2% TDS brine were chosen for their wettability alteration performance in contact angle measurement and IFT reduction, as well as their cloud point stability at high reservoir temperatures as compared to surfactants. Low salinities may aid in stability of minerals in the reservoir and studies have shown higher oil recoveries with higher salinity.

4.2.5. Spontaneous Imbibition Experiments

The final stage of surfactant performance evaluation are spontaneous imbibition experiments carried out using surfactants N1, N2 and 2% TDS Brine. Core plugs 1,2 and 3 from Eagle Ford shale sample 1 are used with N1, N2 and Brine respectively. The OOIP of the cores are 1.26 cc, 1.29cc and 0.38 cc for the N1, N2 and brine cases respectively. The initial OOIP of the brine-plug was low. Computerized tomography (CT) scans are taken of the core plugs throughout the imbibition process to observe rock mineral densities as well as pore structure heterogeneities. Figure 45 shows the recovery factor curves for the imbibition experiments.
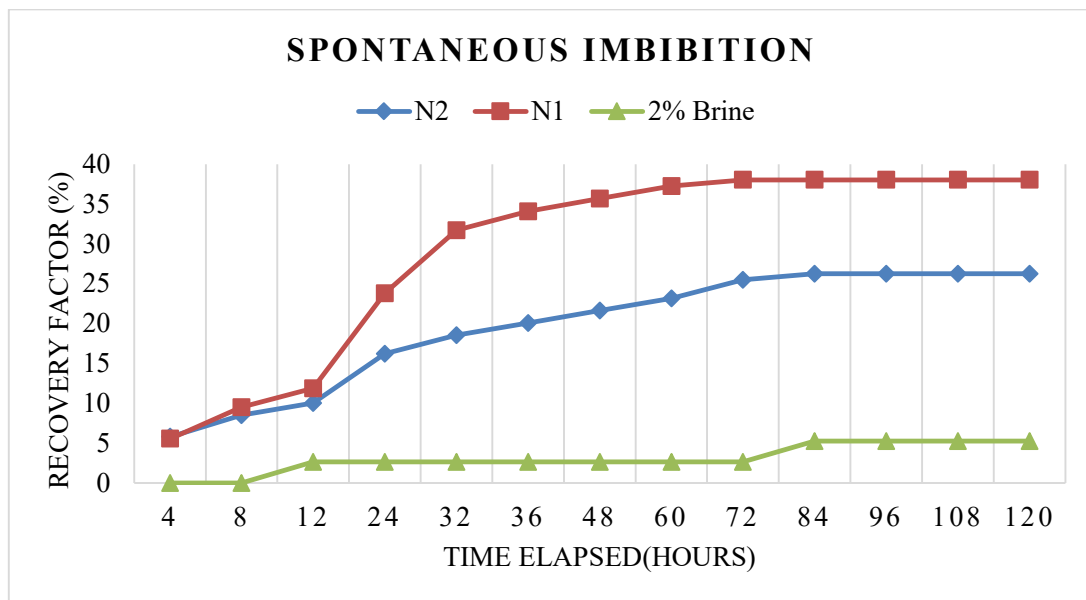
Figure 57: Recovery factor with N1, N2 and brine

A recovery factor of 38% is achieved using surfactant N1, compared to surfactant N2 which improved oil recovery by 26%. The brine case exhibited very low oil recovery

factor of 5%. The performance of surfactants N1 and N2 demonstrates that the presence of surfactant in an aqueous solution leads to higher oil recoveries as compared to a typical brine flooding. We must note that the recovery factor of the core plugs using with surfactant N2 and brine were uncharacteristically low compared to values reported in the literature. Surfactant N1 performs well and is in agreement with recovery factor values reported in lab-scale imbibition tests on Eagle Ford shale rock. An analysis of the CT scan images may aid in understanding the mechanism behind low oil recoveries behind the core plugs 2 and 3 in the case of surfactant N2 and 2% TDS brine.

CT scan images of the core plugs 1,3 and 2 are shown in Figures 54, 55 and 56 respectively with the corresponding ranges of CT number. The change in CT number is observed over the duration of the spontaneous imbibition experiment.
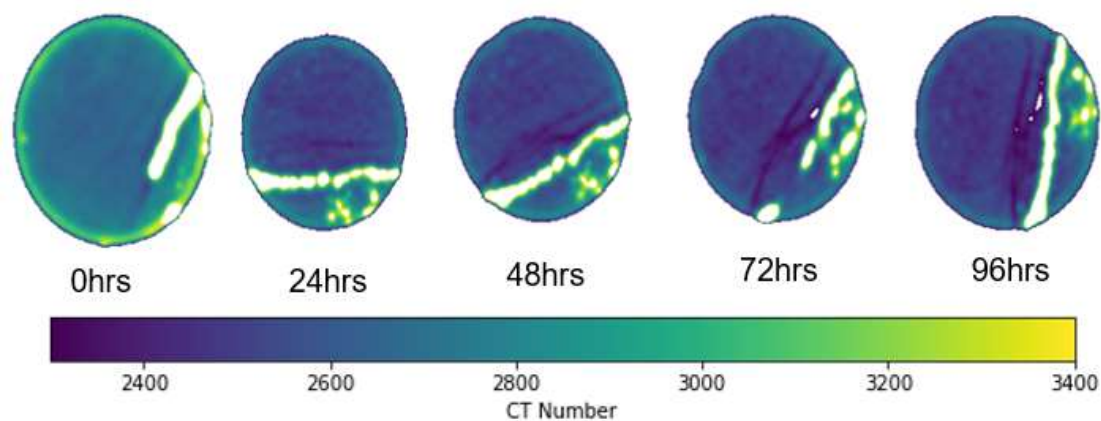
Figure 58: Core Plug 1 (Surfactant N1)
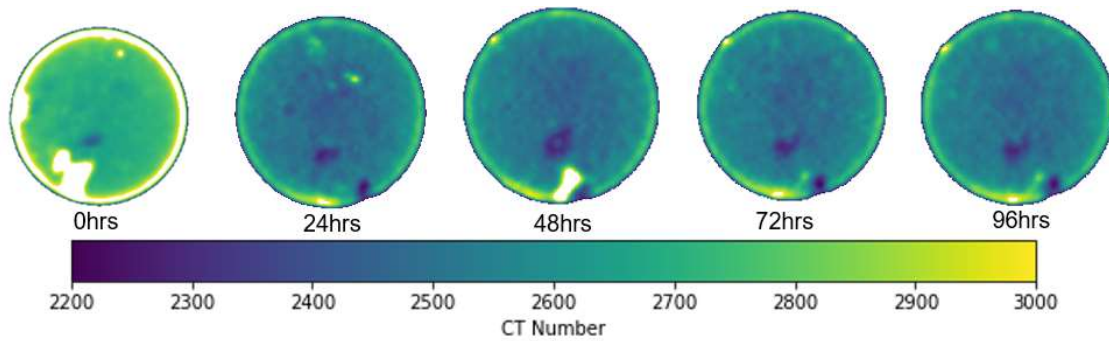
Figure 59: Core Plug 3 (Surfactant N2)
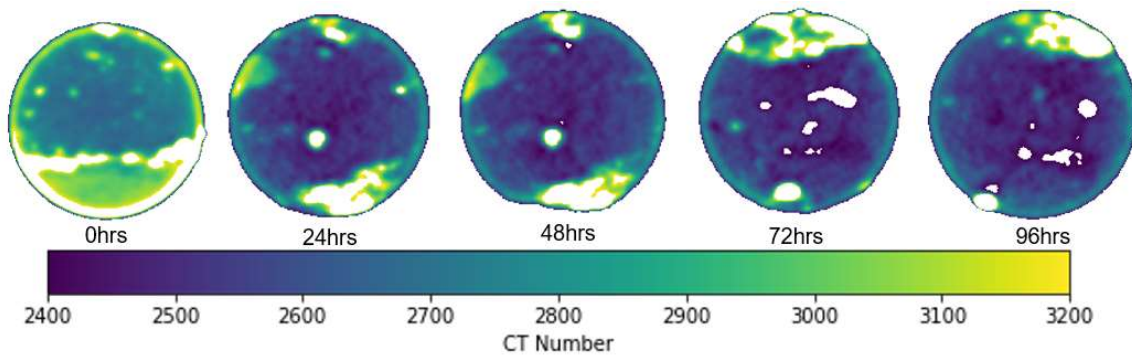
Figure 60: Core Plug 2 (Brine)

The average CT number of the core is noted down for each of the cores at different times through CT scans. The average CT number decreased for each of the cores. The CT number of Core plug 3 was higher than the other core plugs, indicated presence of higher density minerals.

	1	2	3
0hrs	2798.95	2785.51	2920.19
4hrs	2589.01	2571.09	2702.99
8hrs	2591.69	2570.79	2696.51
24hrs	2584.14	2575.51	2707.05
48hrs	2562.67	2578.02	2708.58
72hrs	2549.43	2578.98	2703.99
96hrs	2542.48	2579.89	2701.76
120hrs	2539.1	2584.59	2699.52

Figure 61: Average CT number change

4.2.6. Gel formation tests

As the concentration of surfactant increases in a solution, the surfactant can form a gel as the solubility of the surfactant decreases. The impact of temperature is investigated on the formation of gel. The injection process is scheduled for early December, which indicates the possibility of low ambient temperatures. The purpose of these gel formation tests is to test the feasibility of mixing the concentrated 'stim fluid' under ambient conditions and the ease of transport. The formation of gel is a critical factor in determining the concentration of 'stim fluid' that can be mixed away from the wellsite and transported without practical difficulties. Gel formation can lead to issues with pumping due to the high viscosity of gels and improper mixing of surfactant.

Figure 45 shows the results of the gel formation tests on surfactants N1 and N2 with varying concentrations of 25%, 20% and 15% wt. of surfactant in deionized water at 122

°F, 80 °F and 50 °F. Results show that at high concentration of 25%, gel is formed even at higher temperature of 122 °F. Both N1 and N2 form gels at 80 °F and 50°F. This may be attributed to the lowering of solubility of nonionic surfactants with increasing temperature. At a concentration of 20%, N1 formed a gel at 80 °F, while both N1 and N2 formed gels at 50 °F. The concentration of 15% shows good results with no gel formation even at low temperature of 50 °F. Figure 46 shows the formation of gel at high surfactant concentrations. The temperature was monitored by a thermometer probe and the solution was cooled in an ice bath to ensure gradual decline in temperature. The temperature at which gel was formed was noted. The durations for the concentration solutions to solubilize in fresh water were also recorded to estimate the mixability of the 'stim fluid' with fresh water. Cases with no gel formation dissolved instantly in fresh water to form 0.2 wt. % aqueous surfactant solutions. Based on the gel formation results, a 12.5 wt. % solution of surfactant is chosen to avoid issues arising from pumping highly viscous gel through the pumps.

N1

		Gel	
		Yes	No
25%	122F	Yes	
	80F	Yes	
	50F	Yes	
20%	122F		No
	80F	Yes	
	50F	Yes	
15%	122F		No
	80F		No
	50F		No

N2

		Gel	
		Yes	No
25%	122F		No
	80F	Yes	
	50F	Yes	
20%	122F		No
	80F		No
	50F	Yes	
15%	122F		No
	80F		No
	50F		No

L230 Master Blend Dissolution test

		Dissolution Time (min.)
25%	122F	1-2 min
	80F	3-4 min
	50F	4-5 min
20%	122F	<30 secs
	80F	3-4 min
	50F	5-6 min
15%	122F	Instant
	80F	Instant
	50F	Instant

24-22 Master Blend Dissolution test

		Dissolution Time (min.)
25%	122F	<30 secs
	80F	3-4 min
	50F	5-6 min
20%	122F	Instant
	80F	Instant
	50F	4-5 min
15%	122F	Instant
	80F	Instant
	50F	Instant

Figure 62: Gel test results with N1 and N2
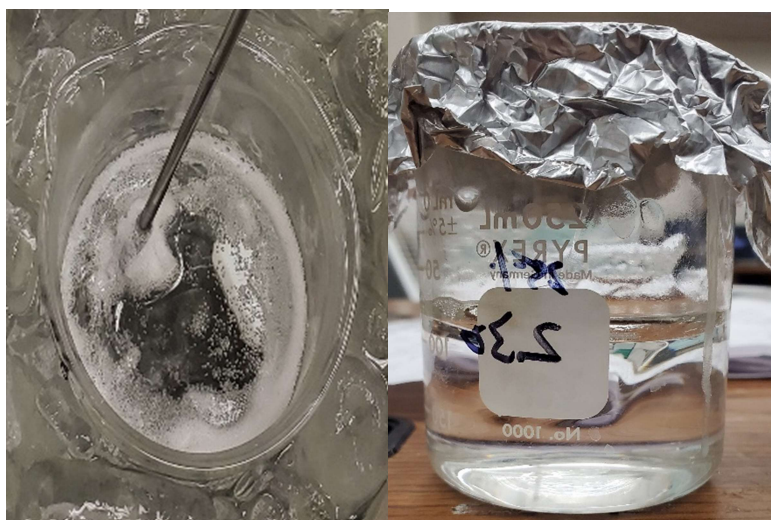
Figure 63: Gel formation test

4.2.7. Pre-injection validation

Prior to injection process, a final check was made using the FW and PW samples from the well to fabricate the injection fluid. The TDS of the PW was measured to be 14.2% TDS which is consistent with the salinity history of the produced water from the LC well. The TDS of the FW was 0%. The PW and FW are mixed together to form the 2% TDS brine. 0.2 wt.% surfactant N1 and 0.01% (64 ppm) of glutaraldehyde are added to the 2% TDS brine to mimic the field scale properties of the injection fluid. Contact angle measurements show that the mixture of field sampled PW and FW are able to successfully alter wettability of oil-aged chips to water-wet when mixed with 0.2 wt. % surfactant N1 and 0.01 wt. % glutaraldehyde.
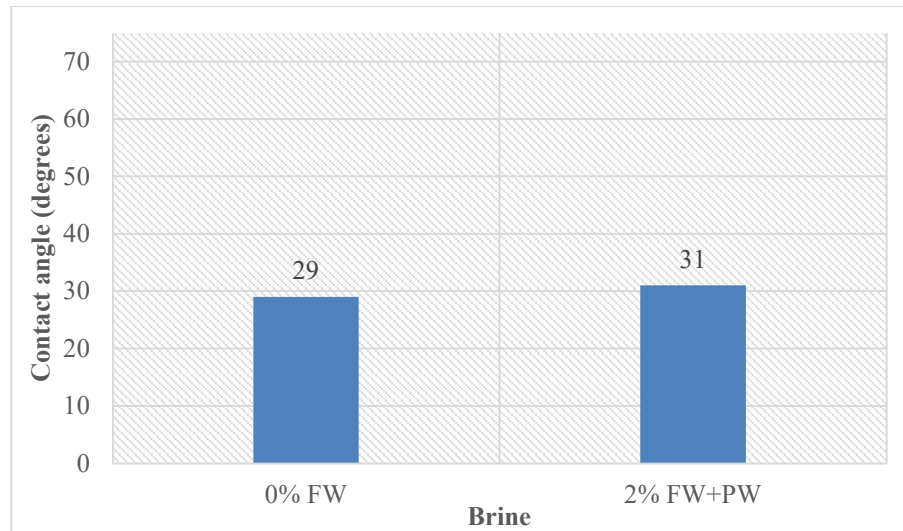
Figure 64: Contact angle with injection fluid

4.2.8. Injection Fluid composition

The wettability performance evaluation on a set of nonionic surfactants N1, N2, N3 and N4 was performed through contact angle, interfacial tension and spontaneous imbibition experiments. The cloud points of the solutions were also investigated into. Based on the results, the 0.2 wt. % solution of surfactant N1 with 2% TDS brine and 0.01% biocide was chosen as the injection fluid composition as it was able to demonstrate high oil recovery factors in spontaneous imbibition tests and low water-wet angles in the contact angle tests. The presence of biocide did not affect the performance of the surfactants. A concentrated master solution (MS) is prepared with a 12.5 wt. % surfactant with DI which is mixed with FW and PW in the field to achieve the desired composition. The well is injected with the injection fluid and allowed to soak for 1 month.

4.3. Post-Injection

4.3.1. Surfactant Concentration measurement analysis

The calibration curves are generated for aqueous solution of surfactant N1 with 6% TDS brine. According to literature, at lower concentrations below the CMC, the slope of the lines when plotted against the respective concentrations result in a linear line. It is then possible to estimate the concentration of an unknown sample of surfactant solution when the concentrations are below the CMC.
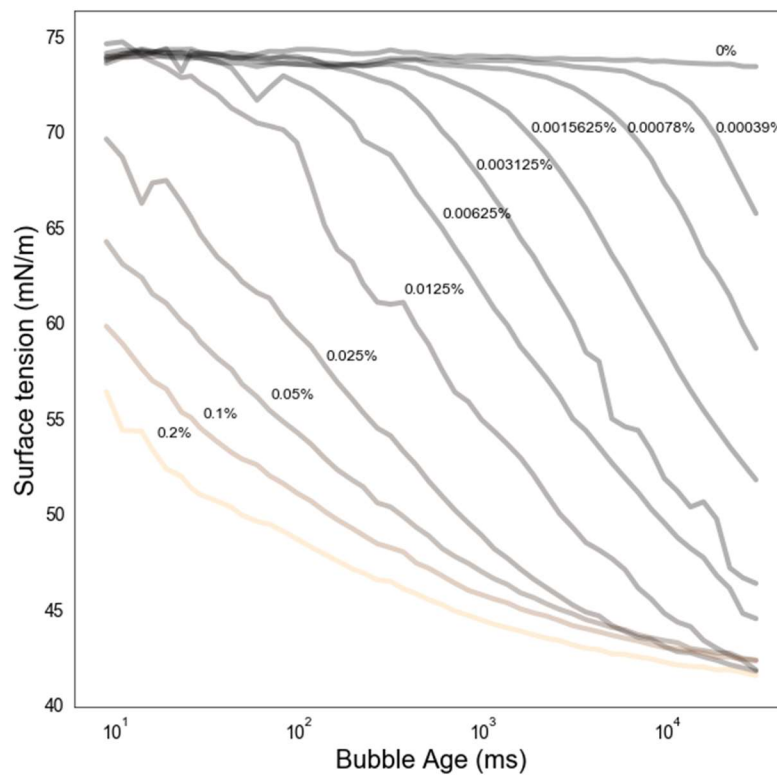
Figure 65: N1 calibration curves with 6% Brine
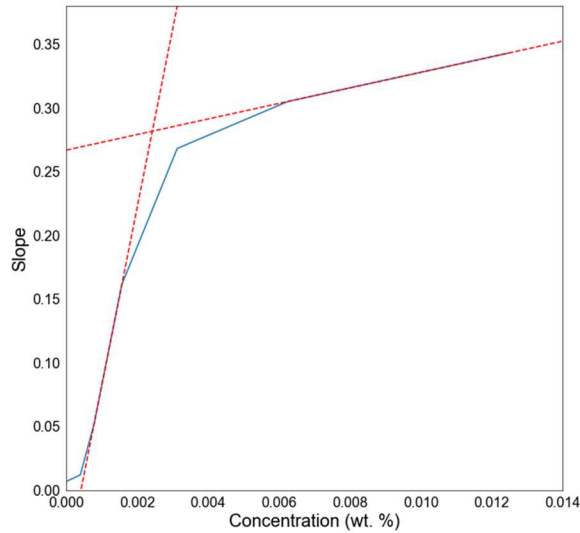
Figure 66: Slope vs concentration (N1 6% brine calibration curves)

Plotting the graph of slopes of the DST curves versus the respective concentrations does not show a linear trend. This may be due to the fact that the surfactant seems to cross a CMC value at around 0.002 % concentration of surfactant. This effect makes it inconvenient to estimate the surfactant concentration using this method. A new methodology will be used whereby the surface tension values at a particular bubble age are plotted against the respective surfactant concentrations to generate a plot shown in the next section.

4.3.2. Produced water analysis

The well was put back on production in January after soaking for 1 month in injection fluid. The produced water from the well was collected and analyzed over the course of several months of well production to evaluate the amount of residual surfactant in flowback waters. Bubble pressure tensiometer is used to generate surface tension data of

produced water fluids which are then integrated with the DST calibration curves of surfactant N1 in a brine with similar TDS. In this case, 6% PW brine is used as the aqueous fluid. Figures 54, 55 and 56 show the surfactant concentration analysis method for produced water samples from January 14th to January 19th. Figure 63 shows the DST measurements for the respective produced water samples from Jan 14th to Jan 15th. The method to estimate concentration is shown in Figure 64, where the curve is generated by plotting surface tensions at constant bubble age (1s, 10s) versus the concentrations of the respective solutions. The X-intercept is found for the surface tension value of the PW sample at the same bubble age as the Y-axis value. This method can allow us to quantitatively measure the surfactant concentrations returning in the produced water samples. The concentrations of the surfactant initially are typically found to be around 0.003125% and 0.00625 % concentrations. Similarly, the analysis is done for produced water samples throughout. A total of 49 samples were processed for surfactant concentration measurements. Figure 57 shows a layout of the produced water analysis performed for all samples from January to July of 2021.
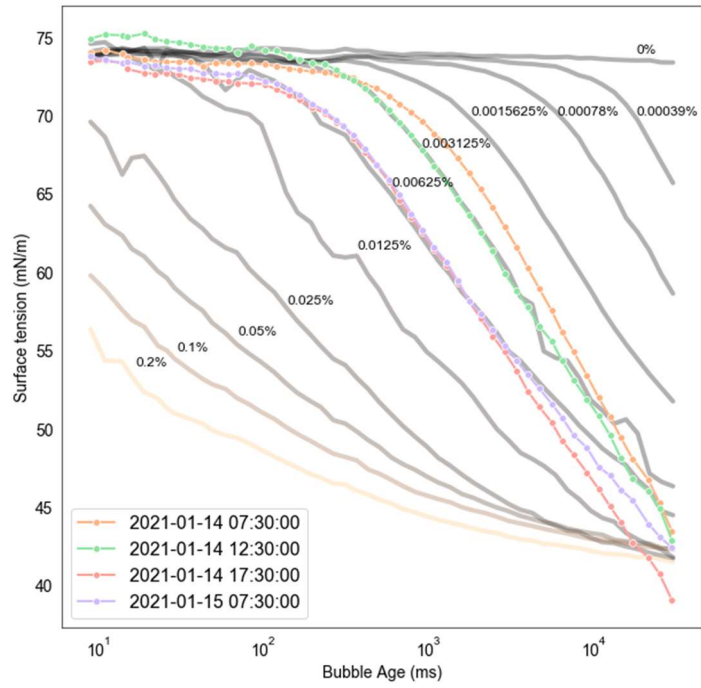
Figure 67: Jan 14th to 15th PW analysis
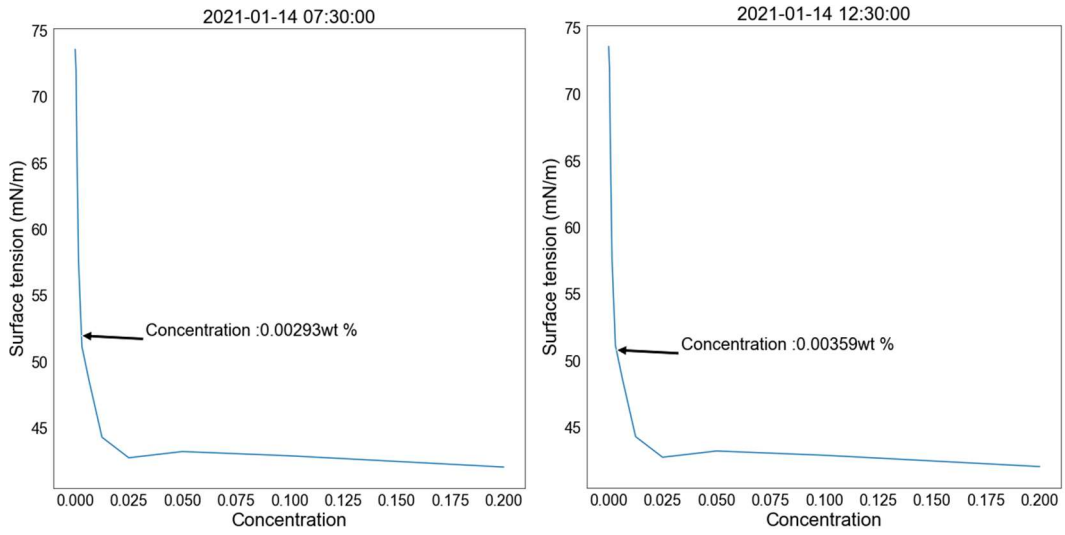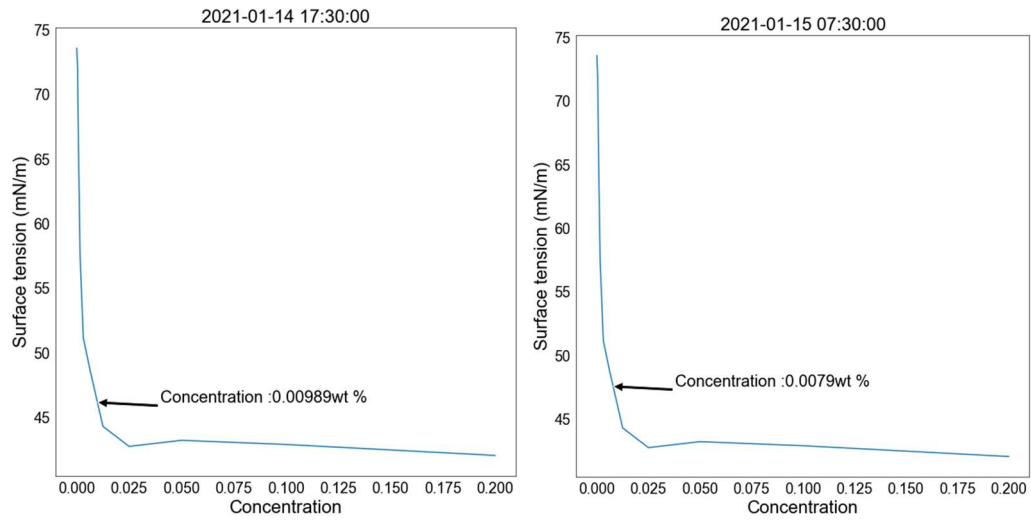
Figure 68: Estimating concentrations from PW samples (Jan 14th to Jan 15th)
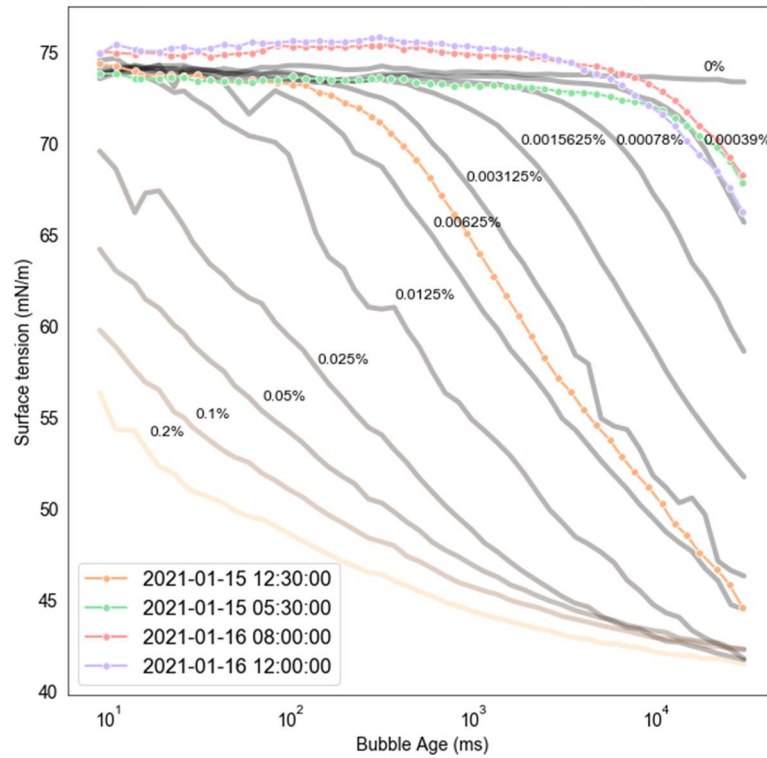
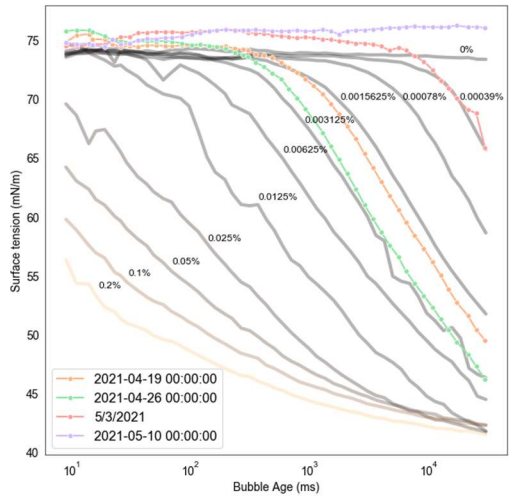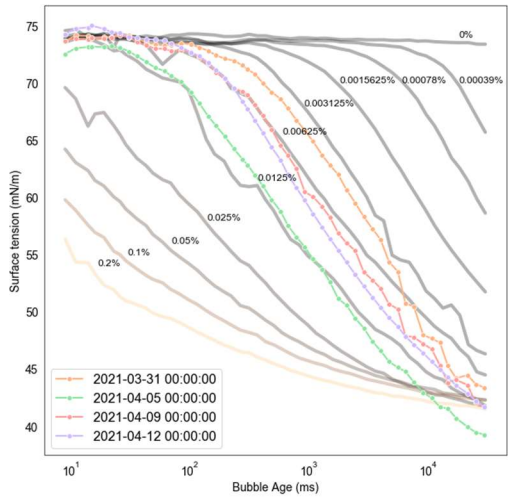
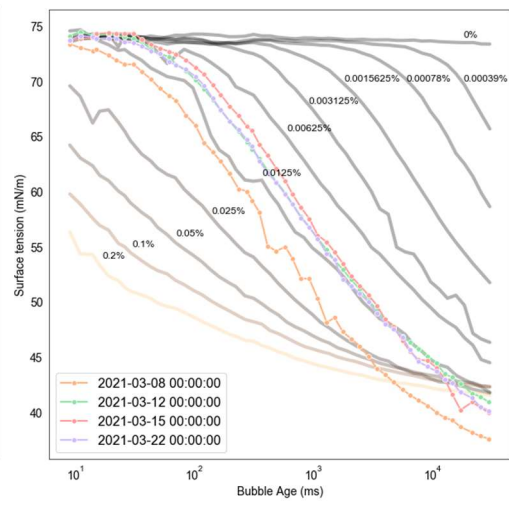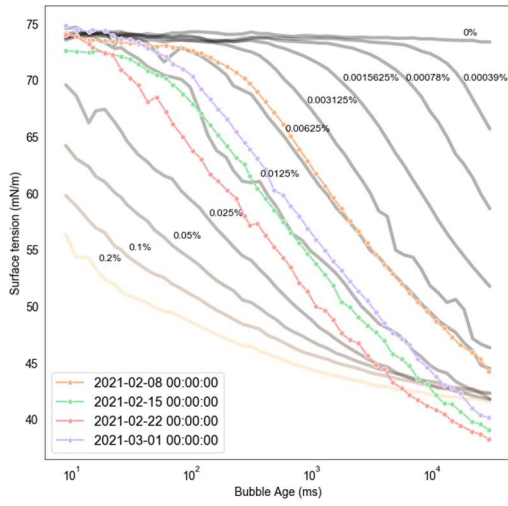**Figure 69: PW analysis from Jan 15th to Jan 16th**

114
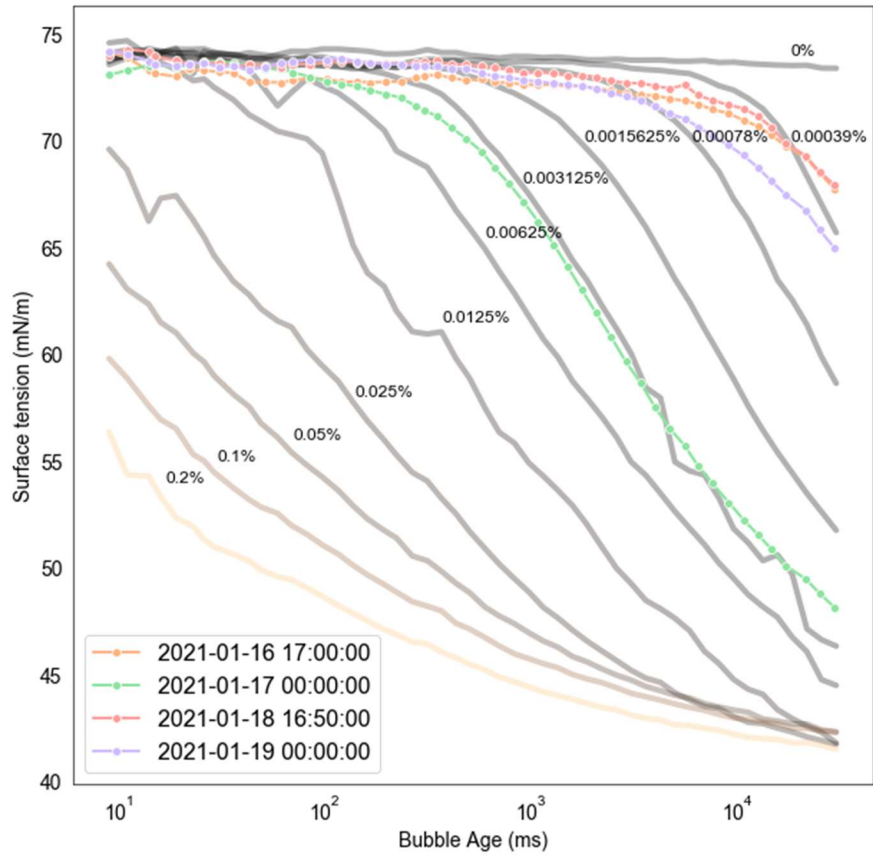
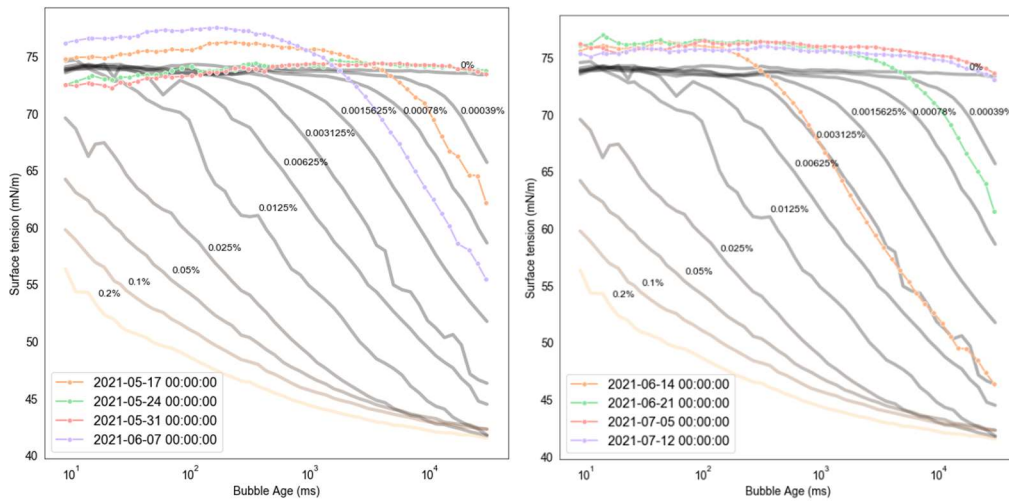**Figure 70: PW sample analysis from Jan 16th to Jan 19th**
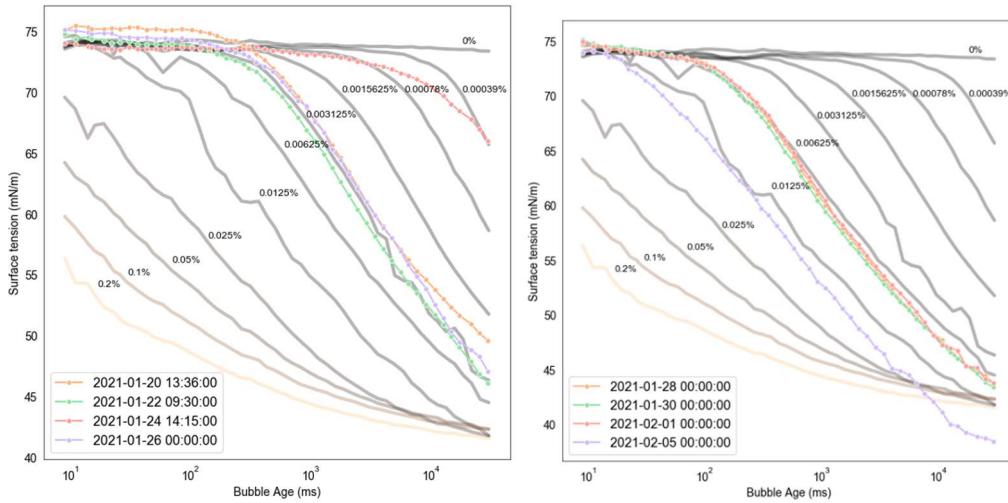
Figure 71: PW sample analysis A) Jan 20th – Jan 26th B) Jan 28th – Feb 5th C) Feb 8th – March 1st D) March 8th – March 22nd E) March 31st – April 12th F) April 19th – May 10th G) May 17th – June 7th F) June 14th – July 12th

The salinity of the produced water samples is also recorded by performing TDS measurements. Figure 58 shows the graph plotting the variation in salinity and surfactant concentration with time. The salinity of the PW from the well pre-injection was about 14% TDS, whereas the salinity of the PW post-injection is nearly 7% TDS. This shows that the injection process has affected the in-situ fluid balance and composition. This may be due to the dilution of reservoir brine by 2% injection fluid, or the injection procedure has resulted in fractures in the rock matrix that have allowed freshwater from an aquifer to leak into the reservoir rock during production. The surfactant concentration noticeably increases over 4 months from the beginning of production to April, and then declines gradually over the months of May to July. The TDS of the produced water remained nearly constant throughout the production of the well.
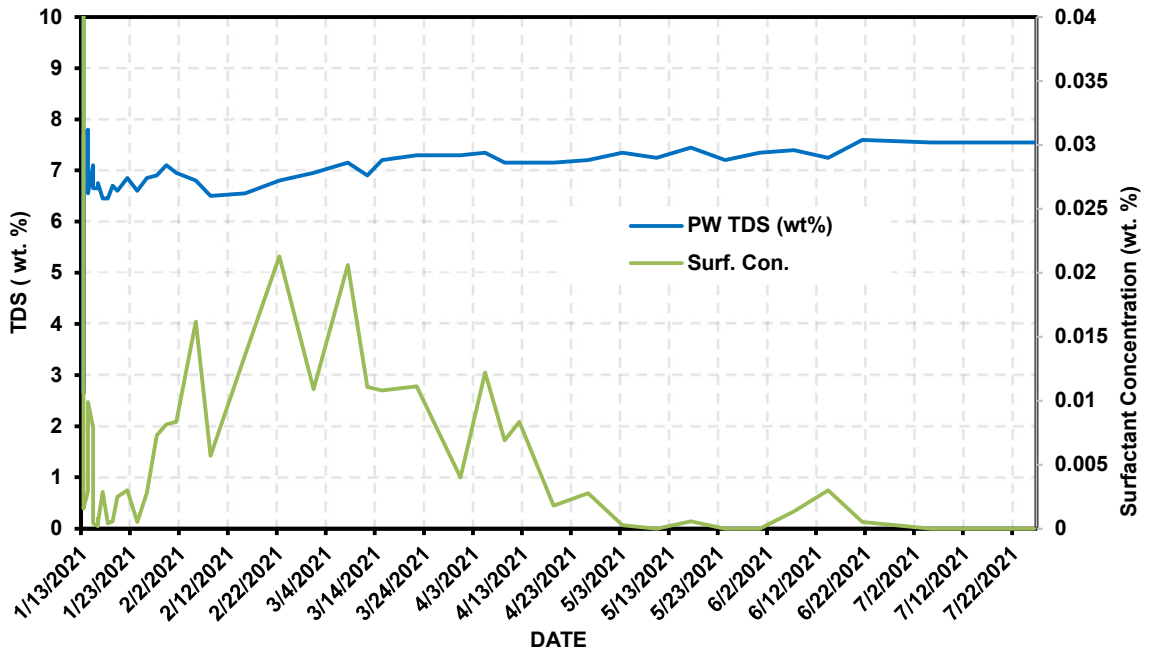
117

Figure 72: PW salinity and surfactant concentration

4.3.3. Water production and Residual surfactant mass

The water production of the well is shown in Figure 59. High surfactant concentrations are observed during peak daily water production in the first 2 months, The water production gradually declines from a peak of 250 bbl. to an average steady production of 80 bbl. The surfactant mass is calculated by multiplying the concentration of the surfactant measured from DST measurements with the daily water production to obtain daily surfactant mass returned values. The total mass of surfactant used in 15000 bbls of injection fluid was 8500 bbls of surfactant N1. By referencing the initial mass of surfactant, it is possible to estimate the mass of residual surfactant in the produced water. The total mass of surfactant returned was calculated to be approximately 563 lbs. This

indicates that only 6.62 % of the initial surfactant mass has been returned to the surface after the injection process. The bulk of the surfactant has been retained in the reservoir matrix which may lead to further penetration of surfactant into the reservoir and wettability alteration of inaccessible zones.
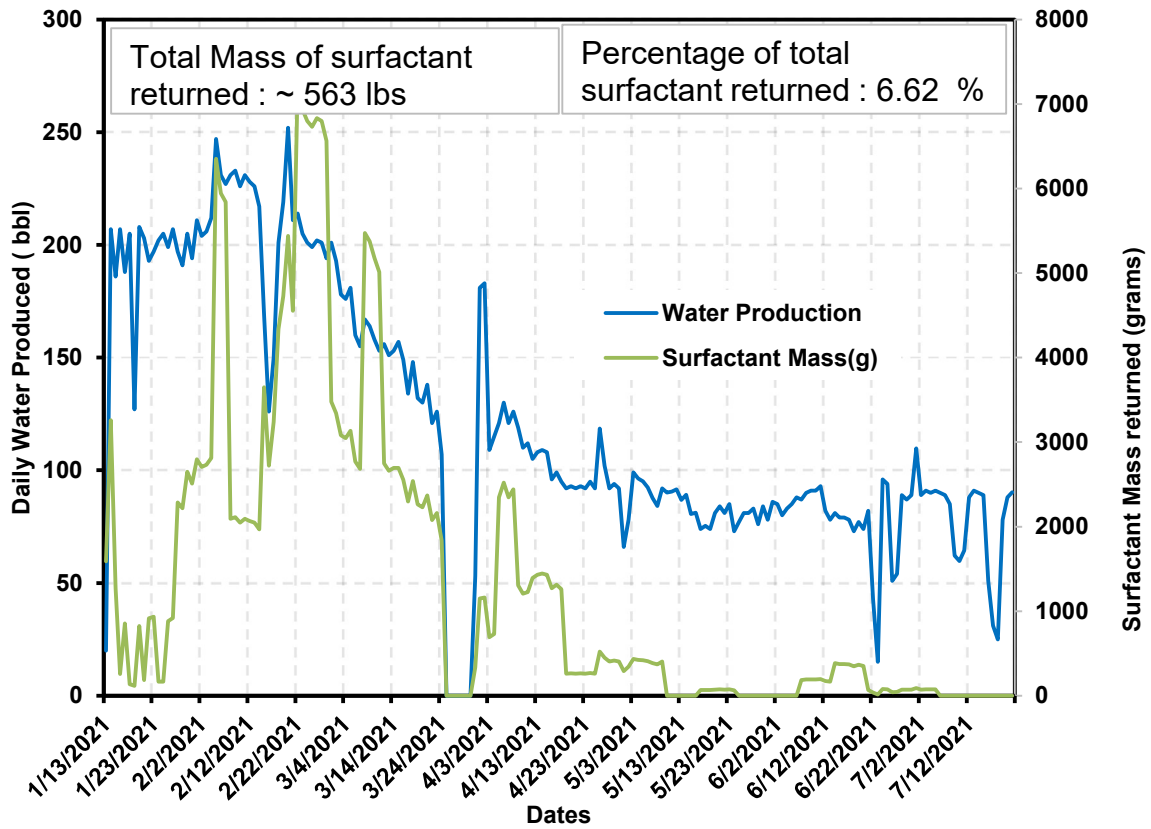

Figure 73: Daily water production (bbls) vs surfactant mass (grams)

4.3.4. Oil production and analysis

The density of the oil produced post-injection was measured to be 0.9045 g/cm^{3,} which is similar to the density of the crude oil prior to injection. The daily oil and water production is graphed in Figure 60. The average daily oil production rate was 14 bbls from February to July.
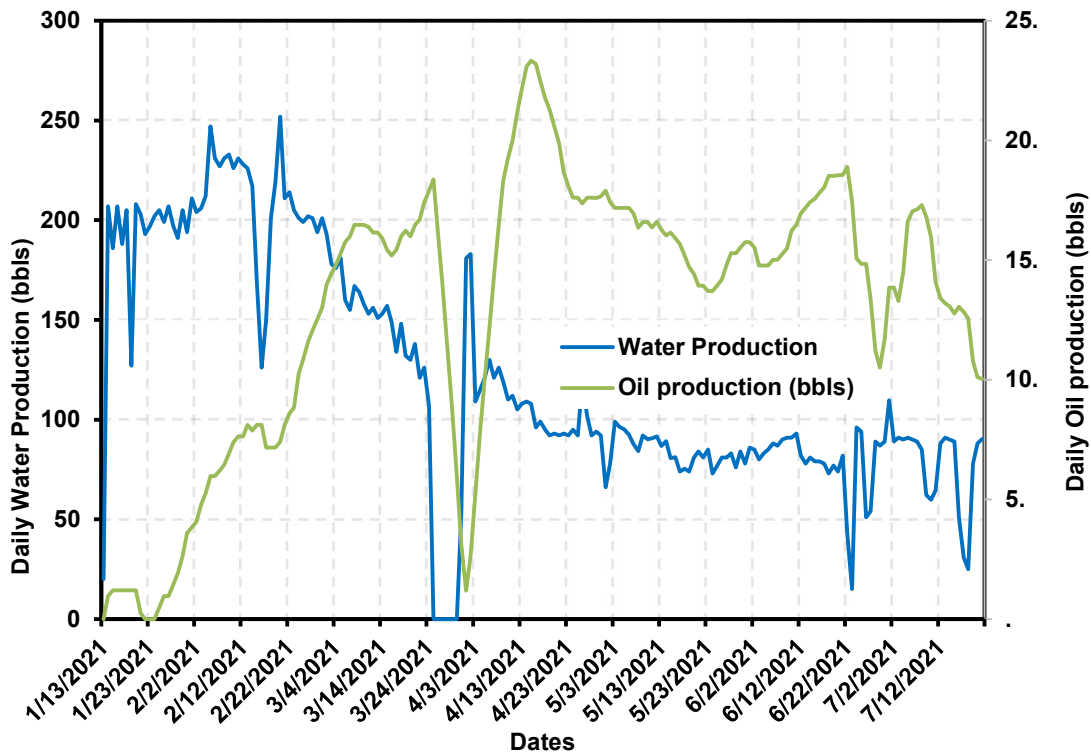
Figure 74: Daily oil and water production of Laughlin Cook (bbls)

4.3.5. Production Performance evaluation

The monthly oil and gas production prior to injection and post-injection is shown in Figure 61 and 62. The average daily oil production rate post-injection from January 2021 to July 2021 was 14 bbls, whereas the average daily oil production rate for 2020 was

approximately 5 bbls. This was an approximately 200% increase in daily oil production rates. This shows that the injection fluid consisting of wettability altering surfactants leads to increased oil production rates and therefore improved ultimate oil recovery potential. The effectiveness of tertiary chemical EOR processes such as surfactant flooding is a viable option to improve oil production rates and oil recovery from mature wells in the Eagle Ford basin that suffer from low oil production.
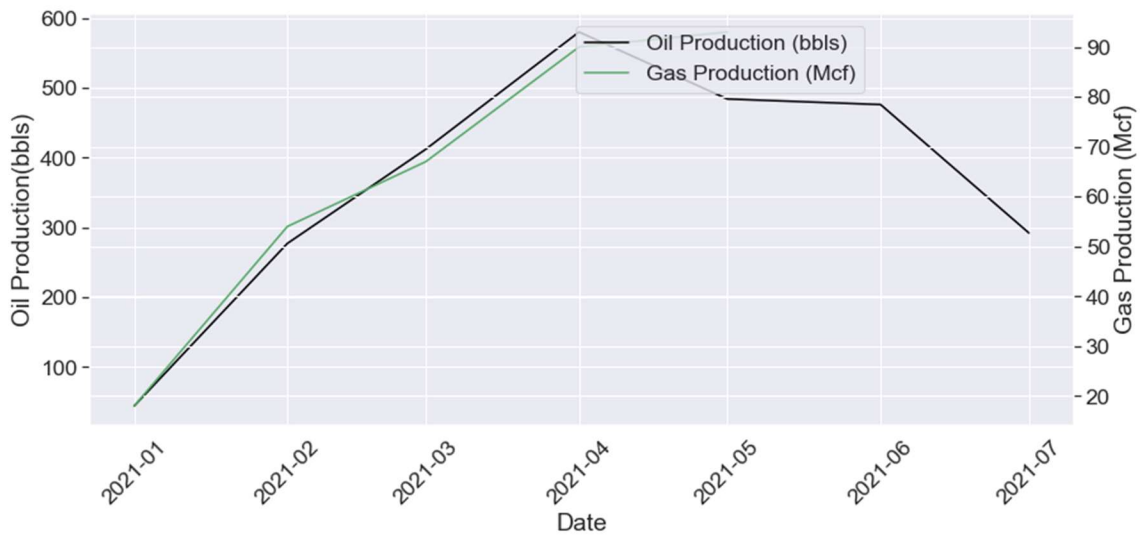

Figure 75: Monthly oil and gas production of LC (bbls) post-injection
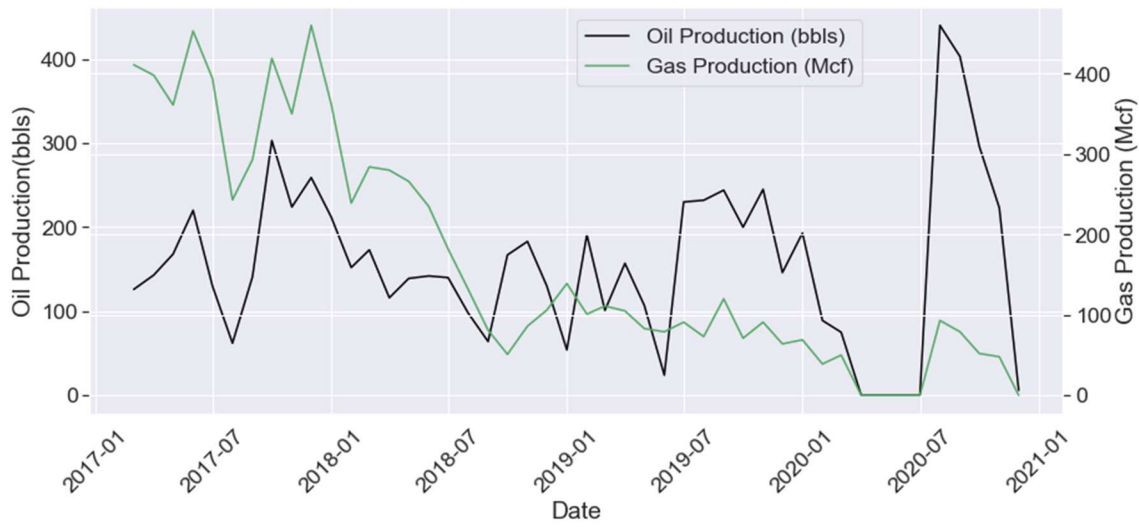
Figure 76: Monthly oil and gas production of LC (bbls) pre-injection

Figure 63 shows the complete data of oil production, water production, salinity of produced water and surfactant concentrations returned in the produced water. The water production was divided by 10 for convenient plotting. The oil production has was observed to reach a daily maximum production rate at the highest concentrations of surfactant in the produced water. The salinity of the produced water is at a plateau with values of 7% TDS. The water production followed the same trend as the oil production. The concentration of surfactants in the produced fluid initially increased within a month of production and slowly declined over the course of a few months, with no noticeable surfactant being returned after 5 months.
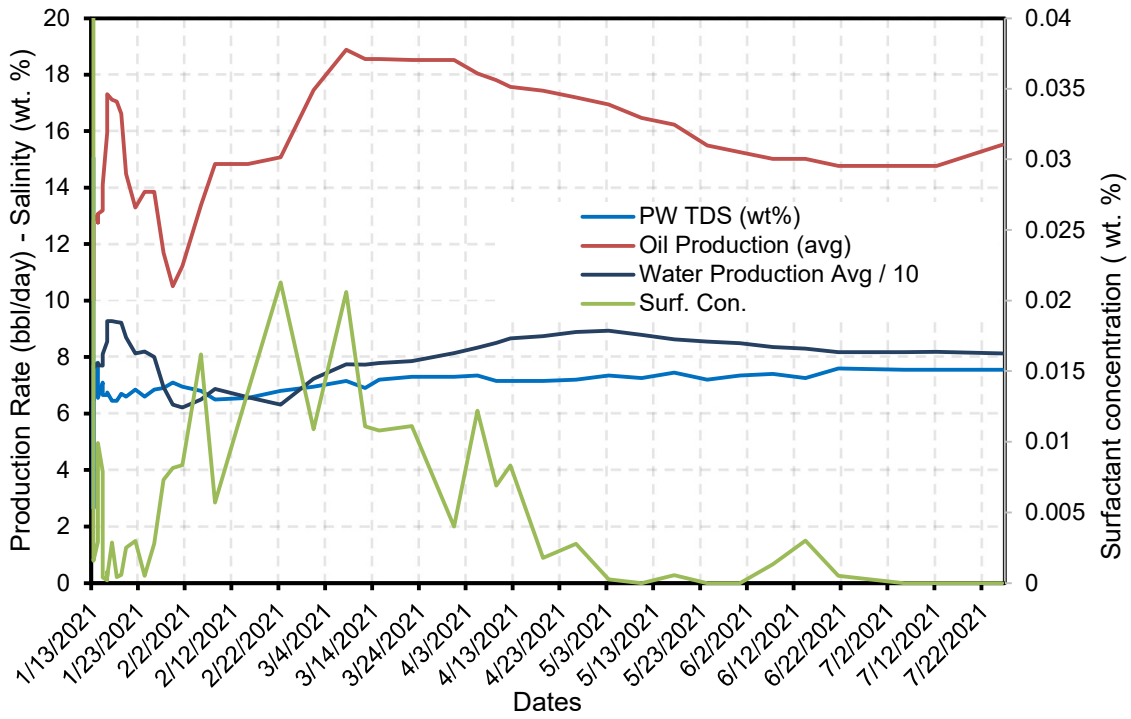
Figure 77: Complete production history of Laughlin Cook well

5. SURFACTANT ADSORPTION EXPERIMENTS

Surfactant adsorption on different rock types have been studied extensively in the literature. The adsorption of a surfactant is typically measured by the adsorption density (mg/gr) of the surfactant onto the rock. The adsorption density has been shown to be dependent upon the surfactant type and the rock type, i.e., the similarity between the charges. Ionic surfactants may lead to wettability alteration through ion-pair formation and surfactant adsorption mechanisms. In the case of surfactant adsorption, the surfactant molecules may adsorb onto the rock surface with either the hydrophobic tail o the hydrophilic head attached to the surface of the rock and may form a double layer depending upon the bulk surfactant concentrations present in the ambient aqueous phase.

This study aims to characterize the surfactant adsorption characteristics of different surfactant types (cationic, anionic, nonionic) with different rock types, with a focus on nonionic surfactants. The rock s used were Eagle Ford Shale Sample 2(EF Shale 2), Limestone outcrop (LS) and Sandstone Outcrop (SS). The effects of surfactant type will be investigated to observe the trends in adsorption dynamics of different types of surfactants. This study attempts to introduce a methodology to quantify the surfactant adsorption density(mg/gr) on the rock surface by measuring the change in surfactant concentration with respect to the weight of the rock. The surface area of the rock is not considered in the study, but instead the adsorption density is correlated with the weights of the rock samples to identify trends in adsorption characteristics between surfactants and

reservoir rock samples. The samples used are taken with weights ranging from 13 grams

to 20 grams approximately. The weights and samples are given in the Table in Figure 71.

sample	sample_wt (g)	sample_no
EF Shale 2	13.940	1A
EF Shale 2	17.721	2A
EF Shale 2	17.720	1B
EF Shale 2	17.657	5B
EF Shale 2	15.628	6B
Sandstone	15.027	1C
Sandstone	16.336	2C
Sandstone	19.316	3C
Sandstone	18.129	4C
Limestone	15.728	5C
Limestone	16.613	6C
Limestone	18.954	7C
Limestone	15.001	8C
Sandstone	16.256	8D
Limestone	19.424	6D
Sandstone	20.230	3D
Limestone	18.490	1D

Figure 78: Rock samples, weights (gr) and sample codes

The different rock samples were immersed in 20 cc of the respective aqueous surfactant solution at 0.05 wt. % concentrations in a glass beaker. The measurements are taken until no further change in concentration is observed.
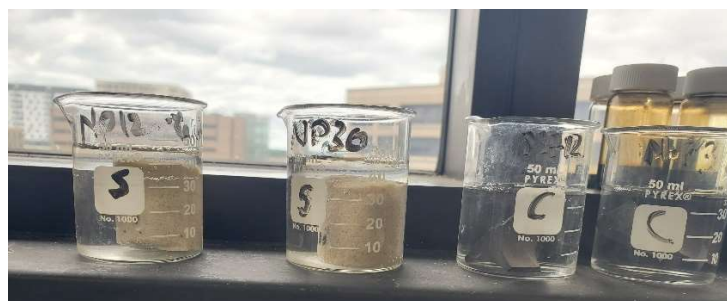
Figure 79: Surfactant adsorption with BPT experiments

5.1. Adsorption of Non-ionic surfactants on different rock types

The focus of this study was to quantify the adsorption of non-ionic surfactants on carbonates and sandstones. The rocks chosen are shale samples from the Eagle Ford (EF Shale 2), Limestone Outcrop (LS) and Sandstone Outcrop (SS). Non-ionic surfactants

have been shown to be effective in altering wettability of carbonate rock. We aim to investigate the adsorption of non-ionic surfactants through the dynamic surface tension measurements. De-sorption experiments were also looked at to investigate the increase in surface activity when the surfactant-saturated rock samples are re-immersed in DI water to notice the increase in surfactant concentration.

5.1.1. Surfactant N1

An example of a concentration measurement for the purposes of surfactant adsorption calculations are presented for surfactant N1 on Eagle Ford shale rock (EF shale 2) with 0.05 wt% surfactant solution. The change in concentration of the surfactant solution in the presence of a rock sample are shown in Figures 73, 74 and 75 for EF Shale 2, Sandstone and Limestone respectively. The concentration is estimated by plotting the change in surface tension versus the concentration at a constant bubble surface age. The surface age of 750ms is chosen for reliability and accuracy to represent the average observed concentration throughout all surface ages. The concentration is then estimated by finding the intercept of the X-axis (concentration) on the Y-axis (surface tension) along the curve generated through interpolation.

 Figure 73 shows the change in concentration in the presence of Eagle Ford shale which shows the concentration gradually change from 0.05 wt. % to approximately 0.0233 wt. % over a range of 144hrs. Figure 74 shows change in surfactant concentration for surfactant N1 with sandstone which shows change in concentration from 0.05 wt. % to 0.0214% over 144 hrs. Figure 75 shows the results for surfactant N1 with Limestone which

shows greater adsorption compared to the shale and sandstone cases with change in concentration from 0.05 wt. % to a final concentration of 0.0133 wt.% over 144 hrs.

N1 calibration curves EF SHALE 2 (5B)

Estimation of concentration from 750ms surface age

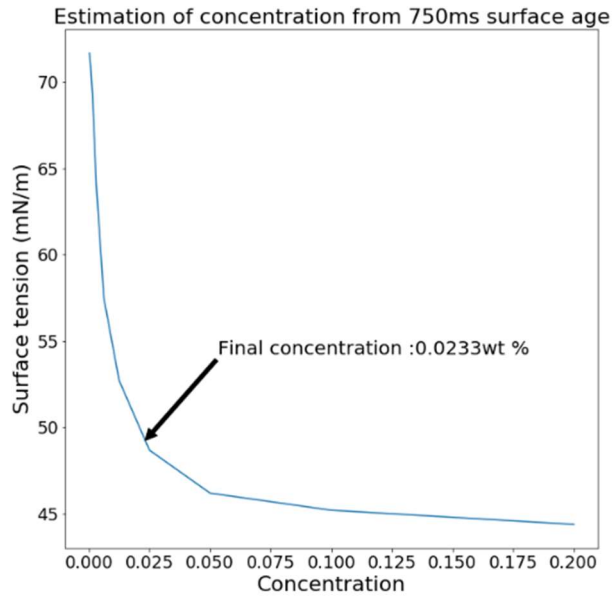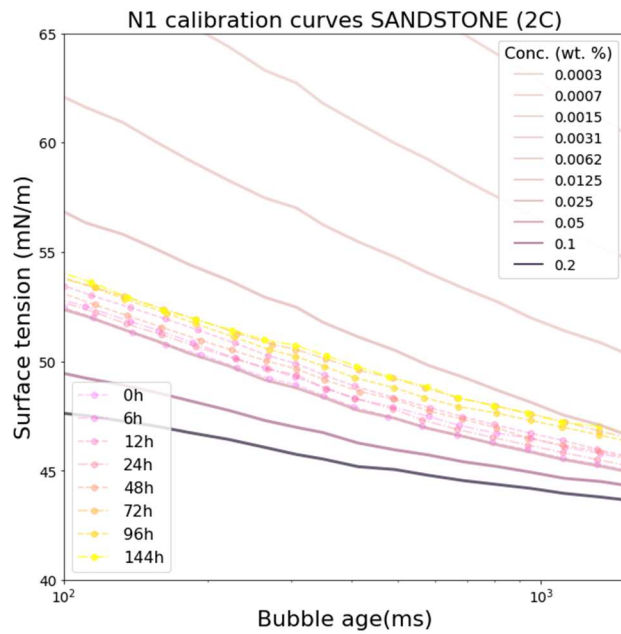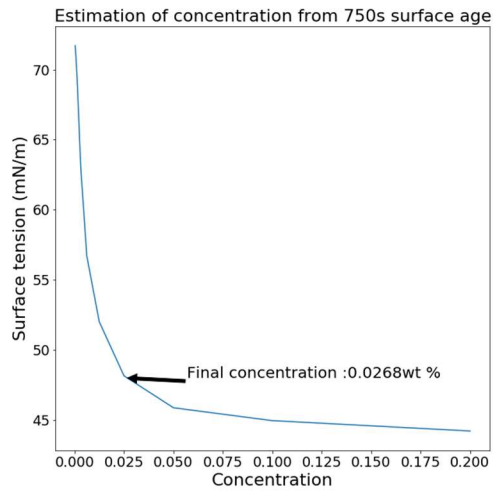Final concentration :0.0233wt %
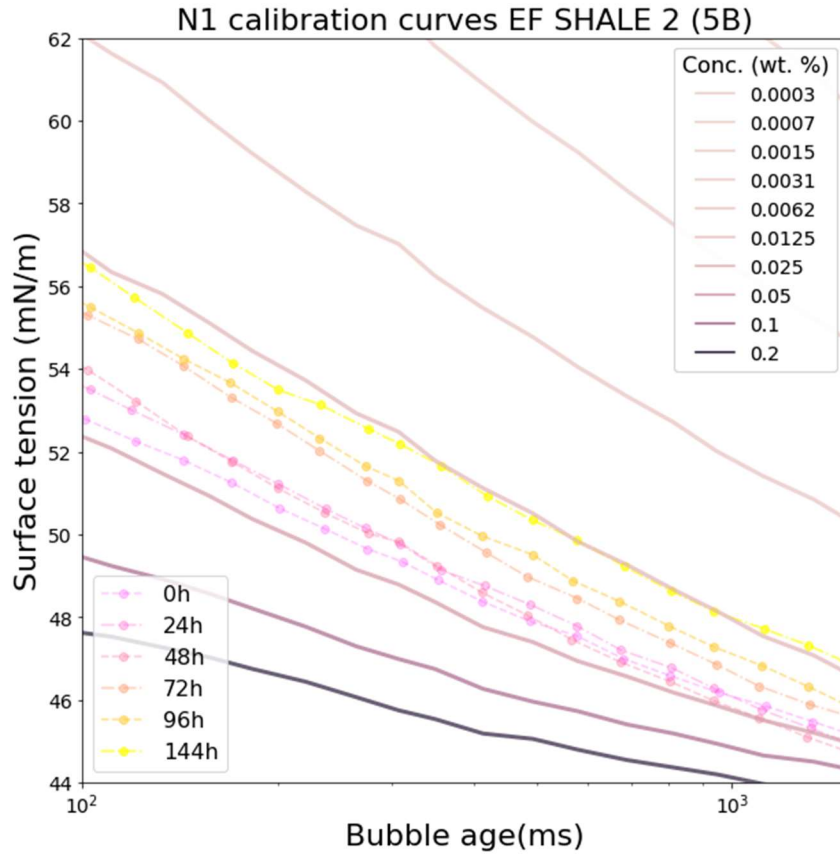
Figure 80: Adsorption measurement (N1 with EF shale) A) DST curves B) Concentration estimation

N1 calibration curves SANDSTONE (2C)

Figure 81: Adsorption measurement (N1 with sandstone) A) DST curves B) Concentration estimation
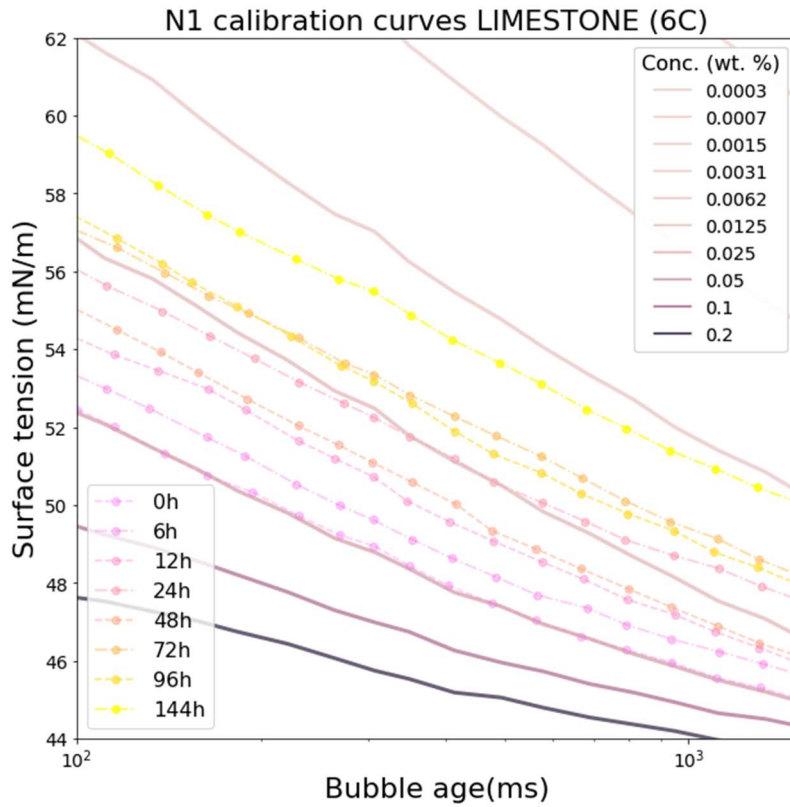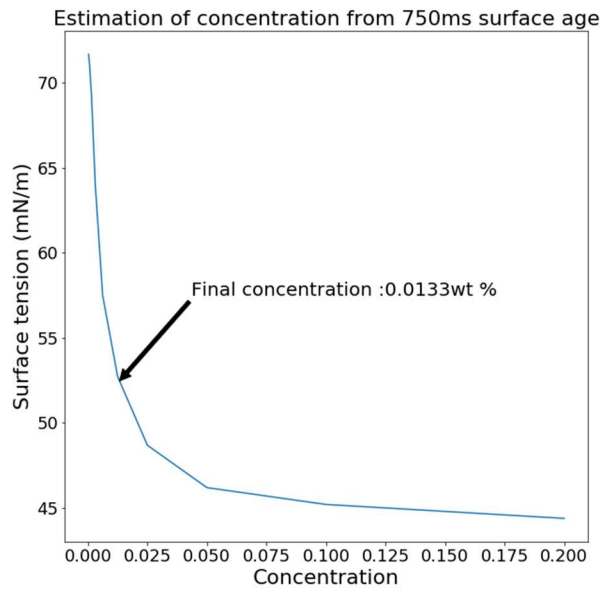
Figure 82: Surfactant adsorption (N1 with limestone) A) DST curves B) Estimated concentration

5.1.2. Surfactant N4

The results of the dynamic surface tension measurement for observing change in surfactant concentration for surfactant N1 on shale, limestone and sandstone are generated using the similar methodology of using the bubble surface age at 750ms for concentration measurements.

The results of surfactant concentration measurement for surfactant N4 on limestone are shown in Figure 76. A change in concentration is observed from 0.05 wt. % to 0.0171 wt. %. Figure 77 shows the measurement taken on sandstone rock which where the concentration was observed to change from 0.05 wt. % to 0.0462 wt. %. The measurements reached a plateau at 144 hours of imbibition. Higher adsorption was observed on the limestone rock compared to the sandstone rock. This indicated a higher

131

affinity for nonionic surfactant N4 for rock higher in calcite content, compared to sandstone rock.
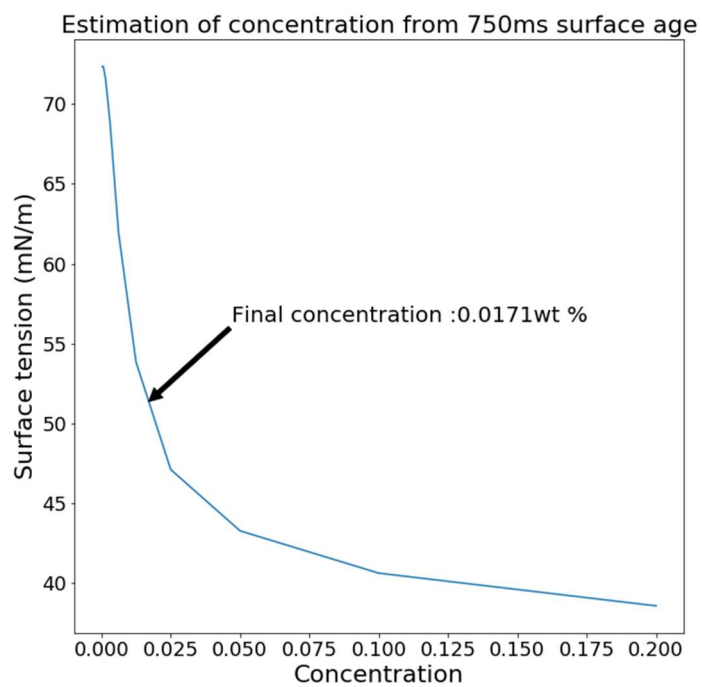

N4 calibration curves LIMESTONE 8C
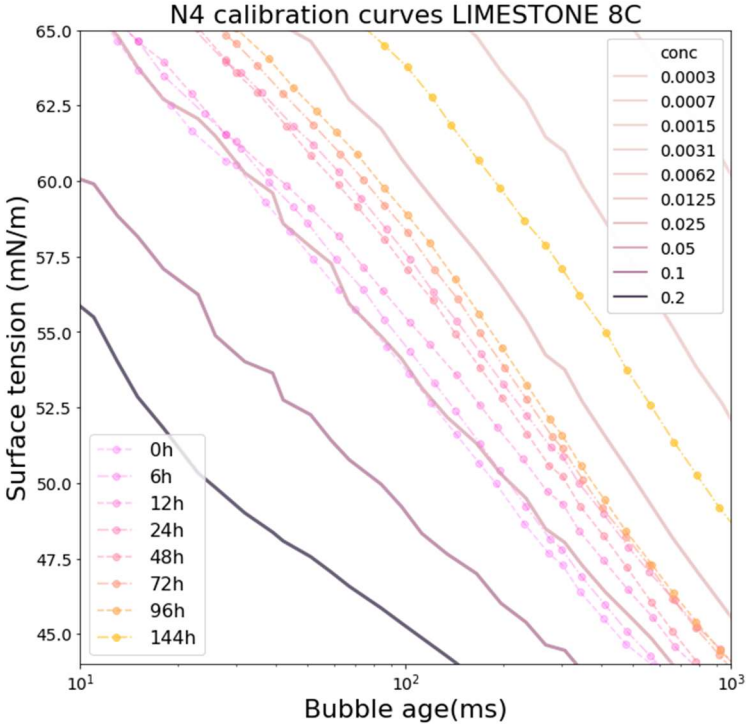
Figure 83: Adsorption measurement (N4 with limestone) A) DST curves B) Estimated concentration
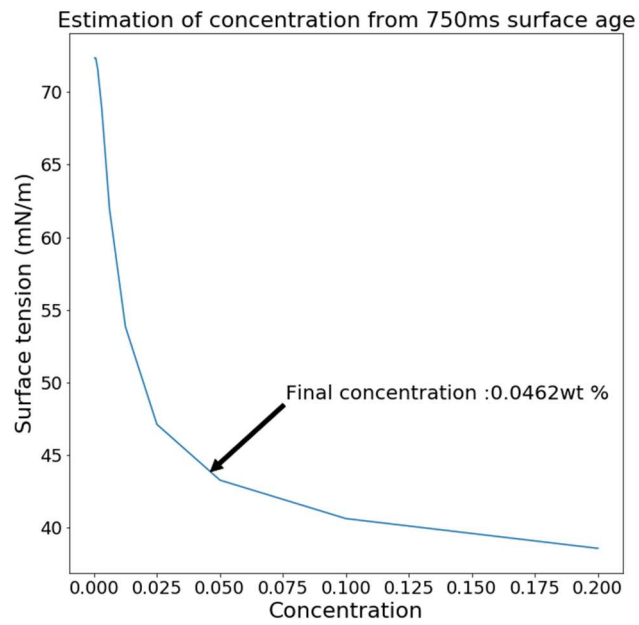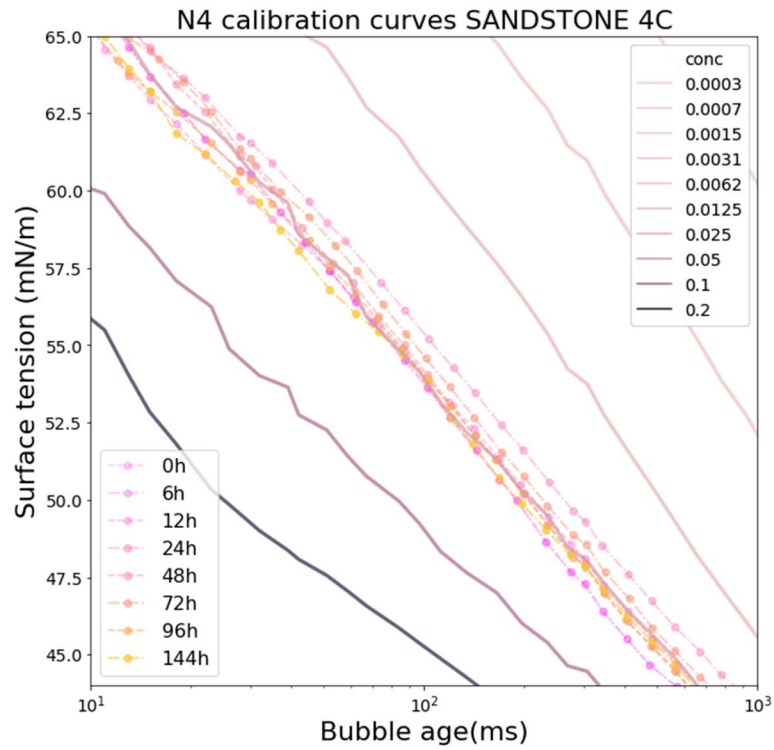
Figure 84: Surfactant adsorption measurement (N4 on sandstone) A) DST curves B) Estimated concentration

5.1.3. Surfactant N5

The results of surfactant adsorption measurements for 0.05 wt. % solution of surfactant N5 on limestone, shale and sandstone are shown in Figures 78, 79 and 80 respectively. Figure 78 shows the change in concentration for surfactant N5 on limestone rock. The concentration changed from 0.05 wt. % to 0.0127 wt. %. Figure 79 shows the measurements for the surfactant N5 on Eagle Ford shale, which showed concentrations change from 0.05 wt. % to 0.0238 wt. %. The change in concentration for surfactant N5 on sandstone was 0.05 % to 0.0416%. All the measurement data points were taken regularly till 144 hrs.

Similar to surfactants N4 and N1, the nonionic surfactants showed increased adsorption onto carbonate rock such as Eagle Ford shale and limestone, and very low adsorption onto rock with high quartz content such as sandstone.
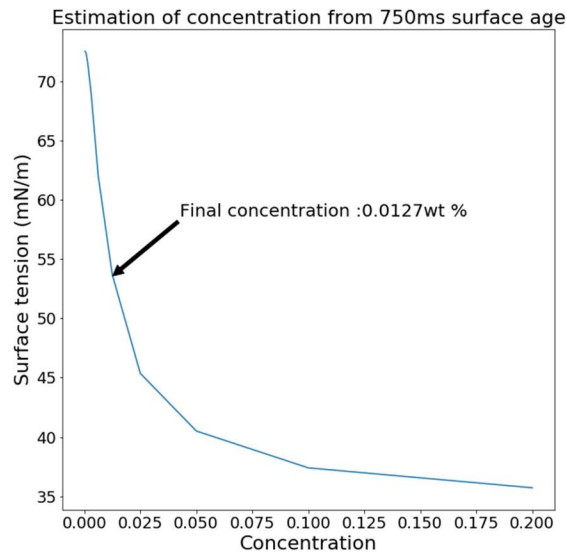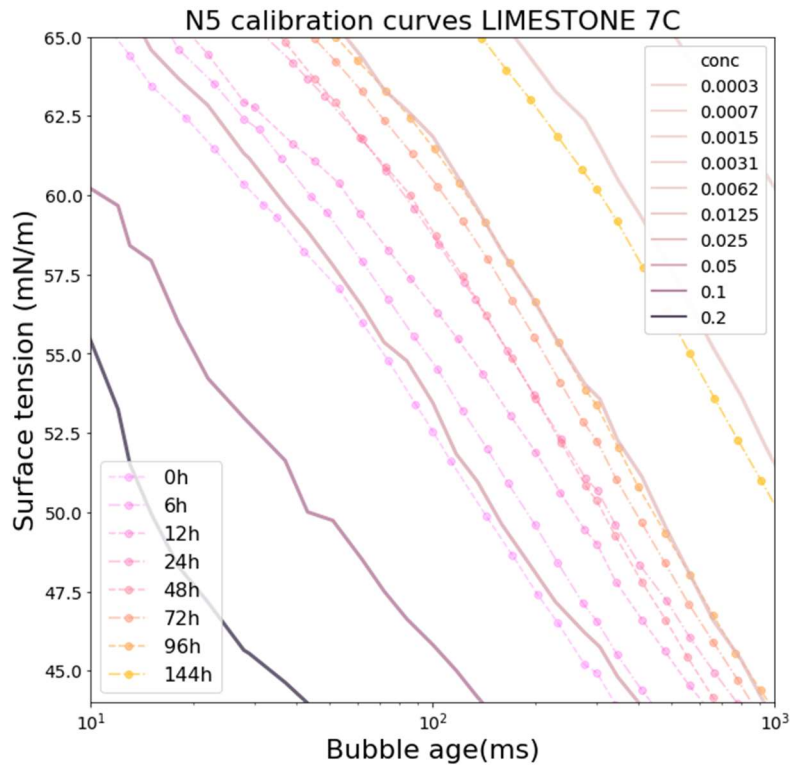
Figure 85: Surfactant adsorption (N5 on Limestone): A) DST Curves B) Estimated concentration

N5 calibration curves EF SHALE 2 (1B)

Estimation of concentration from 750ms surface age

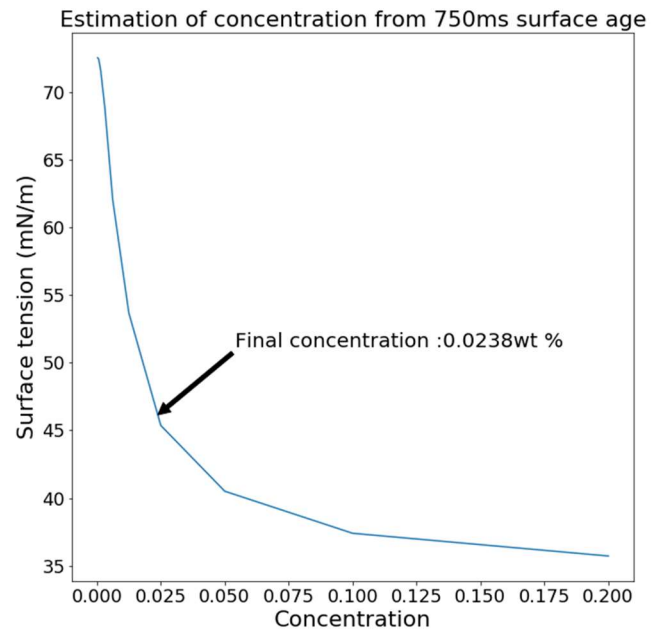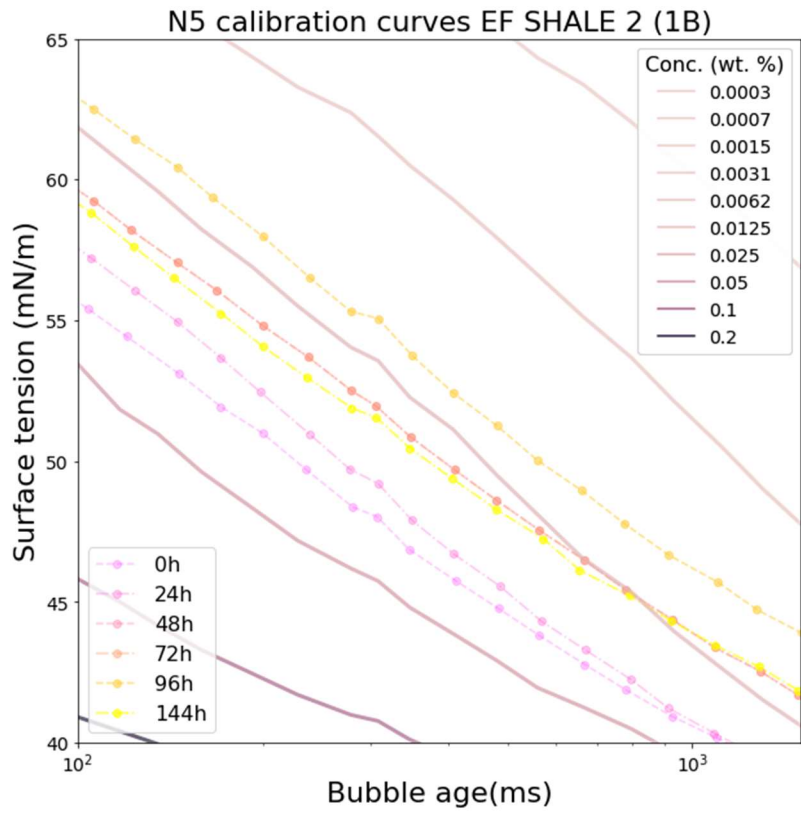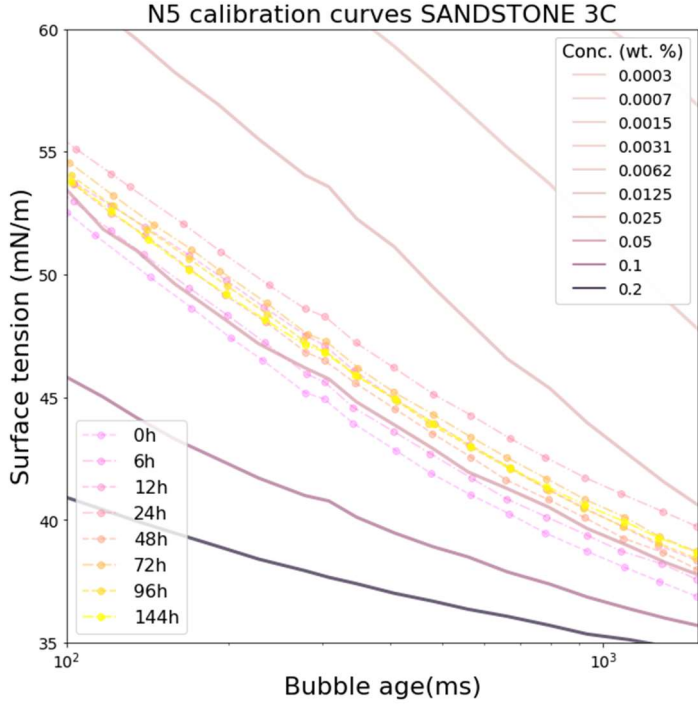Final concentration :0.0238wt %

137

Figure 86: Surfactant Adsorption (N5 on EF Shale 2): A) DST curves B) Estimated concentration
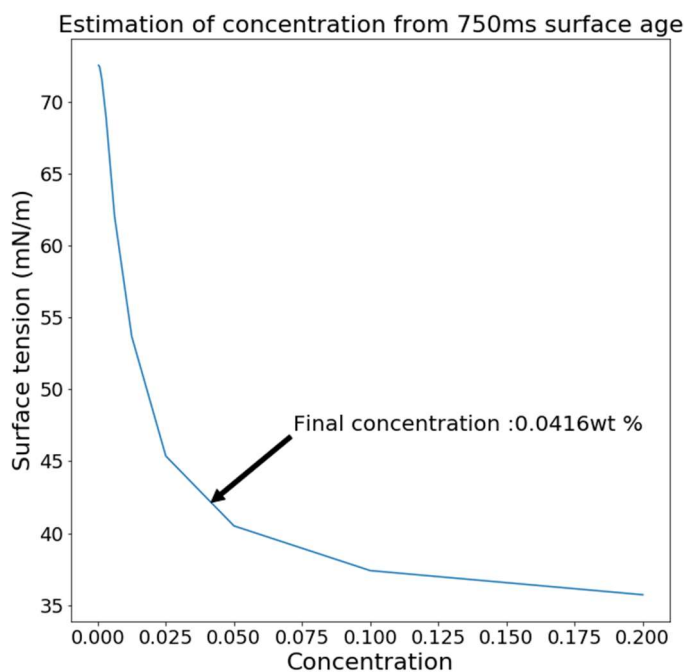
Figure 87: Surfactant adsorption (N5 on sandstone): A) DST Curves B) Estimated concentration

5.1.4. Surfactant N6

The change in surfactant concentration in the presence of different rock types is measured for surfactant N6.

Figure 81 shows the change in concentration of surfactant N6 in the presence of limestone. The concentration changed from 0.05 % to 0.0167 %, over a period of 144 hours. Figure 82 shows the change in concentration of surfactant N6 in the presence of sandstone which changes from 0.05% to 0.0491 %. Figure 83 shows the measurement for surfactant N6 for Eagle Ford shale, which changes from 0.05 % to 0.0241 %, over a period of 120 hours. Similar to previous measurements on nonionic surfactants, the carbonate rocks (shale and limestone) adsorbed significantly higher surfactant content compared to sandstone.
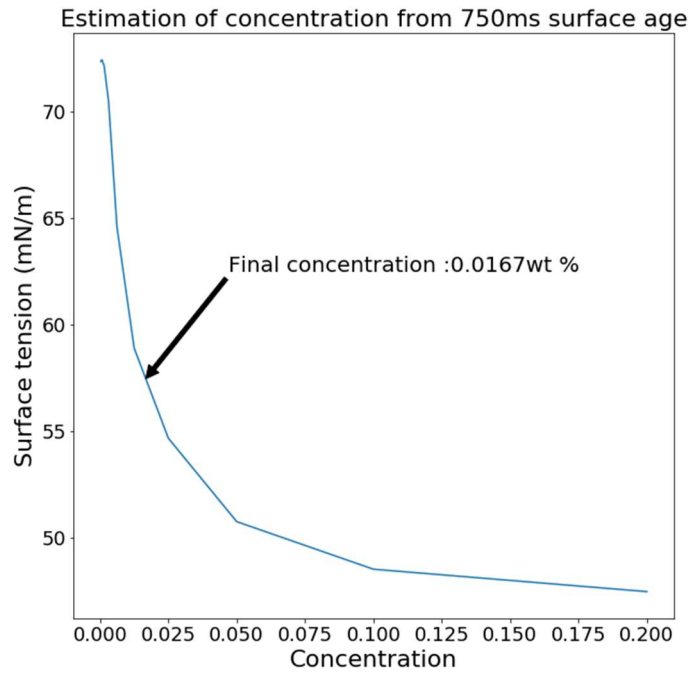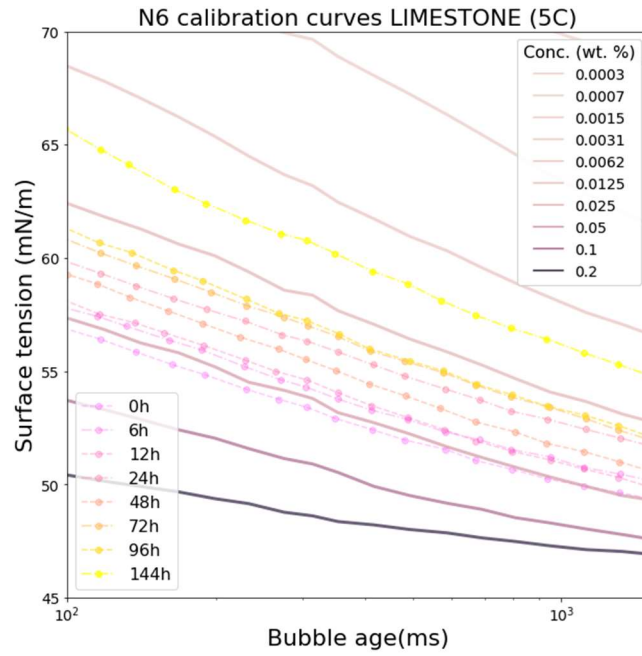
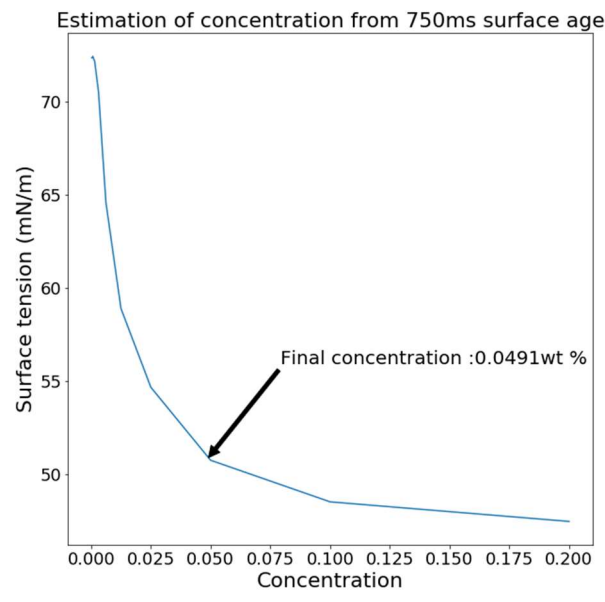**Figure 88: Surfactant adsorption (N6 on limestone): A) DST curves B) Estimated concentration**

Figure 89: Surfactant adsorption (N6 on sandstone): A) DST curves B) Estimated concentration

Figure 90: Surfactant adsorption (N6 on EF shale 2): A) DST curves B) Estimated concentration

5.2. Adsorption of cationic surfactants on different rock types

The adsorption of cationic surfactant C1 on limestone and sandstone outcrops are investigated into (Figures 84 and 85). In both the cases, cationic surfactant C1 does not exhibit significant adsorption onto Limestone or Sandstone rock. The change in concentration is nearly negligible, showing that cationic surfactant has very low adsorption onto limestone and sandstone. The change in concentration was measured of 120 hours to ensure adsorption plateau.

Estimation of concentration from 750ms surface age

Final concentration :~0.05wt %

Figure 91: Surfactant adsorption (C1 on limestone): A) DST curves B) Estimated concentration
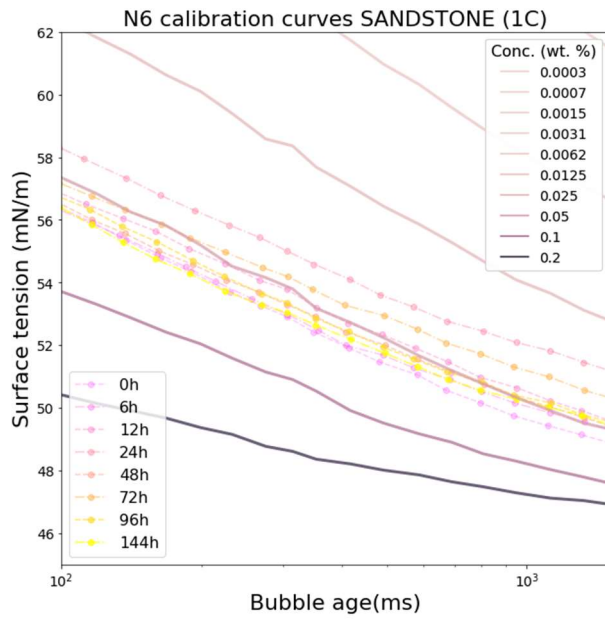

C1 calibration curves SANDSTONE
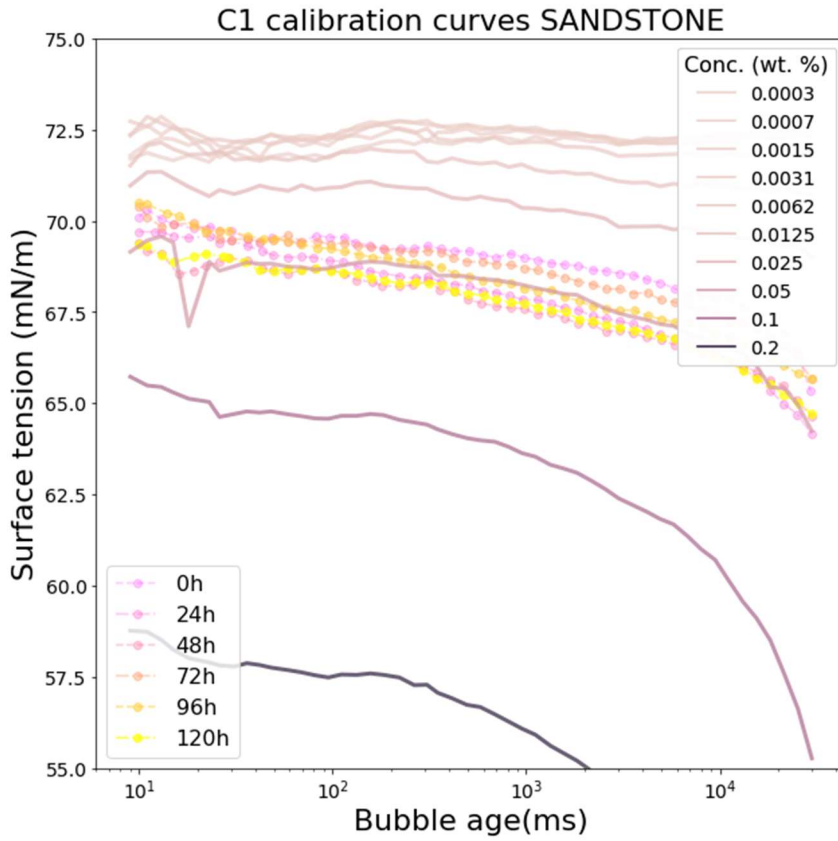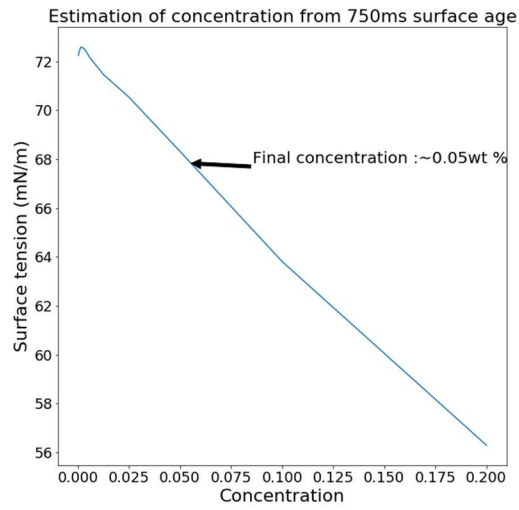
Figure 92: Surfactant adsorption (C1 on sandstone): A) DST curves B) Estimated concentration

5.3. Adsorption of Anionic surfactants on different rock types
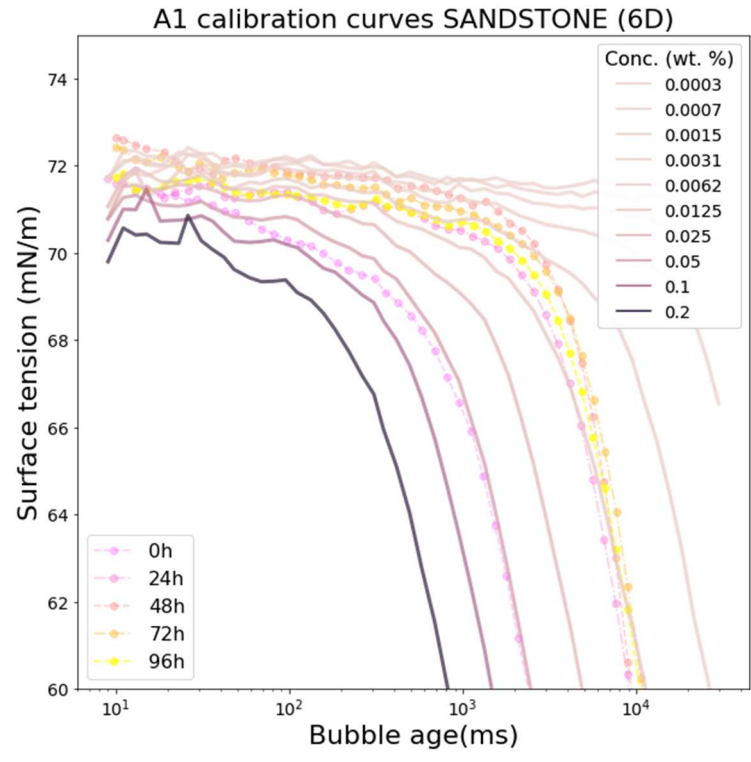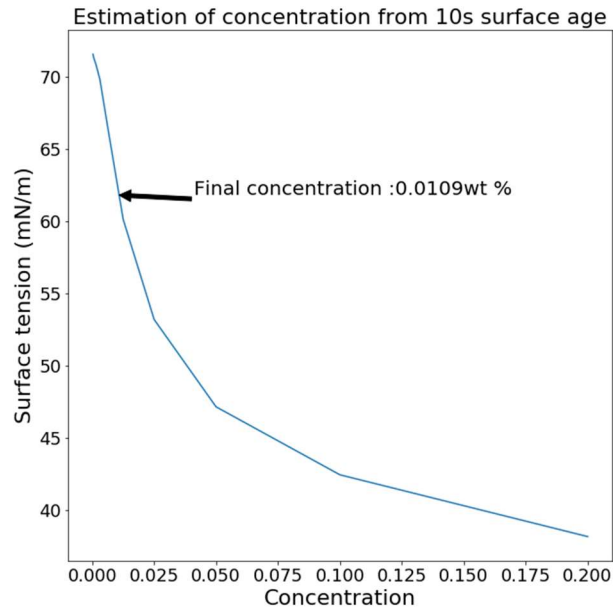
Figure 93: Surfactant adsorption (A1 on sandstone): A) DST curves B) Estimated
concentration

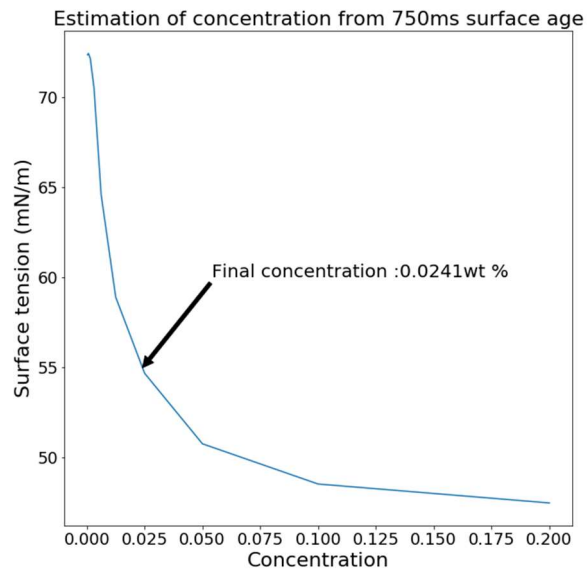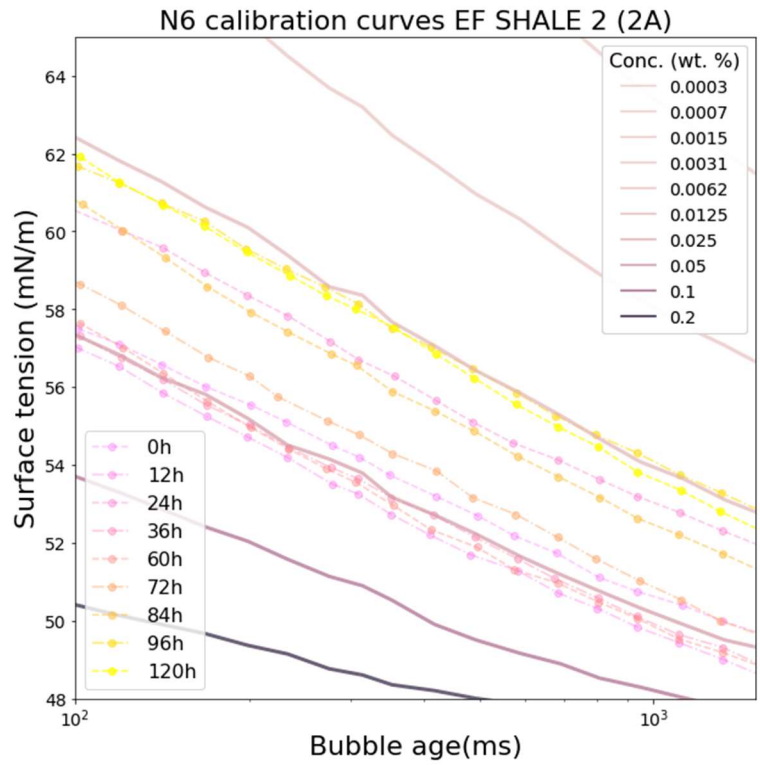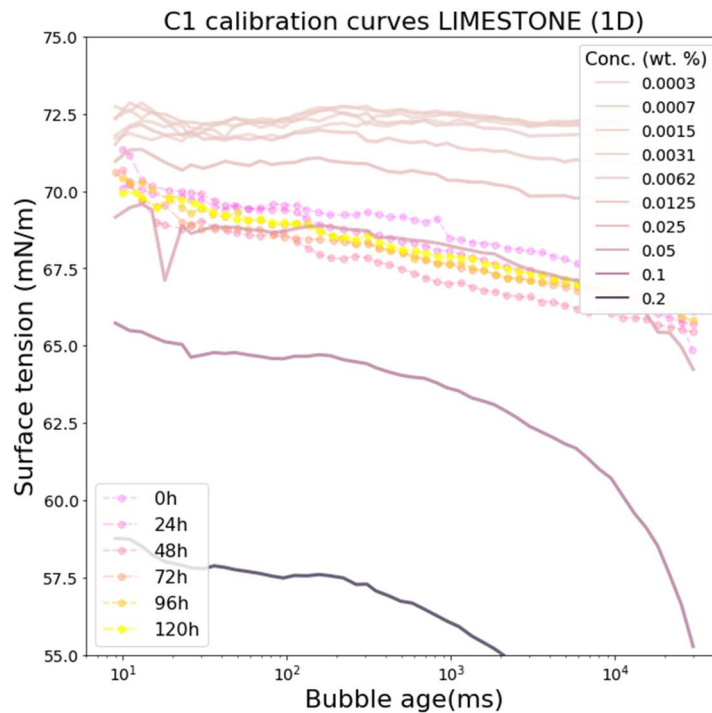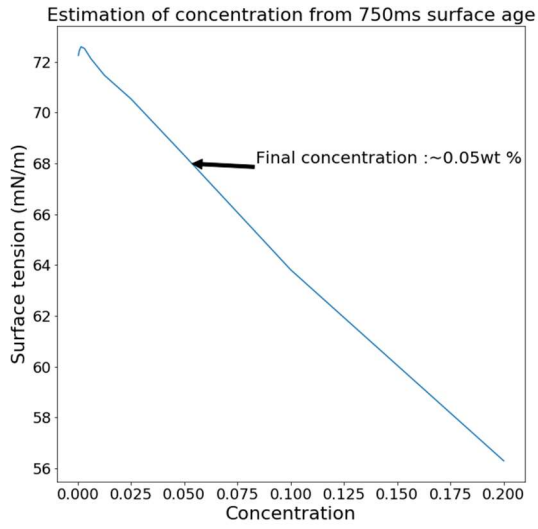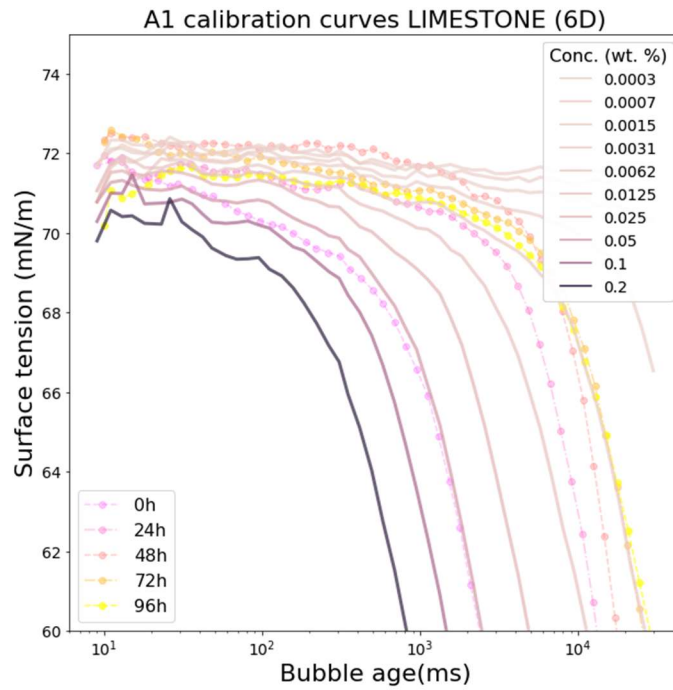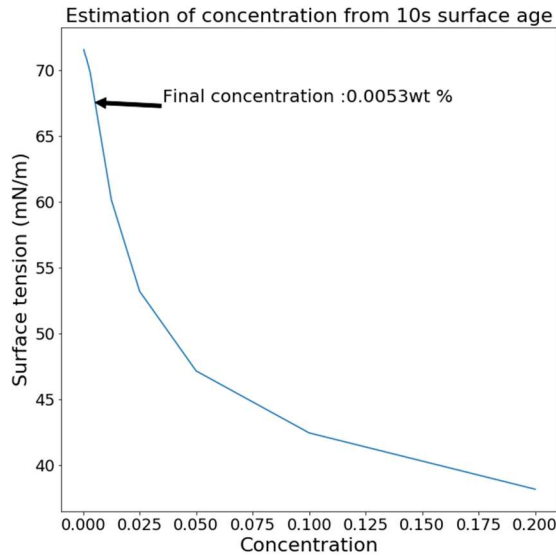**Figure 94: Surfactant adsorption (A1 on limestone): A) DST curves B) Estimated concentration**

5.4. Surfactant adsorption characterization

The total surfactant adsorbed onto the rock samples are compiled and compared in Figure 89. The surfactants used were N1(C_{12-14}23EO), N4(C_{12-14}12EO), N5(Nonylphenol 12EO), N6(Nonylphenol 30EO), A1(C_{20-24}IOS) and C1(C_{12}TAC).

In the case of non-ionic surfactants, we observe a higher adsorption density for across all non-ionic surfactants with a trend of limestone > Eagle Ford shale > sandstone. This shows that non-ionic surfactants tend to adsorb at higher densities on carbonate rocks compared to sandstone rock which is high in quartz content. Compared to non-ionic surfactants, anionic surfactant A1 showed high adsorption densities onto both sandstone and

147

limestone. In stark contrast, cationic surfactant C1 did not show any significant adsorption onto sandstone or limestone. The confidence intervals for shale samples of surfactants N5 and N6 are due to existence of multiple measurements with different similar rock samples, at different weights. A complete summary of the surfactants, rock samples, rock weights and adsorption densities for this study are presented in Figure 88.
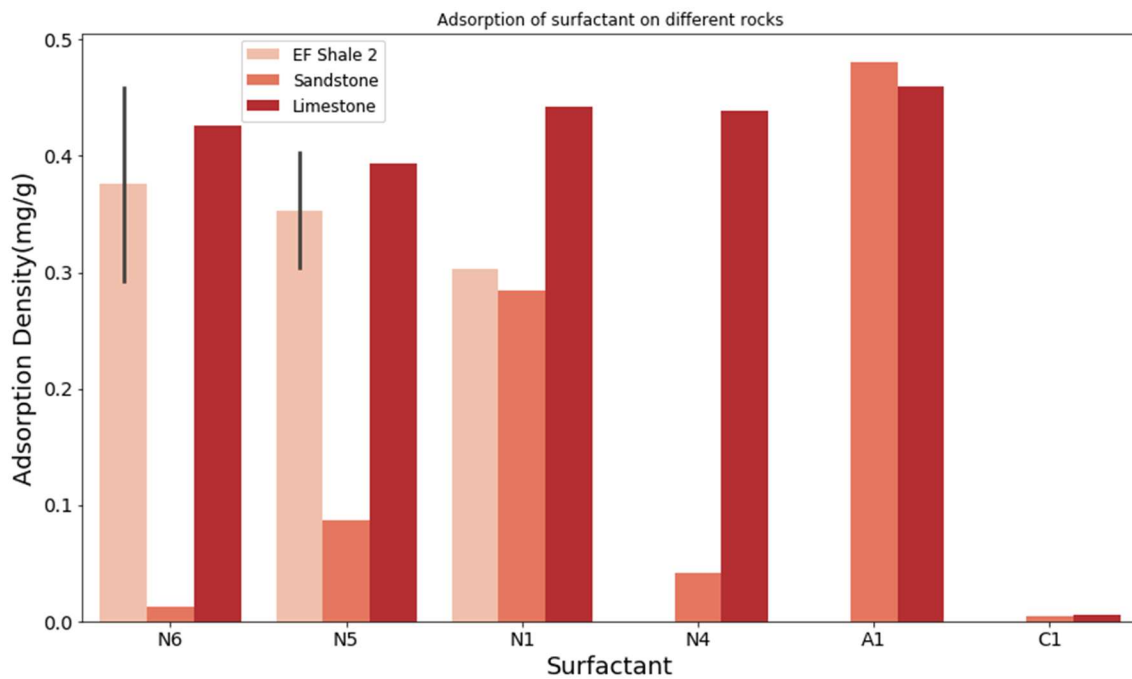
Figure 95: Surfactant adsorption comparison

Surfactant	Rock Sample	Sample Weight (gr)	Adsorption Density(mg/g)	Sample No.
A1	Limestone	19.424	0.460255	6D
A1	Sandstone	16.256	0.481053	8D
C1	Limestone	18.490	0.005408	1D
C1	Sandstone	20.230	0.004943	3D
N1	EF Shale 2	17.657	0.302430	5B
N1	Limestone	16.613	0.441823	6C
N1	Sandstone	16.336	0.284035	2C
N4	Limestone	15.001	0.438637	8C
N4	Sandstone	18.129	0.041922	4C
N5	Limestone	18.954	0.393584	7C
N5	EF Shale 2	15.628	0.403123	6B
N5	EF Shale 2	17.720	0.303612	1B
N5	Sandstone	19.316	0.086975	3C
N6	Limestone	15.728	0.425992	5C
N6	Sandstone	15.027	0.011978	1C
N6	EF Shale 2	17.721	0.292309	2A
N6	EF Shale 2	13.940	0.459110	1A

Figure 96: Summary of surfactants and rock samples utilized

149

5.5. Surfactant Desorption Experiments

Surfactant desorption experiments were performed on a few samples by soaking the surfactant saturated samples in 20 cc of DI water (de-ionized water) after performing surfactant adsorption experiments on the rock sample. Figure 95 shows the change in concentration of DI water when the surfactant-soaked rock sample is immersed in DI water. The change in concentration can quantify the amount of surfactant desorbing from the rock matrix back into the DI water.
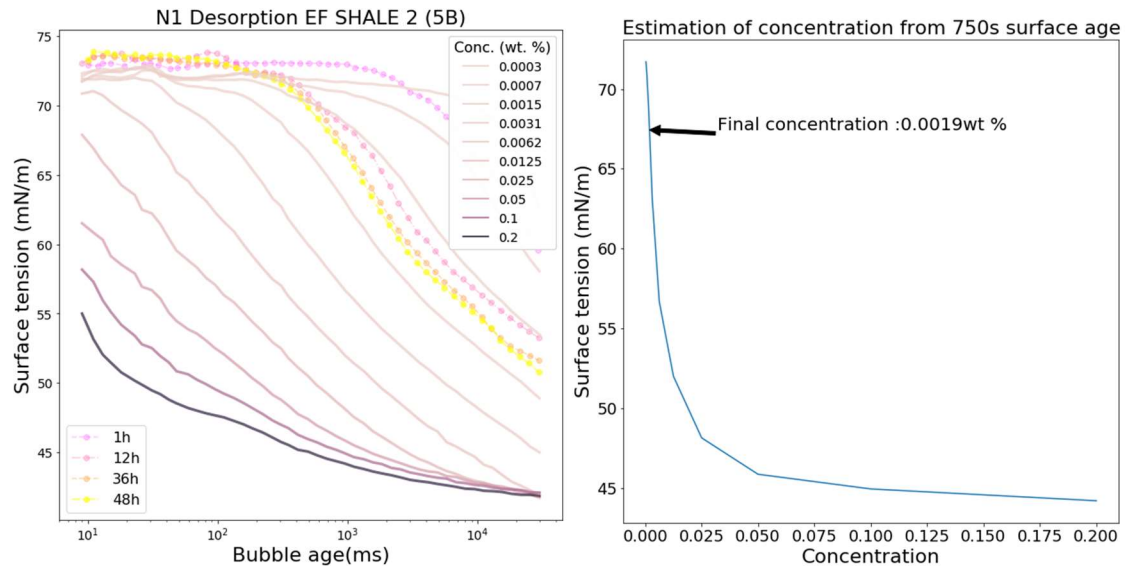
Figure 97: Desorption experiment with N1 sample EF shale 2 (5B)

From Figure 78, the adsorption measurement results show that the concentration decreases from 0.05% to 0.0233% for surfactant N1 and Eagle Ford shale. Desorption experiments show that the surfactant desorbs into the aqueous phase (DI water) and increases the

concentration from 0% to 0.0019%. The amount of surfactant desorbed reached a plateau at around 48 hours, with the total surfactant mass desorbed calculated to be 0.00038 gr. The total surfactant mass adsorbed can be calculated based on values shown in Figure 94 as 0.00533 grams. Approximately 93% of surfactant still remains in the rock sample. Similarly, desorption experiment was carried out on surfactant N5 with Eagle Ford shale. The amount of surfactant adsorbed as calculated from values in Figure 94 was 0.0062 grams. After immersing the sample into DI water, the concentration changed from 0% to 0.00014%. The total surfactant mass desorbed was 0.00028 grams. Approximately 95% by gr. wt. of surf still remained in the rock sample.
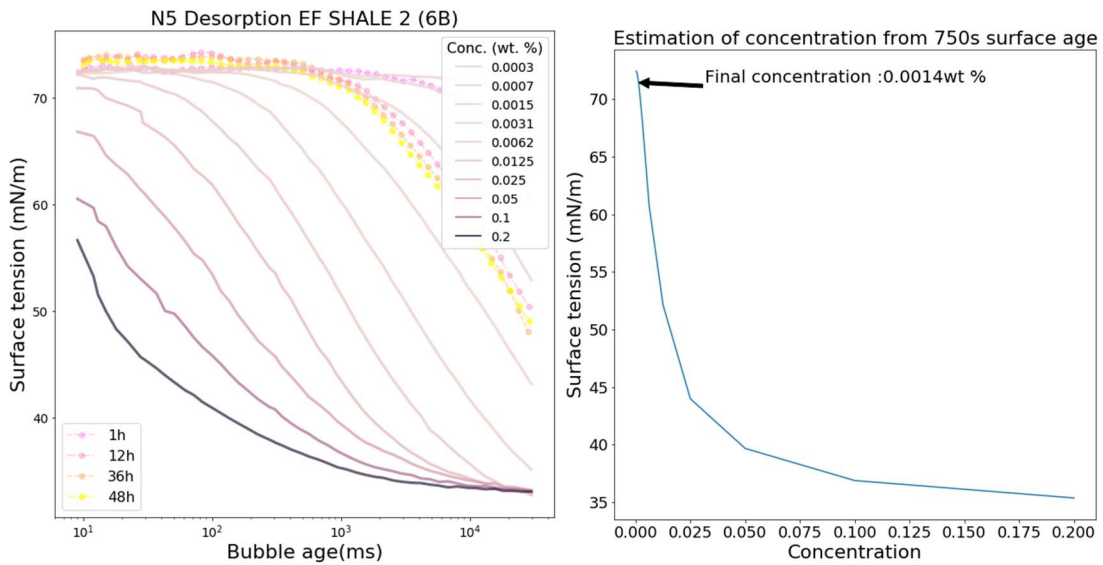
Figure 98: Desorption experiment with N5 sample EF shale 2 (6B)

5.6. Surfactant EOR Project performance

The performance of the EOR project is demonstrated in Figure 95. A 0.2 wt. % surfactant N1 solution with 2% TDS was chosen as the injection fluid after performing laboratory wettability experiments as it showed greater wettability alteration performance while ensuring cloud point and thermodynamic stability.

Post-injection analysis on the well (Figure 95) showed increased average oil production rates compared to the production prior to stimulation with surfactant. The percentage of surfactant returned to the surface through produced water was estimated to be approximately 6.2% of the total surfactant injected by mass. This means that over 90% of the surfactant mass has penetrated the reservoir matrix and remains in the formation. The average oil production rate prior to injection was 5 bbls per day, whereas average oil production after injection was about 14 bbls per day. This increase of over 200% oil production rate can be attributed to wettability alteration process by the injected surfactant solution. Nonionic surfactant N1 resulted in increased oil displacement in the tight pore spaces in unconventional Eagle Ford shale rock as indicated by higher oil production rates. The methodology used for this EOR project can be applied to other mature unconventional wells to improve oil recovery and monitor the well productivity performance.
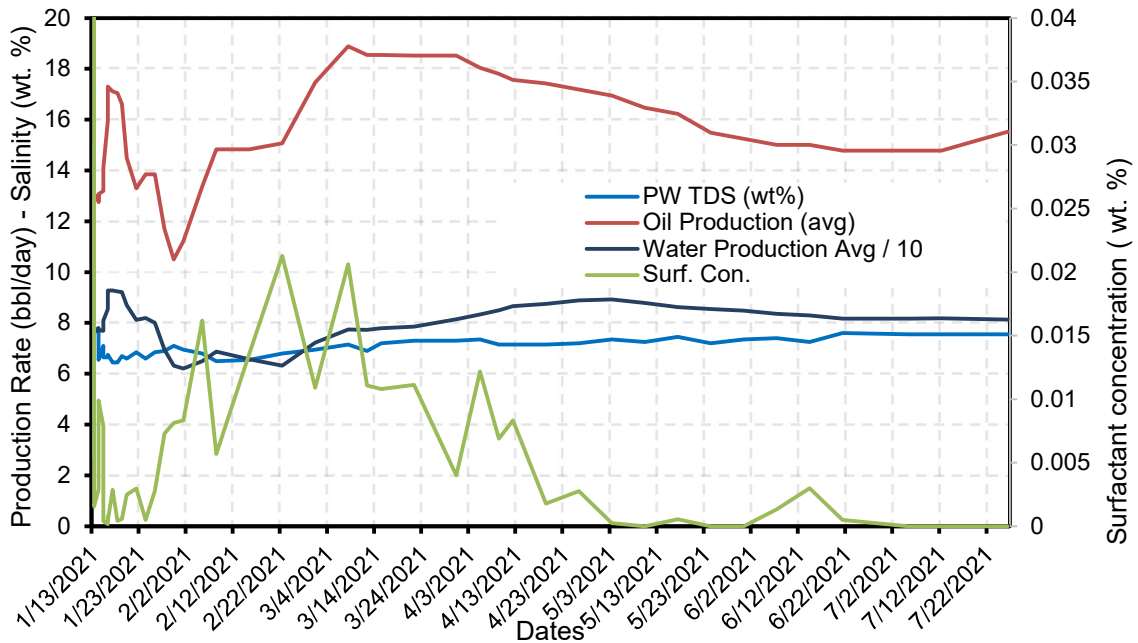
Figure 99: Fluid and surfactant production from EOR project

5.7. Surfactant Adsorption Experiments

Surfactant adsorption measurements were performed to quantify the adsorption density of surfactants on different rock types. The dynamic surface tension methodology for measuring change in concentration was implemented to measure the surfactant adsorbed onto a rock sample over a duration of time until an adsorption plateau was observed. Results show that the nonionic surfactants have high adsorptions on shale and limestones compared to sandstones. Anionic surfactant A1 showed high adsorption on both sandstone and limestone rock, whereas cationic surfactants showed low adsorption densities. Further work is planned to accumulate more data points for adsorption of surfactants on different

rock types to effectively characterize the surfactant adsorption dynamics for wettability

alteration purposes.

Figure 100: Adsorption densities of surfactants on different rock samples

6. CONCLUSIONS

This study aimed to introduce a workflow for applying chemical surfactant EOR methodologies to a mature unconventional well in the Eagle Ford basin. Implementing an effective surfactant EOR project involved wettability alteration performance validation by interfacial tension, contact angle and spontaneous imbibition experiments. The effectiveness of a surfactant formulation for altering wettability is accompanied by investigating the effects of chemical additives to the injection fluid. Th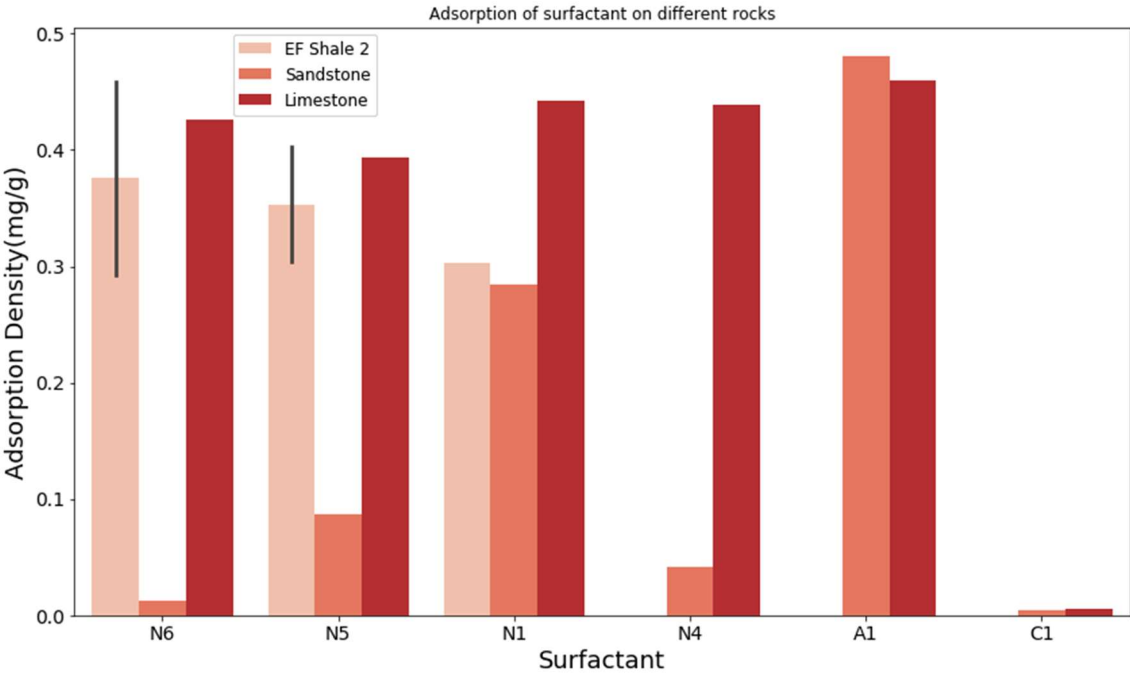e productivity of the well is documented by monitoring the oil and water production over the course of the well production. The surfactant mass balance of the injection process was estimated by calculating the surfactant concentrations in produced water samples using dynamic surface tension analysis. The major conclusions from the surfactant EOR project were:

1. Cloud point measurements on non-ionic surfactants with a range of EO groups in the hydrophilic tail show higher cloud point temperatures for higher EO group numbers. The cloud point temperatures decrease with increasing levels of salinity. These characteristics can be attributed to the lowering of hydrophilicity (water solubility) due to the weakening of hydrogen bonds in EO groups. The presence of salt concentrations leads to lowered solubility.

2. IFT measurements on brines with a range of salinities show IFT increasing with increasing salinity, without the presence of a surfactant. IFT measurements with nonionic-surfactants showed decreasing surface tension with increasing temperatures for a range of brine salinities from 0% TDS to 10% TDS.

155

3. The IFT values showed a decreasing trend in surface tension with increasing brine salinities in the presence of surfactants for a range of salinities. This is due to the electrostatic effects of salts on surfactant molecules which increase surface activity.

4. The cloud point temperature of lower EO group nonionic surfactants can affect the IFT of surfactants solutions, with a reversal in IFT trends observed near the cloud point temperature which can be due to the surfactant phasing out of the aqueous phase near the cloud point temperature.

5. Contact angle measurements show that nonionic surfactants are successfully able to alter wettability to water-wet even in the presence of chemical additives such as biocide (glutaraldehyde).

6. Spontaneous Imbibition experiments show that nonionic surfactants are able to demonstrate oil recovery factor of ~40% with higher recovery factors compared to typical brine imbibition (~5%).

7. Oil production rates were observed to increase by 200% after the surfactant injection process. Surfactant EOR is shown to increase oil production. The amount of residual surfactant returning to the surface in PW was ~6%, which shows that over 90% of the surfactant mass has remained in the reservoir. Surfactant concentration increases initially in the first 2 months and then gradually decreases.

8. PW salinity shows a change from 14% TDS prior to injection to ~6% TDS salinity after surfactant stimulation.

9. The application of dynamic surface tension measurements on aqueous surfactant solutions is shown to be an effective method for estimating surfactant concentrations in produced water fluids and aqueous surfactant solutions based on results from surfactant EOR project and adsorption experiments.

10. Surfactant adsorption experiments show that nonionic surfactants show greater adsorption densities onto carbonate rich rock such as limestone and shale at 0.4 – 0.45 mg/g and 0.3 – 0.4 mg/g. The adsorption density on sandstone was low at an average of 0.1 mg/g.

11. Cationic surfactant adsorbs at high densities on both limestone and sandstone rock at about 0.45 mg/g adsorption density, whereas anionic surfactant showed very low adsorption densities of close to zero.

12. Surfactant desorption experiments show that over 90% of the surfactant remains in the rock matrix, which is analogous to the results observed in the EOR field project where ~93% of the surfactant still remained in the reservoir.

REFERENCES

[1] Green D. W., Willhite G. P. (1998). Enhanced oil recovery. SPE Textbook Series. Richardson, TX: Society of Petroleum Engineers.

[2] Thomas S. (2008). Enhanced oil recovery—An overview. Oil and Gas Science and Technology, 63, 1, 9–19.

[3] Cohen D. (2007). Exaggerated oil recovery. Peak watch. Available from https://peakwatch.typepad.com/peak_watch/2007/07/exaggerated-oil.html. 10 Jan, 2016

[4] Nwidee, L. & Theophilus, Stephen & Barifcani, Ahmed & Sarmadivaleh, Mohammad & Iglauer, S. (2016). EOR Processes, Opportunities and Technological Advancements. 10.5772/64828.

[5] Latil M. (1980). Enhanced oil recovery. Paris: Technip, Gulf Publishing

[6] McInerney M. J., Nagle D. P., Knapp R. M. (2005). Microbially enhanced oil recovery: Past, present, and future. Petroleum Microbiology, 215–23. Washington, DC: ASM Press.

[7] Belyaev S. S., Borzenkov I. A., Nazina T. N., Rozanova E. P., Glumov I. F., Ibatullin R. R., Ivanov M. V. (2004). Use of microorganisms in the biotechnology for the enhance- ment of oil recovery. Microbiology, 73, 590–598.

[8] Van Hamme J. D., Singh A., Ward O. P. (2003). Recent advances in petroleum microbiology. Microbiology, 67(4), 503–549.

[9] Iglauer S., Favretto S., Spinelli G., Schena G., Blunt M. J. (2010). X-ray tomography measurements of power-law cluster size distributions for the nonwetting phase in sandstones. Physical Review E, 82, 056315.

[10] Potts G. D. (2011). Integrating renewable energy resources within the oil industry: Concentrated solar power & enhanced oil recovery. [Online] available from http:ÀÀ wwwžgdpcapitalžcožukÀdocsÀthermalôEORôCSPžpdfž 20 December, 2015.

[11] Terry R. E. (2001). Enhanced oil recovery. Encyclopedia of Physical Science and Technology, 18, 503–518.

[12] Prats M. (1986). Thermal recovery. 2nd edition. Dallas, TX: SPE.

[13] Kovscek A. R. (2012). Emerging challenges and potential futures for thermally enhanced oil recovery. Journal of Petroleum Science and Engineering, 99, 130 – 143.

[14] Satter A., Iqbal G. M., Buchwalter J. L. (2008). Practical enhanced reservoir engineering: Assisted with simulation software. Pennwell: Oklahoma.

[15] Moore R. G., Laureshen C. J., Belgrave J. D., Ursenbach M. G., Mehta S. A. (1994). Insitu combustion in Canadian heavy oil reservoirs. Journal of Petroleum Science and Engineeering, 74(8), 1169 – 1175.

[16] Sarathi S. P. (1999). Handbook of in – situ combustion. US: National Department of Energy.

[17] Baibakov N. K., Garushev A. R., Cieslewicz W. J. (2011). Thermal methods of petroleum production. Amsterdam: Elsevier.

159

[18] Hashemi‐Kiasari H., Hemmati‐Sarapardeh A., Mighani S., Mohammadi A. H., Sedaee‐Sola B. (2014). Effect of operational parameters on SAGD performance in a dip heterogeneous fractured reservoir. Fuel, 122, 82–93.

[19] Parker M. E., Meyer J. P., Meadow S. R. (2009). Carbon dioxide enhanced oil recovery injection operations technologies. Energy Procedia, 1(1), 3141–3314.

[20] U.S. Department of Energy. (2009). Carbon dioxide enhanced oil recovery untapped domestic energy supply and long-term carbon storage solution. Available from http://www.netl.doe.gov/sites/default/files/netl-file/CO2_EOR_Primer.pdf.

[21] Zhang Y., Huang S. S., Luo P. (2010). Coupling immiscible CO2 technology and polymer injection to maximize EOR performance for heavy oils. Journal of Canadian Petroleum Technology, 49(5), 25–33.

[22] Kokal S., Al‐Kaabi A. (2010). Enhanced oil recovery: Challenges & opportunities. [Online] available from http://www.world‐petroleum.org/docs/docs/publications/ 2010yearbook/P64‐69_Kokal‐Al_Kaabi.pdf

[23] Alagorni A. H., Yaacob Z. B., Nour A. H. (2015). An overview of oil production stages: Enhanced oil recovery techniques and nitrogen Injection. International Journal of Environmental Science and Development, 6, 9.

[24] Samanta, A., Bera, A., Ojha, K., Mandal, A.: Comparative studies on enhanced oil recovery by alkali–surfactant and polymer fooding. J. Pet. Explor. Prod. Technol. 2, 67–74 (2012). https:// doi.org/10.1007/s13202-012-0021-2

[25] 8. Wei, B.: Advances in polymer flooding. In: El-Amin, M.F. (ed.) Viscoelastic and Viscoplastic Materials. IntechOpen. https://doi. org/10.5772/64069. https://www.intechopen.com/books/visco elastic-and-viscoplastic-materials/advances-in-polymer-flooding

[26] Sorbie, K.S.: Polymer Improved Oil Recovery. Blackie and Son Ltd, London (1991)

[27] Veerabhadrappa, S.K.: Study of efects of polymer elasticity on enhanced oil recovery by core fooding and visualization experiments (thesis). A Master's thesis submitted to the Department of Civil and Environmental Engineering, University of Alberta (2013)

[28] Mandal, A.: Chemical flood enhanced oil recovery: a review. Int. J Oil Gas Coal Technol. **9**, 241–264 (2015)

[29] Gbadamosi, A.O., Junin, R., Manan, M.A. *et al.* An overview of chemical enhanced oil recovery: recent advances and prospects. *Int Nano Lett* **9,** 171–202 (2019). https://doi.org/10.1007/s40089-019-0272-8

[30] ShamsiJazeyi, H., Miller, C.A., Wong, M.S., Tour, J.M., Verduzco, R.: Polymer-coated nanoparticles for enhanced oil recovery. J. Appl. Polym. Sci. **131**, 1–13 (2014). https ://doi.org/10.1002/app.40576

[31] H. Wang, F. Ma, X. Tong, Z. Liu, X. Zhang, Z. Wu, D. Li, B. Wang, Y. Xie and L. Yang ,Petrol. Explor. Dev., 43 (2016), pp. 925-940, 10.1016/S1876-3804(16)30111-2

[32] A. Rostami and H.A. Nasr-El-Din, Presented at the SPE Western North American and Rocky Mountain Joint Meeting, Society of Petroleum Engineers (2014)

[33] Tianbo Liang, Xurong Zhao, Shuai Yuan, Jiawei Zhu, Xingyuan Liang, Xiuhui Li, Fujian Zhou, Surfactant-EOR in tight oil reservoirs: Current status and a systematic surfactant screening method with field experiments, Journal of Petroleum Science and Engineering, Volume 196, 2021, 108097, ISSN 0920-4105, https://doi.org/10.1016/j.petrol.2020.108097.

[34] Liang, T., Achour, S.H., Longoria, R.A., DiCarlo, D.A., Nguyen, Q.P., 2017a. Flow physics of how surfactants can reduce water blocking caused by hydraulic fracturing in low permeability reservoirs. J. Petrol. Sci. Eng. 157, 631–642. https://doi.org/10.1016/ j.petrol.2017.07.042.

[35] Liang, T., Li, Q., Liang, X., Yao, E., Wang, Y., Li, Y., Chen, M., Zhou, F., Lu, J., 2018a. Evaluation of liquid nanofluid as fracturing fluid additive on enhanced oil recovery from low-permeability reservoirs. J. Petrol. Sci. Eng. 168, 390–399. https://doi.org/ 10.1016/j.petrol.2018.04.073.

[36] Liang, T., Longoria, R.A., Lu, J., Nguyen, Q.P., DiCarlo, D.A., 2017b. Enhancing hydrocarbon permeability after hydraulic fracturing: laboratory evaluations of shut- ins and surfactant additives. SPE J. 22 (1) https://doi.org/10.2118/175101-PA, 011- 1,023

[37] Liang, T., Luo, X., Nguyen, Q., DiCarlo, D.A., 2018b. Computed-tomography measurements of water block in low-permeability rocks: scaling and remedying production impairment. SPE J. 23, 762–771. https://doi.org/10.2118/189445-PA.

[38] Liang, T., Xu, K., Lu, J., Nguyen, Q., DiCarlo, D., 2020. Evaluating the performance of surfactants in enhancing flowback and permeability after hydraulic

fracturing through a microfluidic model. SPE J. 25, 268–287. https://doi.org/10.2118/ 199346-PA.

[39] Liang, T., Zhou, F., Lu, J., DiCarlo, D., Nguyen, Q., 2017d. Evaluation of wettability alteration and IFT reduction on mitigating water blocking for low-permeability oil- wet rocks after hydraulic fracturing. Fuel 209, 650–660. https://doi.org/10.1016/j. fuel.2017.08.029.

[40] Xi Yuan Hua, & Rosen, M. J. (1988). Dynamic surface tension of aqueous surfactant solutions. Journal of Colloid and Interface Science, 124(2), 652–659. https://doi.org/10.1016/0021-9797(88)90203-2

[41] Christov, N. C., Danov, K. D., Kralchevsky, P. A., Ananthapadmanabhan, K. P., & Lips, A. (2006). Maximum Bubble Pressure Method: Universal Surface Age and Transport Mechanisms in Surfactant Solutions. Langmuir, 22(18), 7528–7542. https://doi.org/10.1021/la061239h

[42] Fainerman, V.B., Miller, R. & Joos, P. The measurement of dynamic surface tension by the maximum bubble pressure method. *Colloid Polym Sci* **272,** 731–739 (1994). https://doi.org/10.1007/BF00659287

[43] Qazi, M. J., Schlegel, S. J., Backus, E. H. G., Bonn, M., Bonn, D., & Shahidzadeh, N. (2020). Dynamic Surface Tension of Surfactants in the Presence of High Salt Concentrations. Langmuir, 36(27), 7956–7964. https://doi.org/10.1021/acs.langmuir.0c01211

[44] Ward, A. F. H., & Tordai, L. (1946). Time-Dependence of Boundary Tensions of Solutions I. The Role of Diffusion in Time-Effects. The Journal of Chemical Physics, 14(7), 453–461. https://doi.org/10.1063/1.1724167

[45] Aytouna, M., Bartolo, D., Wegdam, G., Bonn, D., & Rafaï, S. (2009). Impact dynamics of surfactant laden drops: dynamic surface tension effects. Experiments in Fluids, 48(1), 49–57. https://doi.org/10.1007/s00348-009-0703-9

[46] Hua, X. Y., & Rosen, M. J. (1991). Dynamic surface tension of aqueous surfactant solutions. Journal of Colloid and Interface Science, 141(1), 180–190. https://doi.org/10.1016/0021-9797(91)90313-w

[47] Buckley, J. S., Liu, Y., & Monsterleet, S. (1998, March 1). Mechanisms of Wetting Alteration by Crude Oils. Society of Petroleum Engineers. doi:10.2118/37230-PA

[48] Hirasaki, G. J., Miller, C. A., & Puerto, M. (2008, September 21). Recent Advances in Surfactant EOR. All Days. SPE Annual Technical Conference and Exhibition. https://doi.org/10.2118/115386-ms

[49] Anderson, W. G. (1986). Wettability Literature Survey- Part 1: Rock/Oil/Brine Interactions and the Effects of Core Handling on Wettability. Journal of Petroleum Technology, 38(10), 1125–1144. https://doi.org/10.2118/13932-pa

[50] Anderson, W. (1986). Wettability Literature Survey- Part 2: Wettability Measurement. Journal of Petroleum Technology, 38(11), 1246–1262. https://doi.org/10.2118/13933-pa

[51] Reynolds, M. A. (2020). A Technical Playbook for Chemicals and Additives Used in the Hydraulic Fracturing of Shales. Energy & Fuels, 34(12), 15106–15125. https://doi.org/10.1021/acs.energyfuels.0c02527